Aus dem Deutschen Krebsforschungszentrum Heidelberg
(Geschäftsführender Direktor: Prof. Dr. med. Otmar D. Wiestler)
Abteilung für Tumorvirus- Charakterisierung
(Abteilungsleiter: Prof. Dr. Ethel-Michele de Villiers)

Interaction of human papillomavirus 20 and 4-nitroquinoline-1-oxide in carcinogenesis

Inaugural dissertation
zur
Erlangung der Doktorwürde
Der
Naturwissenschaftlich-Mathematischen Gesamtfakultät
der
Ruprecht - Karls - Universität
Heidelberg

vorgelegt von
Elsa Herráez Hernández

aus
Ávila, Spanien
2009

Dissertation
submitted to the
Combined Faculties for the Natural Sciences and for Mathematics
of the Ruperto-Carola University of Heidelberg, Germany
for the degree of
Doctor of Natural Sciences

presented by
Elsa Herráez Hernández
born in Ávila, Spain
Oral-examination: .....

Referees: (Herr) Prof. Dr. G.J. Hämmerling.

(Herr) Prof. Dr. P. Angel.

To Lilín

Table of contents

Abbreviations

A	Adenin
APS	Ammonium persulfate
ß-ME	β-Mercaptoethanol
BaP	Benzo[a]pyrene
bp	Base pair(s)
BPV	Bovine papillomavirus
BrdU	5´ bromo-2-deoxyuridine
BSA	Bovine serum albumin
C	Cytosine
cdk	Cyclin-dependent kinase
cDNA	Complementary DNA
DAB	3,3´-diaminobenzidine substrate
DAPI	4´, 6- Diamidino-2-phenylindole dihydrochloride
DEPC	Diethylpyrocarbonate
DKFZ	Deutsches Krebsforchungszentrum
DMEM	Dulbecco´s modified Eagle´s medium
DMSO	Dimethyl sulfoxide
DNA	Deoxyribonucleic acid
DNase	Deoxyribonuclease
dNTP	Deoxynocleosidetriphosphate
DOSPA	2,3-dioleyloxy-N-[2(spermine-carboxamido)ethyl]-N,N-dimethyl-1-propanaminiumtrifluoro-acetate
DTT	1,4-dithio-DL-threitol
E. coli	*Escherichia coli*
EDTA	Ethylenediaminetetraacetic acid
EGF	Epidermal growth factor
EtBr	Ethidium bromide
EtOH	Ethanol
EV	*Epidermodysplasia verruciformis*
FACS	Fluorescence-activated cell sorting
FCS	Fetal calf serum
Fig	Figure

G	Guanine
G-418	Geneticin
GC-MS	Gas chromatography-mass spectrometry
x g	Centrifugal force
h	Hour(s)
HDAC	Histone deacetylase
HKGS	Human keratinocyte Growth Supplement
HIV	Human immunodeficiency virus
HNSCC	Head and neck squamous cell carcinoma
HPV	Human papillomavirus
HSCG	Heparin sulphate glycosaminoglycan
IHC	Immunohistochemistry
kb	Kilobase(s)
LB	Luria Bertani
MCS	Multiple cloning site
mg	Milligram
ml	Mililiter
µg	Microgram
µl	Microliter
min	Minute (s)
mRNA	Messenger ribonucleic acid
rRNA	Ribosomal ribonucleic acid
NaF	Sodium fluoride
NPT	Neomycin phosphotransferase
NMSC	Non melanoma skin cancer
4-NQO	4-Nitroquinoline-1-oxide
OD	Optic density
o/n	Overnight
ORF	Open reading frame
ori	Origin of replication
PAGE	Polyacrilamide gel electrophoresis
PBS	Phosphate buffered saline
PCR	Polymerase chain reaction
PD	Population doubling

PFA	Paraformaldehyde
pH	Potencial of hydrogen
PV	Papillomavirus
RIPA	Radioimmunoprecipitation assay buffer
RNA	Ribonucleic acid
RNase	Ribonuclease
rpm	Revolutions per minute
RPMI	Roswell Park Memorial Institute medium
RT	Room temperature
RT-PCR	Reverse transcriptase- polymerase chain reaction
SCC	Squamous cell carcinoma
SDS	Sodium dodecyl sulfate
Smad	Signalling mother against decapentaplegic peptide
SR101	Sulforhodamide 101
T	Thymidine
TBS	Tris-buffered saline
TBS-T	Tris-buffered saline-Tween 20
TEMED	N,N,N',N'-Tetramethylethylenediamine
Tm	Melting temperature
TGF-ß	Transforming growth factor-ß
Tris	Trishydroxymethylaminomethane
URR	Upstream regulatory region
UV	Ultraviolet
VLP	Virus like particles
Vol	Volume
v/v	Volume/volume
w/v	Weight/volume

Summary

Human papillomaviruses (HPV) infect mucosal and cutaneous tissue. They induce several epithelial lesions ranging from benign warts to cancer. HPV infection has been demonstrated to play a role in the pathogenesis of cervical, vulvar, penile, anal, skin, head and neck cancers. HPV infection is associated with benign and malignant lesions in the hereditary skin disease *Epidermodysplasia verruciformis* (EV), characterized by cutaneous lesions that progress to squamous cell carcinoma after UV exposure.

Head and neck tumor (HNSCC) patients have been classified into two epidemiological entities, corresponding to either alcohol/tobacco use or HPV infection. High risk mucosal HPV is involved in the pathogenesis of a subset of HNSCC, particularly those that arise from the lingual and palatine tonsils within the oropharynx. Although low risk HPV have been found in several cancers, their gene products do not induce immortalization *per se*, and they probably need other co-factors to modify cellular genes and contribute to tumorigenesis. Cutaneous HPV20 has been found in a number of non melanoma skin cancers as well as in esophageal carcinoma and in HNSCC patients. HPV20 infection combined with UV exposure promotes malignant progression in skin as demonstrated in HPV20 E6/E7 transgenic mice in the presence of chronic UV irradiation. These animals presented papilloma formation that lead to transformation. However, involvement of HPV20 in esophageal cancer and HNSCC have to date not been elucidated.

In this study, the cooperation between HPV20 infection and a chemical carcinogen in the pathogenesis of oropharynx and esophageal cancer was investigated. The synthetic carcinogen 4-NQO is a UV-mimetic that shares the same mechanistic action with the carcinogenic compounds present in tobacco. In order to examine its involvement (comparable with the effect of tobacco) in increasing the viral oncogenic potential, 4-NQO was applied either to cells or organotypic cultures and combined with HPV20 by following two approaches:

Promoter activation assays demonstrated that HPV20 E6 and/or E7 up-regulated its own viral promoter and this effect was further enhanced by 4-NQO treatment. These changes in the viral promoter activity may indicate a positive cooperation between the virus and the chemical in the onset of disease.

Secondly, alterations in proliferation, differentiation, apoptosis and skin barrier functionality were studied in organotypic cultures expressing HPV20 E6 and treated with 4-NQO. Although these cultures were able to stratify and differentiate they failed to form a

normal epidermis. Moreover, the normal differentiation markers pattern was disturbed, resembling simpler epithelia and this phenotype was enhanced after 4-NQO treatment. Cellular protein p53 accumulated whereas $p21^{CIP1}$ and ΔNp63α modifed their expression pattern in the epithelia.

Organotypic raft cultures expressing HPV20 E6 gene presented foamy-like keratinocytes resembling the typical structures found in *Epidermodysplasia verruciformis* patients and pityriasis versicolor -like lesions infected with HPV20. In addition, HPV20 E6 expression was capable of altering the functionality of the skin barrier function by abrogation of tight junction formation in the stratum granulosum and by changes in the lipid metabolism of the skin leading to its accumulation and deregulated composition. Disruption of the skin barrier has been observed in a number of cutaneous diseases as ichthyosis, atopic dermatitis and other eczemas.

These studies provide insight into the functionality of HPV20 E6 in the epidermis. Moreover, the up-regulation in viral promoter activity and alterations in differentiation pattern under the context of HPV20 E6 expression and 4-NQO treatment compared with pLXSN and HPV16 E6/E7 controls showed the cooperation between HPV20 and chemical carcinogens. However, epithelial transformation was not observed and longer 4-NQO treatment would be necessary to analyze its influence in malignancy. Taken together, the conclusions obtained in the present work will be helpful in future experiments to elucidate the role of HPV20 infection and chemical carcinogens in the pathogenesis of esophageal and oropharyngeal tumors.

Zusammenfassung

Humane Papillomaviren (HPV) infizieren das Plattenepithel der Haut und der Schleimhäute. Die daraus folgenden Läsionen des Epithels sind Ursache für die Bildung von gutartigen Warzen bis hin zu Tumoren. HPV-Infektion spielt nachgewiesenermaßen eine Rolle in der Pathogenese von Gebärmutterhals-, Vulva-, Penis-, Anal-, Haut-, Kopf- und Halstumoren. HPV-Infektionen stehen im Zusammenhang mit gut - und bösartigen Hautveränderungen bei der Erberkrankung der Haut Hauterkrankung *Epidermodysplasia verruciformis* (EV). Diese ist charakterisiert durch Hautläsionen, die sich nach UV – Bestrahlung zum Plattenepithelkarzinom weiterentwickeln.

Patienten mit Kopf- und Hals-Tumoren (HNSCC) wurden in zwei epidemiologische Einheiten unterteilt. Die eine bestand aus Patienten mit gesundheitlichen Schäden nach Alkohol- bzw. Tabakverbrauch, die andere aus Patienten mit HPV-Infektion. Infektionen mit „High-risk“ HPV der Schleimhäute hängen mit der Pathogenese bei einem Teil der HNSCC zusammen, insbesondere derjenigen, die aus der Tonsilla lingualis und Tonsilla palatina innerhalb des Oropharynx hervorgehen. Obwohl die „low-risk“ HPV Typen in mehrere Krebsarten vorhanden sind, verursachen ihre Genprodukte per se keine Immortalization. Womöglich benötigen sie weitere Faktoren um zelluläre Gene zu verändern und somit die Tumorentstehung zu verursachen. Der Kutaner HPV20 Typ wurde in einer Reihe von Nicht-melanomatösen Hautkrebs- (NMSC), sowie in Ösophagus-Karzinom- und in HNSCC-Patienten nachgewiesen. Eine HPV20-Infektion in Kombination mit UV-Bestrahlung führt zu malignen Hautveränderungen. Dies wurde in HPV20 E6/E7 transgenen Mäusen, die chronischer UV-Bestrahlung ausgesetzt waren, nachgewiesen. Diese Tiere zeigten ein höheres Proliferationsverhalten und eine Tendenz zur malignen Entartung durch eine größere Anzahl an Papillomen. Die Rolle der HPV20 bei Ösophagus-Karzinom und HNSCC ist bisher nicht geklärt.

In der vorliegenden Studie wurde die Wechselwirkung zwischen einer HPV20-Infektion und einem chemischen Karzinogen in der Pathogenese des Oropharynx- und Ösophagus-Karzinoms untersucht. Das synthetische Karzinogen 4-NQO ist ein UV-Mimetikum, dass die gleichen Pathomechanismen hat wie die karzinogenen Tabakbestandteile. Um den Einfluss auf das virale-onkogene Potenzials zu untersuchen, wurde 4-NQO (ähnlich wie der Tabak) an Zellen bzw. organotypische Kulturen zugesetzt und mit HPV20 infiziert. Folgende zwei Forschungsansätze lagen zugrunde:

Promotor activation assays zeigten, dass HPV20 E6 und / oder E7 seinen eigenen Virus-Promotor hochregulierte und dass dieser Effekt durch die 4-NQO-Behandlung noch zusätzlich verstärkt wurde. Die genannten Veränderungen in der Aktivität des viralen Promotors könnten auf eine positive Wechselwirkung zwischen dem Virus und der Chemikalie hindeuten, und dadurch eine Rolle in der Pathogenese von Krankheiten spielen.

Die Änderungen in der Proliferation, Differenzierung, Apoptose und der Hautbarrierefunktion wurden in organotypischen Kulturen untersucht, wobei die HPV20 E6-Expression betrachtet und mit 4-NQO behandelt wurde. Diese Kulturen konnten Zellschichten bilden und eine Differenzierung konnte zwar stattfinden, doch war die Bildung einer normalen Epidermis nicht möglich. Der normale Differenzierungsmarker war beeinträchtigt und ähnelte einem einfachen Epithel, wobei dieser Phänotyp nach der 4-NQO-Behandlung verstärkt wurde. Es wurde eine Anhäufung des Zellproteins p53 beobachtet, während $p21^{CIP1}$ und ΔNp63α ihre Epithel-Expressionsmuster veränderten.

Organotypische Kulturen, die das HPV20 E6 Gen beinhalteten, bildeten schaumig aussehende Keratinozyten. Diese stellen die typischen Strukturen dar, die in *Epidermodysplasia verruciformis* Patienten und Pityriasis versicolor-aussehenden, HPV 20 infizierten, Läsionen gefunden wurden. Darüber hinaus konnte eine Veränderung der Hautbarrierefunktion durch die HPV20 E6 Expression gezeigt werden. Dies geschah durch eine Unterbrechung der Tight Junctions Bildung im Stratum granulosum und einen Einfluss des Stoffwechsels der Hautlipide, was zu ihrer Anhäufung und unregelmäßigen Zusammensetzung führte. Hautbarrierestörungen wurden bei zahlreichen Hauterkrankungen beobachtet, darunter Ichthyosis, atopische Dermatitis und anderen Ekzemen.

Diese Studien zeigen die Wirkung und Funktion des HPV20 E6 auf die Epidermis. Ferner zeigten die Aktivierung des viralen Promotors und die Änderungen des Differenzierungsmarkers im Rahmen der Expression von HPV20 E6 und der 4-NQO-Behandlung im Vergleich zu den pLXSN- und HPV16-E6/E7-Kontrollen die Wechselwirkungen zwischen HPV20 und den chemischen Karzinogenen. Eine Transformation des Epithels wurde jedoch nicht erreicht. Für die Analyse ihrer Wirkung auf eine maligne Entartung ist eine längere 4-NQO-Behandlung vonnöten.

Die oben erläuterten Beobachtungen können als Grundlage für weiterführende Untersuchungen und Experimente über die Rolle der HPV20-Infektion und der chemischen Karzinogene in der Pathogenese der Ösophagus- und Oropharynx-Tumore dienen.

1 Introduction

1.1 Papillomaviruses

1.1.1 General aspects

Papillomaviruses (PV) belong to the viral family *Papillomaviridae*. They comprise a heterogeneous group with high specificity in host and cell type (Lancaster and Olson, 1982). They infect skin and mucosal epithelia and give rise to different epithelial lesions, ranging from benign hyperplasia (e.g. warts or papillomas) to cancer.

To date, 113 human papillomaviruses (HPV) types have been characterized and more than 300 putative new PV have been identified by PCR amplification (de Villiers *et al.*, 2004). PV infect different hosts: humans, primates, ungulates, rodents, birds, cetaceans and reptiles. They are species specific and therefore, named depending on the species they infect. PV are classified based on their L1 open reading frame (ORF) sequence homology (**Fig. 1**). PV species share between 50-60% nucleotide identity of the ORF L1 within a genus. A PV is defined as new a type if its L1 ORF sequence differs more than 10% to the closest known PV. Subspecies share 2-10% of L1 ORF homology and variants, 2% (de Villiers *et al.*, 2004).

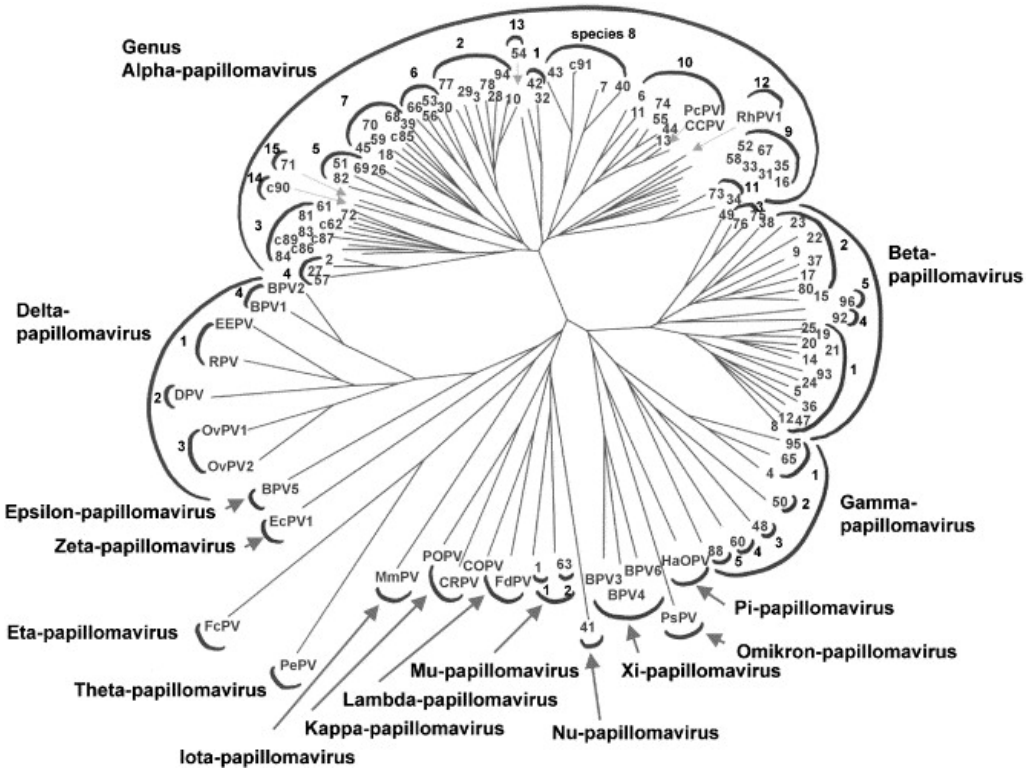

Figure 1. Phylogenetic tree of the *Papillomaviridae* family (de Villiers *et al.*, 2004).

1.1.2 HPV types

HPV play a role in the pathogenesis of several cancers such as cervical, vulvar, penile, anal, skin, esophageal and oropharyngeal cancers. HPV infection is also associated with skin warts (common plantar and flat warts) as well as genital warts. Moreover, infection with HPV6 and 11 is related with recurrent laryngeal papillomatosis. HPV are historically classified in cutaneous and genital/mucosal types depending on the epithelia they infect.

1.1.2.1 Mucosal types

Genital/mucosal PV, mainly grouped within the genus Alpha papillomaviruses, infect the anogenital area, the upper respiratory tract and the head and neck regions. They are classified as high risk (16, 18, 31, 33, 35, 39, 45, 51, 52, 56, 58, 59, 73, and 82) or low risk (6, 11, 40, 42, 43, 44, 54, 61, 70, and 72) types, based on their association with malignant, pre-malignant or benign lesions (Munoz *et al.*, 2003; zur Hausen, 1990).

High risk HPV types are associated with 90% of the cervical cancers, HPV16 and 18 being the most common HPV types found in 70% of the cases. They are also implicated in anal, penile, and head and neck pre-malignant and malignant tumors. HPV16 is the most common HPV type associated with a malignant phenotype regardless of organ origin (Sanclemente and Gill, 2002).

Low risk HPV types are associated with over 90% of HPV-related benign lesions. Laryngeal papillomatosis is a rare disease occurring both in infants and adults caused by low risk HPV6 and 11 (Aaltonen *et al.*, 2002), which also cause genital warts. A few types classified in the genus Alpha papillomaviruses are most commonly associated with cutaneous warts (reviewed in zur Hausen, 1996). HPV2, 27 and 57 have however been described causing benign anogenital lesions in children (de Villiers, 1995; Handley *et al.*, 1997) (reviewed in Cason and Mant, 2005).

1.1.2.2 Cutaneous types

Cutaneous papillomaviruses infect skin epithelia, causing warts with varying clinical entities depending on the HPV type (de Villiers, 1998). HPV have been implicated in the pathogenesis of non-melanoma skin cancer (NMSC), although recent epidemiological data failed to provide convincing evidence. A number of HPV types classified in the genus Beta papillomaviruses are being associated mainly with squamous cell carcinomas (SCC) of the

skin, but it has not been possible to attribute any individual HPV type to its pathogenesis (Asgari *et al.*, 2008; Forslund *et al.*, 2007).

Epidermodysplasia verruciformis (EV) is a rare recessive autosomal hereditary disease that manifests early in childhood. EV is characterized by generalized wart development, with multiple papillomatous lesions, disseminated wart-like and pytiriasis versicolor-like lesions, with infection of a broad spectrum of genus Beta papillomaviruses (reviewed in de Villiers *et al.*, 2004 and in Jablonska and Majewski, 1994). EV patients carry mutations in two genes in chromosomes 2 and 17 that cause defects in cellular innate immunity (Ramoz *et al.*, 2002).

1.1.3 HPV20

HPV20 belongs to the cutaneous genus Beta papillomavirus and is associated with benign and malignant lesions in the skin disease EV (reviewed in Jablonska and Majewski, 1994; Watzig and Jablonska, 1987). It has been detected in a number of NMSC either by DNA detection in biopsies (Astori *et al.*, 1998; de Villiers, 1998) or seroreactivity to HPV20 L1 (Feltkamp *et al.*, 2003) as well as in esophageal carcinoma patients (de Villiers *et al.* 1999) and in patients with head and neck cancer (Lavergne and de Villiers, 1999).

Previous studies in our group demonstrated that chronic exposure of HPV20- and HPV27 E6/E7 transgenic mice to ultraviolet (UV) irradiation resulted in the formation of papillomas and malignant lesions of the skin (Michel *et al.*, 2006). Moreover, using *in vitro* conditions with ectopically expressed proteins, the wtp53-mediated degradation of HPV20 E6 by caspase 3 was described, in contrast to the protective effect exerted by UV-induced mutant p53R248W and ΔNp63α (Fei and de Villiers, 2008).

1.1.4 HPV genomic organization

Viral genome consists of a small, double-stranded circular DNA molecule. It varies in size among HPV types but typically contains around 8000 bp and codes for eight open reading frames (ORF). The genome is organized in three different regions (**Fig. 2**): the long control region (LCR) (also commonly named the upstream regulatory region, URR) and the early (E) and late (L) coding regions. Proteins are expressed from polycistronic mRNAs transcribed from a single DNA strand (**Fig. 3**). E6 and E7 are oncogenes able to induce immortalization in high risk HPV types (Munger *et al.*, 1992). E1 and E2 are regulatory proteins involved in viral transcription and replication (Chiang *et al.*, 1992). E4 regulates viral

replication and induces viral DNA synthesis in suprabasal epithelial layers (Nakahara *et al.*, 2005). E5 is only present in genital HPV types, where enhances E6 and E7 oncogenic effect during early stages of infection (DiMaio and Mattoon, 2001). Late proteins L1 and L2 form the viral capsid (Munger and Howley, 2002).

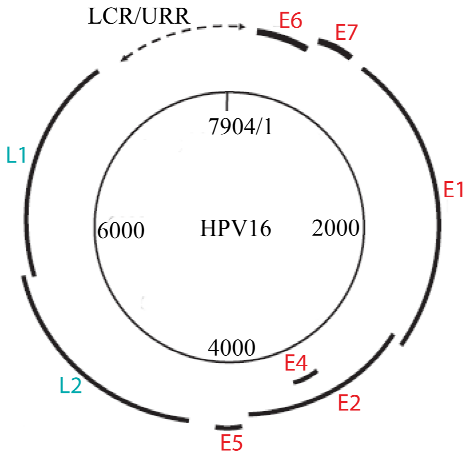

Figure 2. Circular genome representation of HPV16 (adapted from Narisawa-Saito and Kiyono, 2007).

In high risk HPV, transcripts are initiated at two major viral promoters which position varies for each type. The early promoter is located upstream of the E6 ORF. It controls the expression of early viral proteins, and is activated in parabasal epidermal layers prior to replication. In HPV16 and 31 this promoter is referred to as p97 (Smotkin and Wettstein, 1986), while in HPV 18 is named p105 (Butz and Hoppe-Seyler, 1993). The late promoter located within the E7 ORF is activated when the productive replication starts and regulates late protein expression, and is referred to as p670 in HPV16 (Grassmann *et al.*, 1996) and p742 in HPV18 and 31 (Frattini *et al.*, 1997). The location of viral promoters has not been extensively studied in cutaneous HPV types. Recently, putative early promoters for different Beta-papillomaviruses have been identified: p92 in HPV38, p45 in HPV92, p7439 in HPV93 and p256 in HPV96 (Vasiljevic *et al.*, 2008).

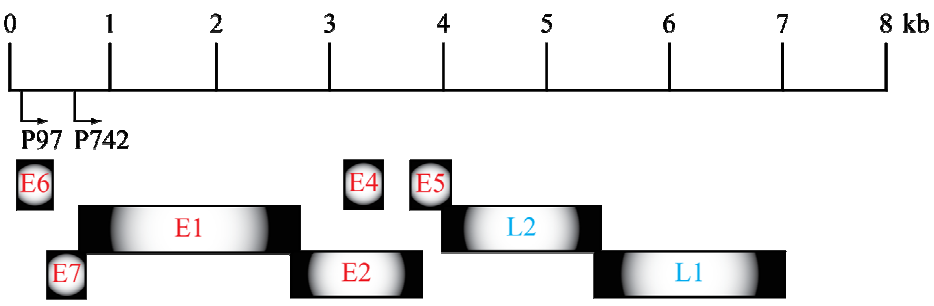

Figure 3. Gene organization in HPV31 (adapted from Longworth and Laimins, 2004).

1.1.4.1 Early proteins

The early region encodes predominantly for proteins that are important in viral DNA replication, which occurs "early" in the viral life cycle. Six different ORFs have been described as E1, E2, E4, E5, E6 and E7. Additionally, E3 and E8 ORFs have been found in BPV 4 (bovine papillomavirus 4): E3 corresponds to a small putative gene of unknown function (Patel *et al.*, 1987) whereas E8 may substitute the E6 gene, absent in BPV4 (Jackson *et al.*, 1991).

E1

E1 is a DNA helicase/ATPase involved in initiating viral DNA replication (Hughes and Romanos, 1993). E1 binds weakly to AT-rich sequences near the origin of replication, controlling the episomal DNA replication (Frattini and Laimins, 1994). When E1 binds to E2 protein, it forms a stable complex, enhancing the protein-DNA interaction. E1 also acts during replication by binding to DNA polymerase, recruiting cellular replication complexes and interacting with cyclins A and E (reviewed in Longworth and Laimins, 2004).

E2

E2 protein facilitates DNA replication (Ustav *et al.*, 1993) and regulates viral transcription through site-specific binding to the early promoter (Frattini and Laimins, 1994). This protein increases viral DNA replication by recruiting the E1 protein to its binding site. When E2 is present at low concentrations, it binds to its recognition sequence and activates the early promoter. At high concentrations, E2 represses the early promoter activity by blocking the binding of cellular transcription factors (Steger and Corbach, 1997). Since the E1 and E2 proteins are expressed from the early promoter, E2 effect on the promoter activity contributes to the control of viral copy number in undifferentiated cells.

Unlike the early promoter, the late promoter is not negatively regulated by E2 protein. Thus, at late stages of viral life cycle E2 contributes to the amplification of viral DNA (Steger and Corbach, 1997).

E4

The E4 ORF is the most highly expressed HPV protein. E4 is translated together with the first 5 amino acids of E1 by formation of a spliced E1^E4 messenger RNA in productively infected keratinocytes (Doorbar *et al.*, 1989). E4 expression is controlled by the HPV late promoter, activated in the differentiating cell layers of the epithelia. Thus, E4 is expressed at

late stages of the virus life cycle, during the viral genome amplification (Middleton *et al.*, 2003).

Genital and cutaneous HPV E4 forms cytoplasmic networks that colocalize with keratin intermediate filaments in the cell. However, only high risk genital types induce collapse of the keratin skeleton facilitating the release of viral particles (Roberts *et al.*, 1993). In addition, HPV11 and HPV16 E4 induce G2 arrest (reviewed in Longworth and Laimins, 2004).

E5

The E5 protein is a strongly hydrophobic protein localized in the Golgi apparatus, endoplasmic reticulum, nuclear membrane and occasionally in cellular membranes of the host cell (Conrad *et al.*, 1993). Genital HPV types encode an E5 protein, whereas cutaneous types lack an E5 gene or a translation start codon (Schiffman *et al.*, 2005). E5 is expressed in the early phase of infection. During malignant progression the HPV genome frequently integrates into the host genome, disrupting the E5 gene (DiMaio and Mattoon, 2001). E5 activates the epidermal growth factor (EGF) receptor, influencing cellular proliferation (Crusius *et al.*, 1998). HPV16 E5 has weak transforming activity *in vitro*; nevertheless, epidemiological and experimental evidences suggest that E5 activity enhances subsequent malignant progression *in vivo* (reviewed in Tsai and Chen, 2003). Targeted expression of HPV16 E5 in basal epithelial cells of transgenic mice induces skin tumors at a high frequency (Genther-Williams *et al.*, 2005). In addition, estrogen-treated transgenic mice expressing HPV16 E5, E6 and E7 develop a higher number of cervical cancers than transgenic mice that express HPV16 E6 and E7 but not E5 (Riley *et al.*, 2003).

Recently it has been demonstrated that E5 and E6 from both low and high risk HPV types cooperate in inducing koilocytosis in cell culture. Formation of koilocytes is inhibited after deletion of 20 amino acids in the carboxiterminal side of E5 protein, also in the presence of E6 protein, showing the key role of E5 in the formation of such structures (Krawczyk *et al.*, 2008).

E6

The E6 protein is composed of approximately 150 amino acids and contains two zinc-binding domains with the motif Cys-X-X-Cys.

In vitro experiments demonstrated that HPV16 E6 is able to transform rodent cells, and primary human mammary epithelial cells (Liu *et al.*, 1999), while cooperates with E7

protein in inducing immortalization in primary human foreskin keratinocytes (Kiyono *et al.*, 1998).

In mucosal high risk HPV types, E6 induces degradation of p53 tumor suppressor protein (**Fig. 4, 5**) by forming a trimeric complex together with the cellular ubiquitin ligase, E6-associated protein (E6AP) (Werness *et al.*, 1990), resulting in inhibition of apoptotic signals (Munger *et al.*, 1992; Scheffner *et al.*, 1990). p53 regulates G1/S and G2/M cell cycle checkpoints. When p53 is degraded, the cell accumulates chromosomal aberrations and centrosomal abnormalities, contributing to malignant progression.

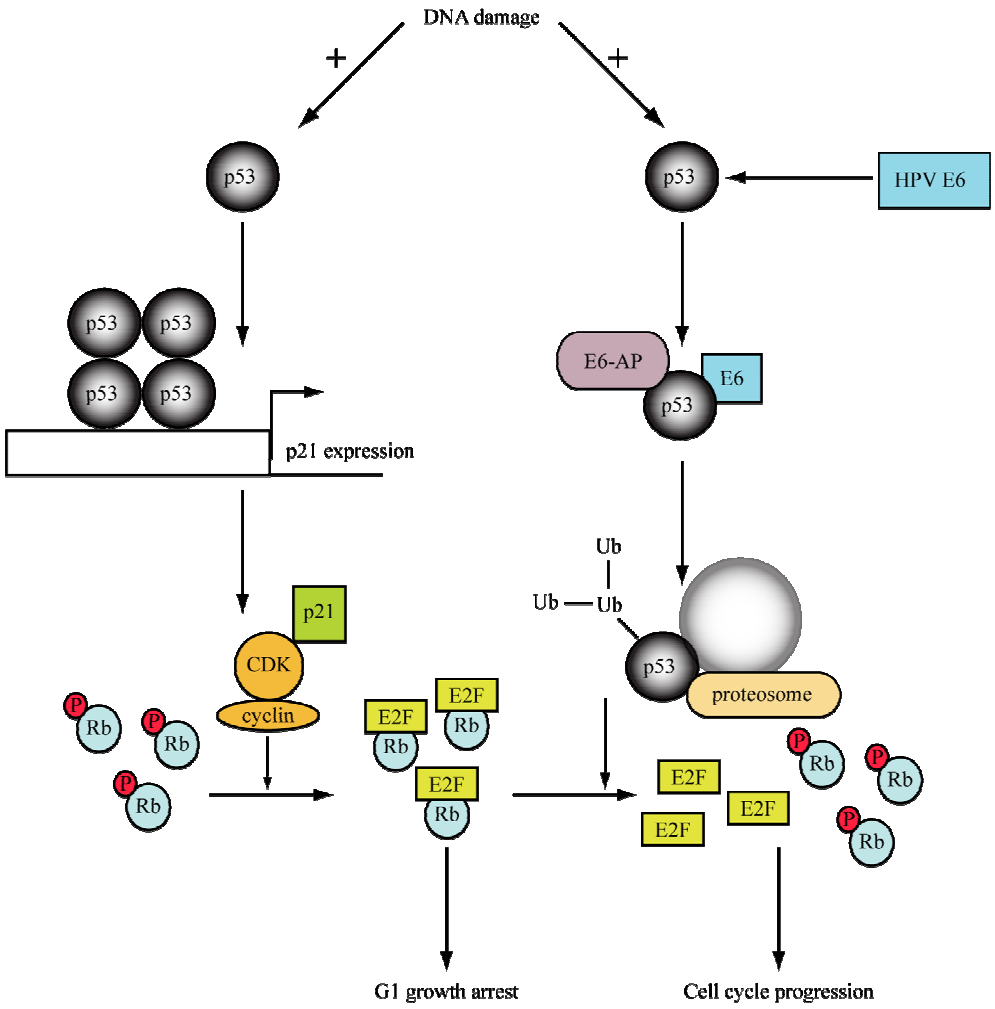

Figure 4. E6-mediated p53 degradation and its effect in cell cycle (adapted from Sterling and Tyring, 2001).

E6 promotes telomerase activity by interacting with hTERT (Kiyono *et al.*, 1998; Klingelhutz *et al.*, 1996). This telomerase activity is a common feature observed in normal proliferating cells and in tumors, which allows an increase in the number of divisions that a cell can undergo.

High risk E6 gene can be also transcribed as E6* by alternative splicing (Pim *et al.*, 1994). This protein interacts with both E6 and E6AP and inhibits E6-mediated p53 degradation (Pim *et al.*, 1997).

PDZ domain (acronym for **P**ost synaptic density protein, PSD95, **D**rosophila disc large tumor suppressor, DlgA, and **Z**onula occludens-1, zo-1) is a structural protein domain present in signalling proteins of bacteria, yeast, plants and animals (Ponting, 1997). E6 presents a PDZ binding motif in the C-terminal of the protein. It interacts with PDZ-containing proteins (i.e. hDlg, MAGI or MUPP1) and targets them for degradation. This activity has only been found in mucosal HPV types and it is believed to play an important role in degradation of tumor suppressor proteins that contain PDZ domains (Lee and Laimins, 2004).

Cutaneous HPV E6 does not induce proteosome-mediated degradation of p53 or PDZ-domain proteins (Elbel *et al.*, 1997; Fei and de Villiers, 2008; Jackson *et al.*, 2000; Pim *et al.*, 2002). However, they indirectly repress p53 function in both mucosal and cutaneous HPV by binding and consequently inhibiting p300/CBP (Hebner *et al.*, 2007; Thomas and Chiang, 2005), which activates p53 by acetylation (Lechner and Laimins, 1994).

High risk E6 also binds and inactivates pro-apoptotic partners like Bak (Thomas and Banks, 1999) and Bax (Li and Dou, 2000) by targeting them for ubiquitin-proteosome degradation. Several cutaneous HPV E6 proteins inhibit UV-induced apoptosis by targeting pro-apoptotic Bak protein for degradation (Jackson *et al.*, 2000; Underbrink *et al.*, 2008). HPV20 and HPV8 E6 inhibit apoptotic response after ultraviolet irradiation of medium wavelengh or B irradiation (UVB) in primary foreskin keratinocytes, contributing to the oncogenic potencial of UV radiation and enhancing transformation in sun-exposed skin sites (Struijk *et al.*, 2008).

Interestingly, recent results indicate that HPV8 and 38 E6 are able to interact with the host cell endogenous E6AP protein (Bedard *et al.*, 2008) and extend the lifespan of human keratinocytes by telomerase activation (Gabet *et al.*, 2008).

E7

E7 is a nuclear protein considered to have the major transforming properties during high risk HPV infection. It shares similar gene sequences and transformation properties with the adenovirus E1A and SV40 large T antigen (reviewed in Lee and Cho, 2002). HPV E7s have three conserved regions: CR1, CR2 and CR3. E7 gene deletion experiments demonstrated that the CR2 region is responsible for the release of E2F from pRb whereas the

CR3 region contains two finger-like motifs that allows the E7 binding to pRb, $p27^{KIP1}$, $p21^{CIP1}$ and p300/CBP (Liu *et al.*, 2006).

The tumor suppressor retinoblastoma protein (pRb) and related pocket proteins p107 and p130 are the main cellular targets for HPV E7 (Dyson *et al.*, 1989). pRb family is the main cell cycle repressor during epithelial differentiation. When unphosphorylated, pRb acts as transcription repressor by complexing to the transcriptional factors E2F/DP, involved in S phase progression and apoptosis (**Fig. 5**). When E7 binds to pRb, E2F is released, allowing the cell cycle progression and the constitutive activation of the repressed genes (Munger *et al.*, 2001). In addition, E7 targets pRb degradation by ubiquitin proteosome pathway (Berezutskaya *et al.*, 1997). Both low and high risk HPV E7s share the ability to bind to pRb and family members, although the affinity is much lower in the low risk types.

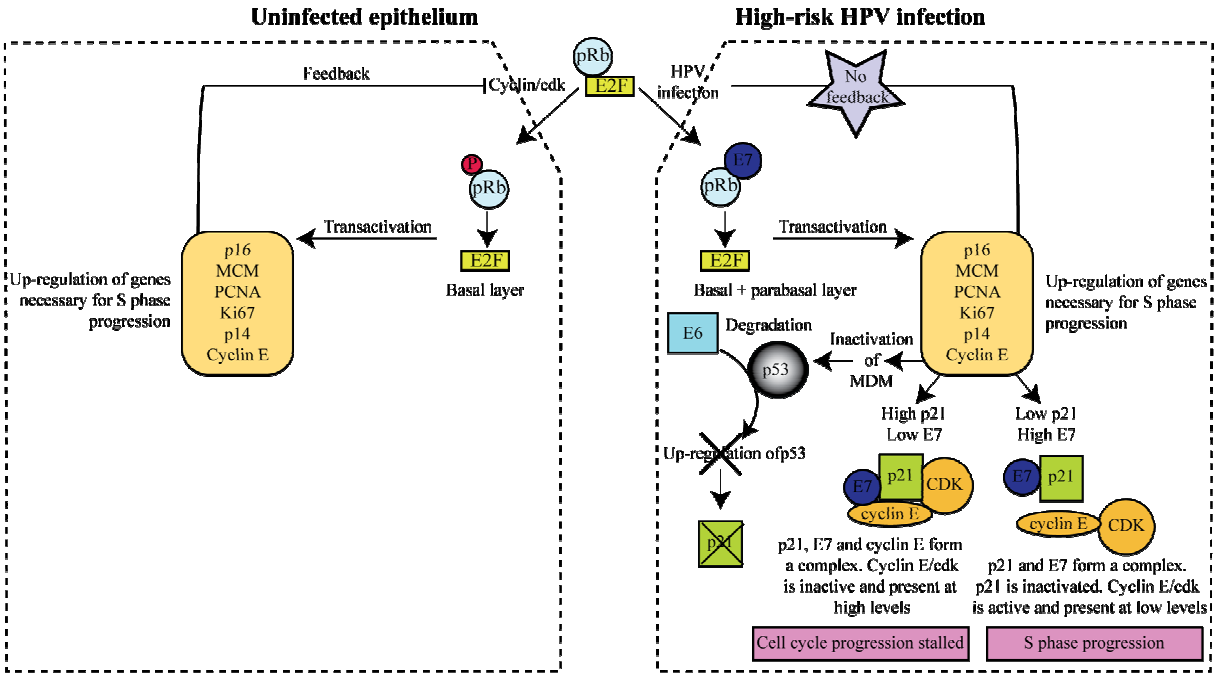

Figure 5. Role of high risk E6 and E7 in HPV infection (adapted from Doorbar, 2006).

Another activity of high risk E7 is interacting with histone deacetylases (HDACs), which helps in the repression effect of E2F. This inhibitory effect of E7 has been described to be crucial in the maintenance of the episomal viral genome (Hurford *et al.*, 1997) although the cellular mechanisms involved in the interaction between E7 and HDAC are not yet fully understood.

Cell cycle progression is controlled by cyclins, which form complexes with cyclin-dependent protein kinases (CDK) (reviewed in Besson *et al.*, 2008). E7 interferes with the activity of the CDK inhibitors $p21^{CIP1}$ and $p27^{KIP1}$ to override normal G1 checkpoint control

(Jones *et al.*, 1997; Zerfass-Thome *et al.*, 1996). It also contributes to cell cycle progression by activation of cyclins E and A (Arroyo *et al.*, 1993), which are involved in pRb inactivation by phosphorylation.

High risk HPV E7 expression leads to transformation of immortalized murine fibroblasts and to immortalization of primary human keratinocytes (Halbert *et al.*, 1991). Centrosomal aberrations have been described as an effect of high risk HPV E7 expression (Duensing *et al.*, 2000), inducing failures in chromosomal segregation, a normal feature in HPV-positive carcinomas.

Low risk genital and cutaneous HPV E7 weakly interact with pRb (Schmitt *et al.*, 1994) and are unable to transform rodent cells unless they are combined with activated H-ras expression (Yamashita *et al.*, 1993). However, single amino acid substitutions can increase the transforming properties of the low risk HPV6 E7 (Sang and Barbosa, 1992). It has been shown that low risk genital HPV1 E7 transforms a mouse fibroblast cell line (Schmitt *et al.*, 1994) and cutaneous HPV38 E7 inactivates pRb and deregulates cell cycle (Caldeira *et al.*, 2003). Moreover, cutaneous HPV5, 15, 17, 20 and 38 E6/E7 showed increased proliferation and aberrant differentiation when constitutively expressed in organotypic cultures of primary keratinocytes (Boxman *et al.*, 2001).

Smad peptides (Signalling Mother Against Decapentaplegic Peptide) are the molecules that control intracellular signalling of transforming growth factor-ß (TGF-ß). Interestingly, both high risk and low risk HPV E7 are able to inhibit the anti-proliferative effect of the TGF-ß by binding to Smad. In this way, E7 from different HPVs preserves keratinocyte proliferation, necessary for the productive viral life cycle (Habig *et al.*, 2006).

1.1.4.2 Late proteins

The late genes L1 and L2 encode for viral structural proteins necessary for the viral capsid production.

L1

The L1 ORF is the highest conserved region in all HPV types and codes for the major capsid protein, which is only expressed in terminally differentiated cells of the epithelia. L1 is the major structural component of HPV and it spontaneously self-assembles in pentamers, known as capsomeres. One virion capsid contains 360 L1 proteins organized in 72 capsomeres (Baker *et al.*, 1991; Modis *et al.*, 2002).

The distinct tissue tropism of genital and cutaneous HPV types might be explained by the positive viral surface charge of L1 in genital types and negative charge of the cutaneous types, as recently demonstrated (Mistry *et al.*, 2008).

L2

The L2 ORF encodes for the minor capsid protein and it is present as a single copy in the centre of the pentavalent capsomeres at the virion vertices (Buck *et al.*, 2008; Modis *et al.*, 2002; Trus *et al.*, 1997). Virus like particles (VLP) can assemble *in vitro* in the absence of L2. However, when L2 is present packaging occurs more efficiently (Stauffer *et al.*, 1998) and the viral infectivity is increased (Roden *et al.*, 2001). Additionally, L2 participates in the disruption of endosomal membranes and the subcellular trafficking of the incoming viral genome (Kamper *et al.*, 2006).

1.1.4.3 Upstream regulatory region

The upstream regulatory region (URR) is located between the L1 and E6 genes of HPV genome. The URR contains the promoters responsible for early genes expression and sequences involved in transcription and replication. A number of binding sites for transcription factors present in the URR are found among all HPV types, as TFIID, Sp-1 and AP-1 (del Mar Pena and Laimins, 2001), NF-1 (Butz and Hoppe-Seyler, 1993), TEF-1 and TEF-2 (Ishiji *et al.*, 1992), AP-2 (Kyo *et al.*, 1997), Oct-1 (O'Connor and Bernard, 1995), Stat-1 (Chang and Laimins, 2000), YY1 and glucocorticoid responsive elements (Gloss *et al.*, 1987).

1.1.5 HPV life cycle

HPV life cycle is linked to the differentiation state of the infected host cell, the keratinocyte. The infection begins when virus particles gain access to proliferative basal cells of the epithelium (**Fig. 6**). The virus reaches epidermal basal cell layer through microlesions. However, the access is naturally occurring in the bulb of the hair follicle and in the transformation zones of the cervix and the anus where columnar and stratified epithelia meet each other (reviewed in Doorbar, 2005 and in Longworth and Laimins, 2004).

The virus initially attaches to the cell surface via Heparin Sulphate Glycosaminoglycans (HSCG) (Giroglou *et al.*, 2001; Joyce *et al.*, 1999). Blocking of HSCG

in the cell surface by heparin sulphates inhibitors like DSTP27 is sufficient for avoiding HPV infection (Selinka *et al.*, 2007).

E1 and E2 proteins are expressed in undifferentiated basal layer cells and first suprabasal layers of the epidermis, where HPV genome is episomally maintained at low copy number (between 20 to 100 extrachromosomal copies per cell). E2 protein anchors the viral circular genome to mitotic chromosomes, ensuring segregation to daughter cells and regulates the early viral promoter (Frattini and Laimins, 1994).

As an infected cell leaves the basal layer, the HPV E7 expression leads to induction of unscheduled re-entry into S-phase of the cell cycle (Cheng *et al.*, 1995). In the upper suprabasal layers, induction of E1, E2, E4 and E5 genes expression necessary for replication is controlled by the late differentiation-specific promoter located in the E7 ORF.

In the stratum granulosum, the capsid proteins L1 and L2 are expressed under the control of the late promoter and are spontaneously assembled into icosahedral capsids. Once the viral assembly occurs, mature viruses are released from the cornified layer of the epithelium, facilitated by the cytokeratin skeleton rearrangements induced by high levels of E4 protein.

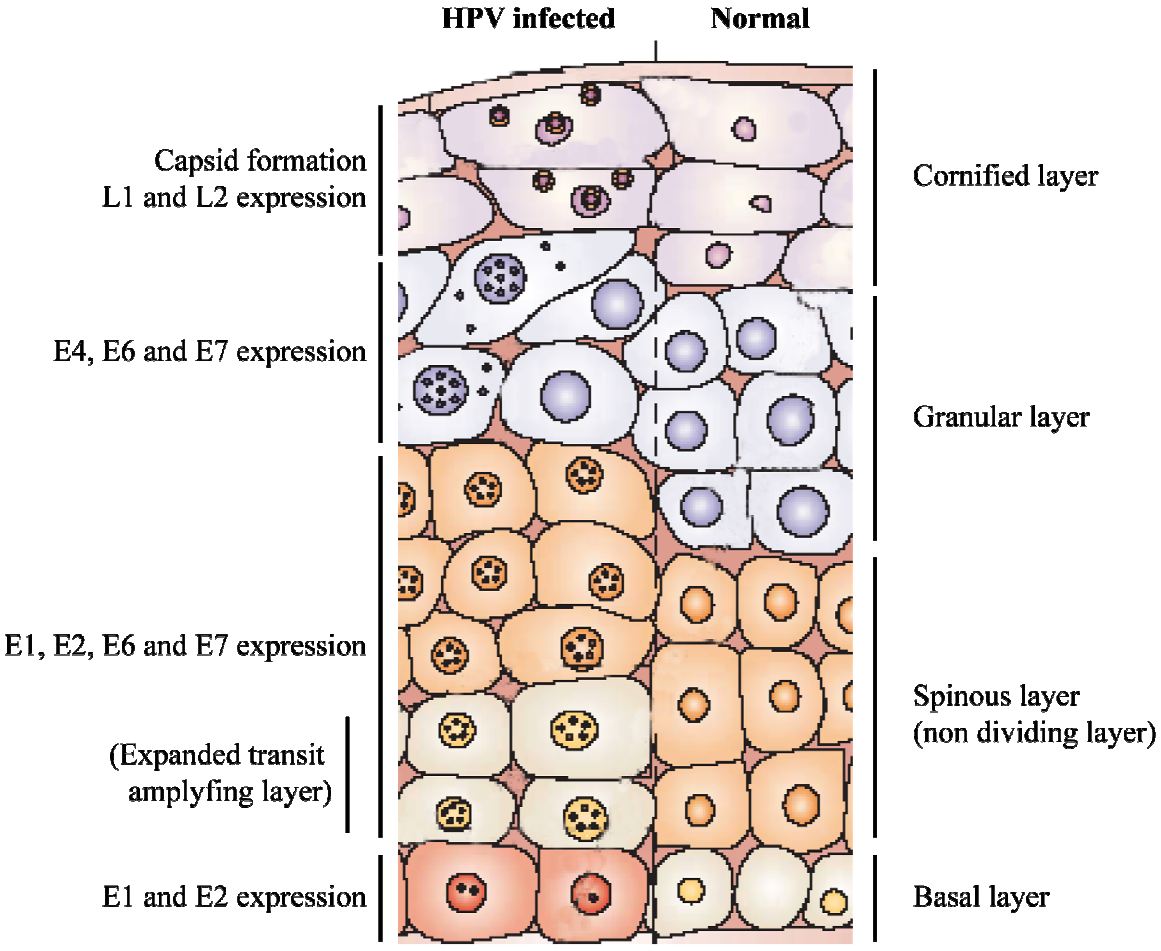

Figure 6. Normal versus HPV infected epithelia. HPV life cycle (adapted from Frazer, 2004).

In low-grade lesions, the high risk HPV is presented in episomal copies in the host cell whereas during progression to high grade lesions or carcinomas the genome is often integrated into the host cell genome (reviewed in Pett and Coleman, 2007; Schwarz *et al.*, 1985). The integration usually occurs in the E2 ORF, disrupting the gene and releasing the repressing effect of E2 protein on E6 and E7 expression, leading to higher levels of these transforming proteins (Chan *et al.*, 2007; Dowhanick *et al.*, 1995).

1.1.6 HPV and cancer

HPV infection causes 5.2% of all cancers worldwide (Parkin and Bray, 2006). HPV is associated with cancer of the genital tract, skin and the head and neck region. The distribution of HPV positive cases is shown in **table 1**.

Anatomical distribution	HPV positivity
Cervix	100%
Anus	90%
Penis	40-50%
Vulva, vagina	40%
Oropharynx	14%
Oral cavity	4%

Table 1. Percentage of HPV-positive tumors (Parkin and Bray, 2006).

1.1.6.1 Cervical cancer

Cervical cancer is the second most common cancer in women worldwide with approximately 493,000 new cases and 274,000 deaths per year (Parkin and Bray, 2006).

Most of cervical cancer corresponds to SCC, whereas adenocarinomas are less common. Developing countries have the highest incidence in cervical cancer (83%) (Parkin *et al.*, 2005), while the incidence in industrialized countries has decreased during the past decades, due to a highly effective screening program (Koong *et al.*, 2006; Peto *et al.*, 2004).

HPV infection is linked to cervical carcinoma (zur Hausen *et al.*, 1974) and it is known to be an essential factor in cervical and anogenital carcinogenesis (Walboomers *et al.*, 1999; zur Hausen, 1996; reviewed in zur Hausen, 2002).

HPV16 together with HPV18 infections accounts for approximately 70% of cervical cancers (IARC, 2005); other types demonstrated in cervical cancer are HPV31, 33, 35, 39, 45, 51, 52, 56, 58, 59 and 66 (Clifford *et al.*, 2003; IARC, 2005). Significant co-factors in HPV-associated cancer include co-infection with *Chlamydia* or human immunodeficiency virus (HIV), smoking and parity (> 3 children). The role of hormonal contraceptives and nutrients is presently unclear (IARC, 2005).

1.1.6.2 Head and neck cancer

Head and neck squamous cell carcinoma (HNSCC) refers to mucosal malignancies arising from the lips, oral cavity, oropharynx, nasopharynx, hypopharynx, larynx, maxillary sinus, nasal cavity, ethmoid sinus, and salivary glands. It is the fifth most common cancer in males and the eight most common in females (Parkin *et al.*, 2005). The total number of new HNSCC cases is globally more than 600,000 annually, with 350,000 deaths per year.

The etiology of HNSCC is considered multifactorial. Tobacco use and alcohol consumption are considered the main risk factors for this disease (Castellsague *et al.*, 2004; Franceschi *et al.*, 1990), and the incidence rates vary depending on different geographically customs. The mode of tobacco use varies depending on customs in different countries. Tobacco smoking is common in Europe, Australia and Latin America whereas chewing tobacco is the major exposure in India, Papua New Guinea and Southeast Asia. Alcohol increases the risk of oral cancer, regardless of the type of beverage (Parkin and Bray, 2006). Cancer risk is higher when tobacco and alcohol consumption are combined (Morse *et al.*, 2007).

Viral agents also contribute to the development of HNSCC. Esptein-Barr virus is associated with nasopharyngeal cancer (Deyrup, 2008). HPV infection, mainly HPV16, has been demonstrated in oropharyngeal cancer (Loning *et al.*, 1985; Syrjanen *et al.*, 1983; Syrjanen *et al.*, 1982; reviewed in Fakhry and Gillison, 2006; Kreimer *et al.*, 2005).

Oropharyngeal tumors are classified into two subgroups: tobacco and alcohol negative tumors associated with HPV infection and those associated with tobacco and alcohol consumption and HPV negative (Smith *et al.*, 2004; Tachezy *et al.*, 2005). However, a synergistic effect of HPV infection and alcohol/tobacco in the onset of the disease is still unclear (Smith *et al.*, 2004). Tumors of never smokers and never drinkers contain more often HPV DNA than tumors of cases with tobacco and alcohol history. HPV DNA positivity varies depending on the anatomical localization of the tumor; tumors of oropharynx are more often HPV DNA positive (57%) than tumors of the oral cavity (25%) (Gillison *et al.*, 2000; Miller

and Johnstone, 2001; Tachezy *et al.*, 2005). The highest prevalence of HPV in HNSCC has been found in tonsillar cancer with HPV positivity in 40-75% of the cases (Dahlstrand and Dalianis, 2005). Interestingly, HNSCCs patients infected with HPV have a better prognosis when compared with HPV-negative patients (Fakhry and Gillison, 2006).

1.1.6.3 Non melanoma skin cancer

Non melanoma squamous skin cancer (NMSC) is the second most common cancer among Caucasian populations (Preston and Stern, 1992). Main risk factors described are UV light exposure, smoking, age, male sex, chronic skin ulcers, burn scars and immunosuppression (Alam and Ratner, 2001). Infection with HPV has been found in healthy individuals (Antonsson *et al.*, 2000; Astori *et al.*, 1998; Harwood *et al.*, 2004) and it has been related to benign and malignant lesions of NMSC immunocompetent and immunosuppressed patients (Akgul *et al.*, 2006; Biliris *et al.*, 2000; de Jong-Tieben *et al.*, 1995; de Villiers *et al.*, 1997; Kiviat, 1999; Shamanin *et al.*, 1994).

A number of cutaneous HPV types have been associated with multiple lesions in EV patients. These patients have an inherited disorder of cell-mediated immunity, and develop flat warts which in 40-60% of the cases lead to malignancy in sun-exposed sites (reviewed in Jablonska and Majewski, 1994).

Immunosuppressed and solid organ transplant patients infected with HPV present warts that develop into squamous cell carcinoma (SCC), especially on sun-exposed skin sites (Akgul *et al.*, 2006; Berkhout *et al.*, 1995; de Villiers *et al.*, 1997; Shamanin *et al.*, 1994; Shamanin *et al.*, 1996; Tieben *et al.*, 1994). HPV is specially detected in sun-exposed sites in both lesion and control skin (Asgari *et al.*, 2008; Forslund *et al.*, 2007), what suggests that combined effect of viral infection and UV light may lead to persistent infection and malignant progression.

Interestingly, a recent report in non-immunosuppressed patients showed that 12% of healthy skin contained HPV sequences whereas its presence was 26% in benign lesions, 22% in actinic keratoses, 18% in BCC and 26% in SCC. However, only infection with genus Beta papillomavirus of the subgroup 2 showed a direct correlation with disease (Forslund *et al.*, 2007). This observation demonstrates the involvement of HPV in skin SCC also in non-immunosuppressed individuals. Individual involvement of cutaneous HPV types with the onset and development of skin SCC remain to be elucidated.

1.2 4-NQO

Chemical carcinogens present in tobacco (e.g. DMBA and benzenes) need metabolic activation and are therefore rarely used in *in vitro* studies.

4-nitroquinoline-1-oxide (4-NQO) is a quinoline derivative compound active when applied directly either to cells or whole organisms. It was initially developed with chemotherapeutic purposes (Nakahara *et al.*, 1957) but it acts indeed as chemical carcinogen, inducing oral carcinogenesis in mice when applied in the drinking water and being widely used for studying oral carcinogenesis (Miyamoto *et al.*, 2008; Srinivasan *et al.*, 2008; Vered *et al.*, 2005) and tumors of the head and neck region (Aubry *et al.*, 2008).

4-NQO is used as a model for studying genetic susceptibility to different types of cancers; it has been described that when lymphocytes are exposed to 4-NQO they are more sensitive in samples from melanoma patients than those from head and neck cancer patients or healthy subjects (Hsu TC, 1993). Recently, another study demonstrated that sensitivity to 4-NQO reflects susceptibility to UV in the development of NMSC (Wang *et al.*, 2007).

Treatment with 4-NQO has been employed in mammalian cells as a model for DNA damage-induced carcinogenesis (Kyng *et al.*, 2005; Ninomiya *et al.*, 2004). 4-NQO has been characterized as UV-mimetic with respect to its genotoxic properties; it behaves very similarly to ultraviolet irradiation of short wavelengh or C irradiation (UVC) as DNA damaging agent. Both bulky 4-NQO adducts and UV-induced pyrimidine dimers are repaired by nucleotide excision repair mechanism (Snyderwine and Bohr, 1992). It induces a potent intracellular oxidative stress (Nunoshiba and Demple, 1993) and generates reactive oxygen species (ROS) such as superoxide radical or hydrogen peroxide (Arima *et al.*, 2006; Hozumi, 1969; Sugimura *et al.*, 1968). 4-NQO causes bulky DNA adducts primarily at G and A bases (Bailleul *et al.*, 1989; Galiegue-Zouitina *et al.*, 1985), chromosomal aberrations (Darroudi *et al.*, 1989), apoptosis when applied at high doses and cell cycle arrest in G0-G1 phases (Han *et al.*, 2007).

p16, cyclin D1 and p53 are altered during oral carcinogenesis (Opitz *et al.*, 2001; Shah *et al.*, 2007; Wayne and Robinson, 2006). Interestingly, these proteins have also been observed to change under experimental 4-NQO-induced oral cancer (Kanojia and Vaidya, 2006). DNA damage induced by 4-NQO treatment leads to increased levels of tumor suppressor p53 and up-regulation of $p21^{CIP1}$ (Seo *et al.*, 1999). In a 4-NQO mouse model, up-regulation in expression of keratin 1, keratin 14, EGF receptor and a decrease in p16 expression in tongue tumors have been reported as observed in human oral SCC (Tang *et al.*,

2004), simultaneously with over-expression of apoptotic related Bcl-2 and Bax proteins (Nishimura, 1999). These similarities between human patients and mouse models treated with the carcinogenic agent points the suitability of 4-NQO as inducing agent for studying oral carcinogenesis.

1.3 p53 gene family

p53, p63 and p73 form a protein family that shares a similar gene structure, containing alternative splicing, initiation of translation and promoters sites. The basic structure of the family includes an N-terminal domain required for transcriptional activation, a DNA binding domain and an oligomerization domain in the C terminus. All the members have very similar sequences, especially in the DNA binding domain, which enable p63 and p73 to transactivate p53-responsive genes (reviewed in Irwin and Kaelin, 2001). However, each protein has specific functions that are not shared by all the family members (reviewed in Bourdon, 2007).

1.3.1 p53

p53 is a tumor suppressor protein. It acts as transcription regulator and plays a key role in cell cycle by regulating growth arrest, DNA repair and apoptosis. Mutations in the p53 gene that unable it to bind its target DNA sequences have been observed in 50% of all the human tumors (Soussi and Beroud, 2001).

DNA damage and other stress signals as UV radiation, osmotic stress, chemical agents and oncogene expression activate p53. Its expression is regulated by an E3 ubiquitin ligase, Mdm2, which recognizes the transactivation domain of the protein and inhibits its transcription.

p53 regulates the transcription of genes encoding proteins involved in cell cycle arrest as $p21^{CIP1}$, GADD45 and 14-3-3σ, avoiding replication of damaged DNA (**Fig. 7**). Once growth arrest occurs, p53 activates the transcription of genes involved in DNA repair such as ribonucleotide reductase p53R2 (implicated in DNA replication and reparation) and the AP endonuclease, which forms part of the base excision repair machinery (reviewed in Bourdon, 2007). In irreversible DNA-damaged cells, p53 can target them to apoptosis by activating the pro-apoptotic proteins Bax (Chipuk *et al.*, 2004), Apaf-1 (Robles *et al.*, 2001), PUMA (Nakano and Vousden, 2001) and NoxA (Shibue *et al.*, 2003).

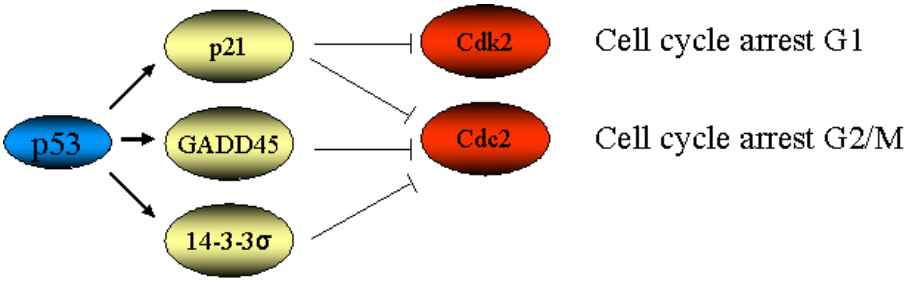

Figure 7. Role of p53 in G1 and G2/M growth arrest (modified from http://mol-biol4masters.org/).

The p53 gene codes for nine different isoforms (p53, p53β, p53γ, Δ133p53, Δ133p53β, Δ133p53γ, Δ40p53, Δ40p53β, Δ40p53γ) named depending on its promoter use (in exon 1 or in intron 4) and alternative splicing of intron 9 in the carboxiterminus side (β and γ forms) (reviewed in Bourdon, 2007). Although the function of the different forms still need to be further investigated, it has been shown that p53β binds preferably $p21^{CIP1}$ and Bax target promoters, while p53 has a high affinity to Mdm2 (Bourdon *et al.*, 2005).

1.3.2 p63

p63 gene is composed of 15 exons and codes for 6 protein isoforms (TAp63α, TAp63β, TAp63γ, ΔNp63α, ΔNp63β and ΔNp63γ). The transactivating isoforms, TAp63, are transcribed from the promoter located upstream of the exon 1 whereas truncated ΔNp63 forms lacking the transactivation domain are expressed under the control of the second promoter, located in the intron 3. The different C-terminal spliced proteins correspond to α, β and γ forms (reviewed in Candi *et al.*, 2007).

The role of p63 isoforms is still controversial. ΔNp63 plays a crucial role during embryogenesis, epithelial development and differentiation (McKeon, 2004). However, other reports defined TAp63 isoforms as the first appearing during development (Koster *et al.*, 2004). The more likely explanation is that both TA and ΔNp63 isoforms are required for development and their effect is exerted by protein counterbalance. In disease, the p63 gene is amplified in cervical carcinomas (Wang *et al.*, 2001).

The role of p63 isoforms in epidermal differentiation has been studied recently by iRNA in organotypic raft cultures (Truong *et al.*, 2006). In this study, they demonstrated that failure in ΔNp63 isoforms expression abolishes proliferation and differentiation, whereas TAp63 isoforms expression has a minor contribution to epidermal differentiation.

1.4 Cell cycle control by cyclin-dependent kinase inhibitors

Cell cycle progression is regulated by the activity of cyclin/CDK complexes (reviewed in Besson *et al.*, 2008). Cell cycle inhibitor molecules (CDI) interact with these cyclin/CDK complexes. CDI are classified into two gene families:

- INK4 tumor suppressor family. They inhibit cell cycle by avoiding CDK4 and CDK6 union to cyclin D (reviewed in Sherr and Roberts, 1999). The INK4 family is formed by $p16^{INK4a}$, $p15^{INK4b}$, $p18^{INK4c}$ and $p19^{INK4d}$ proteins.
- Cip/Kip family, refered to $p21^{CIP1}$, $p27^{KIP1}$ and $p57^{KIP2}$ proteins. They bind to cyclins D, E, A and B and to CDK molecules, modulating the activity of these cyclin/CDK complexes (reviewed in Sherr and Roberts, 1999).

$p21^{CIP1}$ acts by binding to the complexes cyclin E/CDK2 and cyclin B/CDK1 and blocking the CDK kinase activity, inducing both G1 and G2 arrest (Agarwal *et al.*, 1995). Moreover, $p21^{CIP1}$ controls cellular proliferation by binding to proliferating cell nuclear antigen (PCNA) and inhibiting DNA synthesis (Luo *et al.*, 1995). Its transcription is regulated by p53 (el-Deiry *et al.*, 1993). In addition, $p21^{CIP1}$ activates pRb, linking both tumor suppressor pathways. The role of Cip/Kip proteins as tumor suppressors or oncogenes remains still controversial (reviewed in Besson *et al.*, 2008). However, in pancreas, breast, prostate, ovary, cervix and brain tumors, $p21^{CIP1}$ overexpression correlates with a poor prognosis (Roninson, 2002).

1.5 The skin

1.5.1 Skin organization

The skin is a complex, multilayered organ that serves as the first barrier to the outside environment and prevents unnecessary loss of water from the organism. Both adherens junctions and desmosomes mediate cell-cell adhesion within the skin. It is composed of two parts, the dermis in the inner most layer and the epidermis as the outer layer (Elder *et al.*, 2005).

The dermis is a connective tissue containing fibroblasts embedded in collagen and elastic fibers. It harbors the nerve receptors, hair follicles, sweat glands, sebaceous glands, apocrine glands, lymphatic vessels and blood vessels.

The epidermis consists primarily of cells with little connective tissue. It is a stratified, continually renewing epithelium, exhibiting progressive differentiation in a basal to superficial direction. It is comprised mainly of keratinocytes (90-95% of the cells) and also melanocytes, Langerhans and Merkel cells. The structure of an individual keratinocyte correlates with its position within the epidermis and its state of differentiation (reviewed in Houben *et al.*, 2007).

1.5.2 Epidermal layers

Different cellular layers can be distinguished in the epidermis corresponding to progressive stages of differentiation: basal, spinous, granular and cornified layers (**Fig. 8**). Keratinocytes arise from stem cells in the basal layer of the epidermis and in the bulge region of the hair bulb, and move through a series of differentiation events until they are finally sloughed into the environment (Eckert *et al.*, 1997). During epidermal differentiation, keratinocytes undergo dehydration, loss of proliferation properties, cell flattening and increase in size. The cells create and reorganize the organelles, change their plasma membrane properties, cell surface antigens and receptors and synthesize different proteins and lipids.

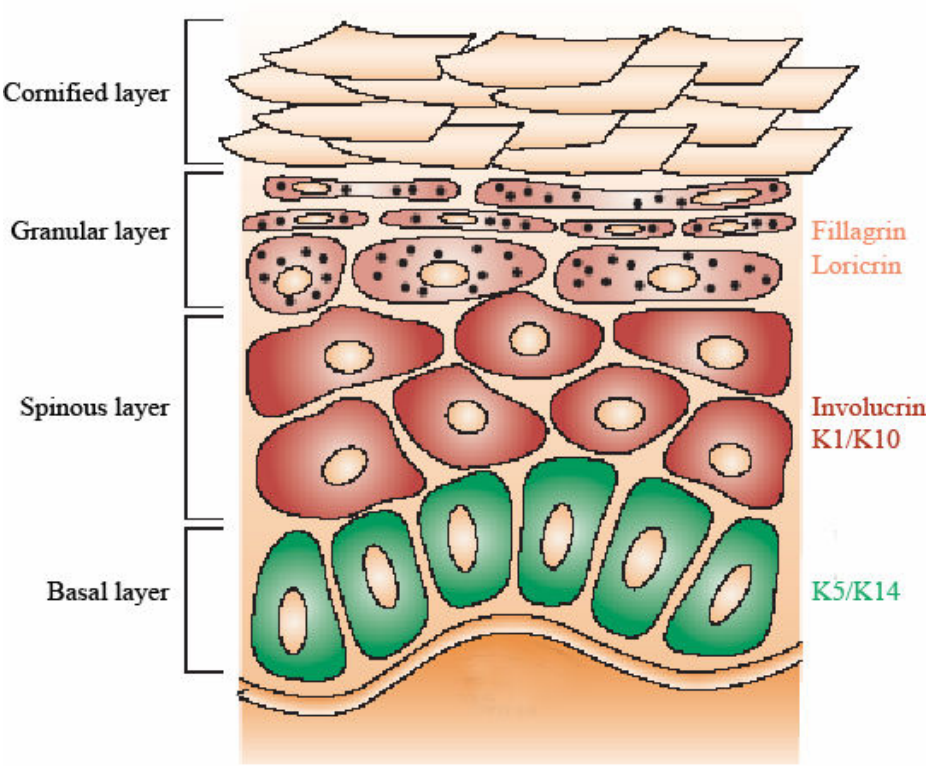

Figure 8. Epidermal layers and protein expression pattern in the epidermis (adapted from Radtke and Raj, 2003).

The basal layer of keratinocytes is in contact with the basement membrane, which separates the epidermis from the dermis. Cells in the basal layer are the only keratinocytes in intact skin capable of mitosis and, as such, are the source of all other keratinocytes in the epidermis. They attach to the dermis through hemidesmosomes and to adjacent cells through desmosomes and adherens junctions (Borradori and Sonnenberg, 1996). Basal layers are columnar in shape and tipically express keratins 5 and 14 (Steinert, 1993).

The first suprabasal keratinocyte layer is the stratum spinosum, with many desmosomal contacts between cells. Morphologically, spinous cells are larger and more flattened than basal cells. Suprabasal keratinocytes express differentiation-specific keratins 1 and 10. Cells begin to produce late differentiation markers such as involucrin in the upper spinous layers followed by expression of loricrin and epidermis-specific transglutaminases in the upper stratum spinosum (Fuchs, 1993; Rossi *et al.*, 1998).

As keratinocytes differentiate further, they form the stratum granulosum. Distinct electron-dense keratohyalin granules characterize cells of this layer. They contain a late stage protein, the profilaggrin, the protein precursor of filaggrin. Filaggrin functions as an intermediate filament-associated protein, which aggregates keratin filaments in cornified cells (Ishida-Yamamoto *et al.*, 1999). Granular cells also contain lipid-filled granules. These lipids granules fuse with the plasma membrane and release their contents into the intercellular spaces in the transition zone between the stratum granulosum and stratum corneum.

The uppermost epidermal layer is the stratum corneum. The corneocyte is a flattened cell that loses the nuclei, whose organelles have broken down, and which is metabolically inactive (reviewed in Candi *et al.*, 2005). Macrofibrils are the basic structural unit of the cornified envelope. In this epidermal layer, the extracellular matrix is replaced by lipid lamellae, conferring hydrophobicity to the surface. Corneocytes attached by desmosomes are ultimately desquamated on the skin surface (Eckert *et al.*, 1997).

In palmar and plantar skin additional keratins, 6a, 6b, 9, 16, and 17 are expressed (Fuchs, 1993).

1.5.3 The skin barrier

The outermost layer of the stratified squamous epithelia, the stratum corneum, is responsible for skin impermeability. This layer is composed of dead cells (corneocytes) filled with keratins. They are embedded in a filaggrin matrix and surrounded by intercellular lipid lamellae structures. At the molecular level, a functional corneocyte contains loricrin,

involucrin attached to lipids and in the uppermost cell membrane free fatty acids, ceramides and cholesterol. A balanced composition of these elements is necessary for keeping an effective physical and water barrier function in the epidermis (reviewed in Candi *et al.*, 2005). Loricrin constitutes 80% of the proteins in the cornified envelope. It acts as reinforcement together with small proline rich protein (SPR) in the lower part of the corneocyte cellular membrane (Hohl *et al.*, 1991).

Lipids are accumulated in the trans-Golgi of the cells in the granular layer and released as lamellar bodies (Wertz and van den Bergh, 1998), mostly composed of ceramides. The ceramides link to specific scaffold proteins, involucrin, envoplakin and periplakin in the cornified layer (Marekov and Steinert, 1998). This attachment occurs via transglutaminase enzymes that form ester bounds (reviewed in Kalinin *et al.*, 2002).

Several hereditary diseases involve impaired barrier function. These alterations in skin barrier can be caused by:

- Protein alterations: as in the lamellar ichthyosis disease, where mutations in the transglutaminase 1 gene lead to aberrant crosslinking of the proteins in the cornified layer (Huber *et al.*, 1995) or the Netherton syndrome, characterized by a severe skin barrier defect induced by defects in the serine protease inhibitor Kazal type 5 (SPINK5) (reviewed in Sevilla *et al.*, 2007).
- Defects in lipid metabolism: as X-linked ichthyosis, with cholesterol sulphate accumulation in the intercellular spaces; nonbullous congenital ichthyosiform erythroderma with mutations in lipid lipoxygenase-3 or -12R that leads to aberrant lipid extrusion (reviewed in Elias *et al.*, 2008 and in Sevilla *et al.*, 2007) and the Chanarin–Dorfman syndrome where lipid droplets accumulate into vacuoles in the epidermis (reviewed in Candi *et al.*, 2005).

1.5.4 Keratins

Keratins are the intermediate filaments that provide the structural integrity of the skin by interacting with the microfilaments and microtubules. Different keratin polypeptides have been described, 20 corresponding to epithelial cells and 10 to hair (reviewed in Moll *et al.*, 2008; Moll *et al.*, 1982; Tseng *et al.*, 1982; Wu *et al.*, 1982). They can be classified into two classes, the acidic, type I (K10-K20) and basic-neutral, type II (K1-K9) based on amino acid sequence, charge, size, immunological properties and homologies with wool keratins (Sun, 1984). Keratins form heterodimers between one acid and one basic keratin of similar

molecular weight. They are expressed in highly specific patterns related to the cell type, functional state and stage of cellular differentiation (**table 2, fig. 8**) (O'Guin *et al.*, 1987).

	Simple epithelia		Stratified epithelia				
Type II/type I keratins	K8/ K18	K7/ K19	K5/ K14	K15	K6/ K16	K1/ K10	K4/ K13
Non-keratinizing stratified squamous epithelia	Some basal cells	K19 in many basal cells	Basal cell layer	Basal cell layer	Suprabasal layers	Focal, suprabasal layers	Suprabasal layers
Epidermis			Basal cell layer	Basal cell layer		Suprabasal layers	

Table 2. Characteristic expression patterns of keratins. (Adapted from Moll *et al.*, 2008).

1.5.4.1 Keratin expression in simple epithelia

The pair K8/K18 is the typical keratins expressed in simple epithelia. They appear firstly during embryogenesis and are present in simple epithelia as ductal, gastrointestinal and urothelial cells but not in differentiating keratinocytes (reviewed in Moll *et al.*, 2008). Interestingly, since cancers tend to behave as simple epithelia, K8/K18 has been found in most cancers, except some differentiated SCC (Malzahn *et al.*, 1998; reviewed in Moll, 1998).

K7/K19 pair can be expressed in some simple ductal epithelia as bile and pancreatic ducts but its profile is not as well defined as K8/K18 (reviewed in Moll *et al.*, 2008).

1.5.4.2 Keratin expression in stratified epithelia

The K5/14 pair of keratin filaments is expressed in the basal cells of epidermis and mucosal non-keratinizing stratified squamous epithelia (Moll *et al.*, 2008). As basal cells of the epidermis begin to differentiate, they down-regulate their expression and begin to produce differentiation-specific keratins.

K6/K16 are typically found in hyperproliferative tissue as nails, mucosa, palmoplantar epidermis and skin wounding (Moll *et al.*, 1982; Sun *et al.*, 1983). They are highly expressed after injury and UV exposure, in squamous metaplasia and poorly differentiated SCCs (Moll, 1998). K6/K16 are rarely found in cervix adenocarcinomas and invasive breast carcinomas. K17 is restricted to basal/myoepithelial cells and shares the same expression profile in healthy and carcinoma tissue as the K6/K16 pair.

The K1/K10 pair is expressed in the suprabasal layers of the epidermis and is the main keratins associated with differentiation and keratinization. In normal skin, they are expressed from the first suprabasal layer throughout the surface of the tissue (Boukamp *et al.*, 1990; Stoler *et al.*, 1988) and provide mechanical integrity to the epidermis. K9 is a very specific keratin that couples with K1; it is only present in the palm and sole in terminally differentiating keratinocytes (Moll *et al.*, 1987).

The pair K4/K13 is expressed in suprabasal mucosal squamous epithelial cells, involving non-keratinizing epithelia (intern organs) but not epidermis (Mischke *et al.*, 1990).

K77 expression is restricted to secreting cells of eccrine sweat gland ducts, what makes it a suitable marker for secreting epithelia (Langbein *et al.*, 2005).

1.5.4.3 Keratin expression in squamous cell carcinoma

Keratin expression profile deeply changes during disease depending on the keratin type, being therefore a very important tool for diagnostic in tumor pathology.

SCC mainly expresses stratified-epithelia keratins but may retain expression of simple-epithelia types too. Most SCCs and mesotheliomas, but not adenocarcinomas, strongly express K5/K14 and K17 (McDonald *et al.*, 1998). The K6/16 pair, associated with hyperproliferative tissue, is generally up-regulated in SCC (McGowan and Coulombe, 1998). Histological examinations in SCCs revealed focal expression of K1/K10 depending on its level of maturation and keratinisation. High differentiated tumors focally express K4/K13 as well as K1/K10 in horn pearls formations. Considering the epidermal origin of HNSCC results surprising that focal K4/K13 expression has been found in this disease, especially in poorly differentiated carcinomas (Moll, 1998).

K1/K10 are present in 50% of oral and pharyngeal SCC (Moll, 1998). In contrast, low differentiated SCC expresses typical keratins for simple epithelia, as K8/K18 and K19. In the case of oral SCC, K8/K18 expression is used as a marker for poor prognosis (Fillies *et al.*, 2006).

1.5.5 Differentiation markers

1.5.5.1 Involucrin

Involucrin is a soluble protein localized in the cytoplasm of granular and cornified cells (Mansbridge and Knapp, 1987; Murphy *et al.*, 1984) of stratified squamous epithelia and primary keratinocyte organotypic cultures (Boukamp *et al.*, 1990; Watt *et al.*, 1987). This protein consists of repeating peptide units with a high Gly and Asp amino acid content. It is an early component during the cornified envelope formation, getting crosslinked to other proteins and thus forming a scaffold structure. Involucrin localizes in the cell membrane and is the substrate for lipid (mainly ceramides) attachment, being a crucial component of the lipid envelope (Marekov and Steinert, 1998). Involucrin expression has been demonstrated to be crucial for maintenance of epidermal barrier function (reviewed in Sevilla *et al.*, 2007).

1.5.5.2 Loricrin

Loricrin is expressed in granular layer cells during cornification as aggregates in the cytoplasm. It is the main component of the cornified layer and plays a key structural role as reinforcement protein and maintenance of barrier function (Candi *et al.*, 1995; Segre, 2006). Its sequence is very rich in Gly, Ser and Cys residues and the protein lacks an ordered structure, providing elasticity to the cornified layer. Loricrin crosslinks with other loricrin molecules and to a lesser extends to SPR proteins, forming the scaffold of the cornified envelope (reviewed in Candi *et al.*, 2005).

1.6 Aim of the project

The etiology of cancer of the oral cavity and esophagus is multifactorial with alcohol and tobacco consumption considered to be the main risk factors. Mucosal high risk HPV plays an important role in the pathogenesis of a subset of HNSCC, particularly those that arise from the lingual and palatine tonsils within the oropharynx. The smaller proportion of smokers in patients with HPV DNA positive tumors suggests that these tumors might form a distinct epidemiological entity.

Cutaneous HPV20 is associated with benign and malignant lesions in the skin disease EV. It has been demonstrated in a number of NMSC as well as in esophageal carcinoma and in HNSCC patients.

Chemical carcinogens present in tobacco need metabolic activation and therefore are rarely used in *in vitro* studies. In our studies, we combined HPV20 with a chemical carcinogen that would act as a co-factor for investigating the immortalization and transformation properties of this virus. 4-NQO is considered as an UV-mimetic with respect to its genotoxic properties. It has been largely applied as model for oral carcinogenesis and it is active when applied directly either to cell culture or whole organisms.

The aim of the project was studying the cooperation between HPV20 and the chemical carcinogen 4-NQO in the pathogenesis of malignant tumors by characterization of:

- The HPV20 promoter activation profile under the context of 4-NQO treatment together with HPV20 E6, E7 or E6/E7 expression.
- The expression of cellular proteins involved in cell cycle control, proliferation and differentiation (p53, ΔNp63α, PCNA and p16) in keratinocytes expressing HPV20 E6 and treated with 4-NQO.
- The cell cycle profile, apoptosis rates and effect on life span of primary keratinocytes treated with 4-NQO combined with HPV20 E6 expression.
- Epidermal morphology; differentiation and proliferation markers expression pattern; effect in cellular proteins p53, ΔNp63α and $p21^{CIP1}$; skin barrier functionality and lipid organization in organotypic cultures expressing HPV20 E6 and treated with 4-NQO.

2 Materials

2.1 Equipment

Cell culture	
Incubator for cell culture	Forma Scientific, Ohio, USA
Laminar flow hood	The Baker Company Inc., Sanford, USA
Neubauer cell counting chamber	Brand GmbH, Wertheim, Germany
Tissue grinder (Dounce)	Sigma-Aldrich, Taufkirchen, Germany

Centrifuges	
Floor centrifuge for large volumes (up to 500 ml) RC5C	Sorvall Instruments, USA
High speed refrigerated centrifuge 1-15K	Sigma, Osterode, Germany
Non-refrigerated bench top centrifuge 5415	Eppendorf, Hamburg, Germany
Refrigerated centrifuge Megafuge for conical tubes 1.0R	Heraeus Sepatech, Hanau, Germany

Freezers	
Freezer 4°C and -20°C Premium	Liebherr, Ochsenhausen, Germany
Freezer -80°C Hera	Kendro Laboratory, Hanau, Germany
Liquid nitrogen freezer	Chronos Biosafe, Griesheim, Germany

Gel electrophoresis, UV visualization and film developing	
Electrophoresis chamber for DNA and RNA	Owl Separation Systems, Inc. Portsmouth, USA
Electrophoresis power supplier Power Pac	Bio-Rad, München, Germany
Film developing hyperprocessor	Amersham Biotech, Freiburg, Germany
Protein Minigel Wet Transfer System	Bio-Rad, München, Germany
SDS-PAGE electrophoresis equipment	Bio-Rad, München, Germany
UV transilluminator 366 nm	Konrad Benda, Wiesloch, Germany
UV transilluminator 254 nm	Bio-Rad, Milan, Italy

Microscopes, microtome and cryostat	
Binocular microscope Wilovert S	Helmut Hund GmbH, Wetzlar, Germany
Cryostat Leica CM3050S	Leica, Nussloch, Germany
Fluorescence camera F-View II firewire	Soft Imaging System Münster, Germany
Fluorescence microscope Leitz DM RBF	Leitz Instruments, Wetzlar, Germany
Light camera Colorview II	Olympus, Hamburg, Germany
Microtome Leica RM2235	Leica, Nussloch, Germany
Transmission electron microscope EM 900	Zeiss, Oberkochen, Germany
Ultramicrotome Leica Ultracut UCT for electron microscopy sectioning	Leica, Nussloch, Germany

Other equipment	
Balance PB 602	Mettler- Toledo, Greifensee, Switzerland
Bunsen burner	Integra Biosciences, Chur, Switzerland
Cytofluorograph 30-L	Ortho Diagnostics, Westwood, USA
Gas chromatograph HP5890	Agilent Technologies, Waldbronn, Germany
Flow cytometer FACScalibur	Becton Dickinson, Heidelberg, Germany
Block heater	Gebr. Liebisch, Bielefeld, Germany
Magnetic stirrer	Heidolph Instruments, Schwabach, Germany
Mass spectrometer HP5973	Agilent Technologies, Waldbronn, Germany
Microwave oven	B. Braun, Melsungen, Germany
pH meter	WTW, Weilheim, Germany
Platform shaker Str6	Stuart Scientific, United Kingdom
Scanner Perfection 4990 PHOTO	Epson, Tokyo, Japan
Shaking water bath 3047	Köttermann, Hänigsen, Germany
Sonicator Bioruptor™	Diagenode, Liege, Belgium
Spectrophotometer Ultrospec 3000pro	Amersham Pharmacia Biotech, Freiburg
SpeedVac concentrator Savant	Instruments Inc., Farmingdale, NY, USA
Thermocycler GeneAmp PCR 9700	Applied Biosystems, Darmstadt, Germany
Vacuum pump	Pfeiffer, Asslar, Germany
Vortex Genie 2	Bender & Hobein AG, Zurich, Switzerland
Water bath	Julabo Labortechnik, Seelbach, Germany

2.2 Consumables

Bacterial culture	
Bacterial culture plates	Greiner bio-one, Solingen, Germany

Cell culture	
Cell culture plates	Greiner bio-one, Solingen, Germany
Cell scrapers	Corning Costar GmbH, Bodenheim, Germany
Cryo tubes	Nunc, Invitrogen, Karlsruhe, Germany
Organotypic culture transwells inserts 3 µm	Neolab, Heidelberg, Germany
Organotypic culture trays	Neolab, Heidelberg, Germany

Sterile filtration	
Bottle Top Filter 500 ml, 0,22 µm	Corning Costar GmbH, Bodenheim, Germany
Filter Millex 0,22µm and 0,45 µm	Millipore, Schwalbach, Germany
Filter Puradisc for viruses, 0,45 µm	Whatman, Madistone, USA

Western blot	
BioMax MR film, Kodak	Kodak, Stuttgart, Germany
Cuvettes for protein cuantification	Greiner bio-one, Solingen, Germany
Nitrocellulose membrane	Whatman Optitran, Dassel, Germany
Whatman 3MM paper	Whatman, Madistone, USA

Other consumables	
Capillary columns for gas chromatography HP 5MS	Agilent Technologies, Waldbronn, Germany
Centrifugation tubes 1,5 ml and 2 ml	Eppendorf, Hamburg, Germany
Centrifugation tubes 15 ml and 50 ml	BD Falcon™, New Jersey, USA
Microscope Slides Super-Frost® Plus	Menzel-Gläser, Braunschweig, Germany
Parafilm M	Greiner, Frickenhausen, Germany
QIAshredder™ columns	Qiagen, Hilden, Germany

2.3 Reagents

Bacterial culture	
Ampicillin	Sigma-Aldrich, Taufkirchen, Germany
Bacto-agar	Invitrogen, Karlsruhe, Germany
Trypton	AppliedChem GmbH, Darmstadt, Germany
Yeast extract	Difco, Beckton and Dickinson, USA

Cell culture	
Adenine	Sigma-Aldrich, Seelze, Germany
Cholera toxin	Sigma-Aldrich, Taufkirchen, Germany
Dimethyl sulfoxide	Sigma-Aldrich, Taufkirchen, Germany
Dulbecco´s modified Eagle´s medium (DMEM) 1x	Sigma-Aldrich, Taufkirchen, Germany
Dulbecco´s modified Eagle´s medium (DMEM) 10x	Promocell, Heidelberg, Germany
Earl´s salt solution	Sigma-Aldrich, Taufkirchen, Germany
Epidermal growth factor (EGF)	R & D systems, Wiesbaden, Germany
Fetal calf serum (FCS)	PAA laboratories, Pasching, Germany
Geneticin	Calbiochem, Darmstadt, Germany
Ham´s F-12 medium	Invitrogen, Karlsruhe, Germany
Hepes	Sigma-Aldrich, Taufkirchen, Germany
Hydrocortisone	Merck, Darmstadt, Germany
Insulin	Sigma-Aldrich, Taufkirchen, Germany
Keratinocyte medium 2	Promocell, Heidelberg, Germany
Keratinocyte medium supplements 2	Promocell, Heidelberg, Germany
Keratinocyte EpiLife medium	Cascade Biologics, Mansfield, UK
Keratinocyte medium supplements HKGS	Cascade Biologics, Mansfield, UK
Mitomycin C	Roche, Mannheim, Germany
4-Nitroquinoline-1-oxide 99%	Sigma-Aldrich, Taufkirchen, Germany
OPTI-MEM medium	Gibco, Invitrogen, Germany
Penicillin 10,000 units/ml /streptomycin 10 mg/ml (P/S)	Sigma-Aldrich, Taufkirchen, Germany
Polybrene (Hexadimethrine bromide)	Sigma-Aldrich, Taufkirchen, Germany

Rat tail collagen type I 4mg/ml	BD Biosciences, Heidelberg, Germany
Roswell Park Memorial Institute medium (RPMI)	Sigma-Aldrich, Taufkirchen, Germany
Transfection reagent FuGENE HD	Roche, Mannheim, Germany
Transfection reagent Lipofectamine™	Invitrogen, Karlsruhe, Germany
Transfection reagent Lipofectamine™ 2000	Invitrogen, Karlsruhe, Germany
Transfection Plus™ Reagent	Invitrogen, Karlsruhe, Germany
Trypan blue dye	Sigma-Aldrich, Taufkirchen, Germany
Trypsin-EDTA	Sigma-Aldrich, Taufkirchen, Germany

Gas chromatography- mass spectrometry	
Chloroform	Sigma-Aldrich, Taufkirchen, Germany
Dimethoxypropane	Sigma-Aldrich, Taufkirchen, Germany
Oleic acid	Campro Scientific, Berlin, Germany
Palmitic acid	CDN, Pointe-Claire, Quebec, Canada
Stearic acid	CDN, Pointe-Claire, Quebec, Canada
Sulfuric acid H_2SO_4	Sigma-Aldrich, Taufkirchen, Germany
Toluene	Sigma-Aldrich, Taufkirchen, Germany

DNA and RNA	
Agarose	Gibco, Invitrogen, Karlsruhe, Germany
Bromophenol blue	Serva, Heidelberg, Germany
Deoxynocleosidetriphosphate (dNTP)	Qiagen, Hilden, Germany
Diethylpyrocarbonate (DEPC)	Sigma-Aldrich, Taufkirchen, Germany
Ethidium bromide 95% (EtBr)	Carl Roth GmbH, Karlsruhe, Germany
Isoamylalcohol	Merck, Darmstadt, Germany
Isopropanol	J.T. Baker, Deventer, Holland
Random hexamers	Qiagen, Hilden, Germany
RNase inhibitor RNasin®	Promega, Mannheim, Germany
Xylene cyanol	Sigma-Aldrich, Seelze, Germany

Immunohistochemistry and electron microscopy	
Bovine serum albumin (BSA)	Sigma-Aldrich, Taufkirchen, Germany
5´ bromo-2-deoxyuridine (BrdU)	Calbiochem, Darmstadt, Germany
Citric acid	Merck, Darmstadt, Germany
3,3´-diaminobenzidine substrate (DAB)	BD Biosciences, Heidelberg, Germany
4´, 6- Diamidino-2-phenylindole dihydrochloride (DAPI)	Serva, Heidelberg, Germany
Eosin Y-solution 0,5%	Merck, Darmstadt, Germany
Eukitt®	Kalo GmbH, Freiburg, Germany
Fluoromount-G™	Southern Biotech, Biozol, Eching, Germany
Glutaraldehyde solution 25%	Sigma-Aldrich, Taufkirchen, Germany
Haematoxylin	Merck, Darmstadt, Germany
Hoechst 33258 dye	Invitrogen, Karlsruhe, Germany
Hydrogen peroxide H_2O_2	Serva, Heidelberg, Germany
Lead citrate	Merck, Darmstadt, Germany
Meyers´ hemalaum solution	Carl Roth GmbH, Karlsruhe, Germany
Oil red O	Sigma-Aldrich, Taufkirchen, Germany
Paraffin Paraplast® Plus	Ted Pella Inc., Redding, CA, USA
Paraformaldehyde (PFA)	Merck, Darmstadt, Germany
Resin Araldite® 506 epoxy	Sigma-Aldrich, Taufkirchen, Germany
Sodium cacodylate trihydrate $(CH_3)_2AsO_2Na{\cdot}3H_2O$	Serva, Heidelberg, Germany
Sodium citrate dihydrate $C_6H_5Na_3O_7{\cdot}2H_2O$	Merck, Darmstadt, Germany
Streptavidin Alexa 488-conjugated	Invitrogen, Karlsruhe, Germany
Sulforhodamide 101 dye (SR101)	Eastman Kodak, Sttutgart, Germany
Tissue-Tek O.C.T	Sakura Finetek, Tokyo, Japan
Triethyl-phosphate 60% $(C_2H_5)3PO_4$	Sigma-Aldrich, Taufkirchen, Germany
Trypsin powder	Biochrom AG, Berlin, Germany
Uranyl acetate	Merck, Darmstadt, Germany
Xylol	Sigma-Aldrich, Taufkirchen, Germany

Protein extraction and Western blot	
Ammonium persulfate $(NH_4)_2S_2O_8$ (APS)	Merck, Darmstadt, Germany
Protein quantification reagent	BioRad Laboratories, Munich, Germany
1,4-dithio-DL-threitol (DTT)	Sigma-Aldrich, Taufkirchen, Germany
Western blotting detection reagent ECL	Amersham Biotech, Munich, Germany
β-Mercaptoethanol (ß-ME)	Sigma-Aldrich, Taufkirchen, Germany
Nonidet NP40 10%	Roche, Mannheim, Germany
Non-fat milk powder	Carl Roth GmbH, Karlsruhe, Germany
Pefabloc® AEBSF	Roche, Mannheim, Germany
Polyacrylamide	Carl Roth GmbH, Karlsruhe, Germany
Protease inhibitor cocktail 100x	Sigma-Aldrich, Taufkirchen, Germany
Restore™ Western Blot Stripping Reagent	Perbio Science, Rockfold, USA
Sodium dodecyl sulfate $C_{12}H_{25}SO_4Na$ (SDS)	Gerbu, Gaiberg, Germany
Sodium orthovanadate Na_3VO_4	Merck, Darmstadt, Germany
N,N,N',N'-Tetramethylethylenediamine (TEMED)	Sigma-Aldrich, Taufkirchen, Germany
Triton X 100	Applichem, Darmstadt, Germany
Tween®20	Serva, Heidelberg, Germany
Urea	Fluka, Deisenhofen, Germany

Other reagents	
Ammonium acetate CH_3COONH_4	Merck, Darmstadt, Germany
Ammonium chloride NH_4Cl	Merck, Darmstadt, Germany
Calcium chloride $CaCl_2$	Fluka Chemie AG, Buchs, Switzerland
Ethylenediaminetetraacetic acid (EDTA)	Merck, Darmstadt, Germany
Glycerol	Fluka, Deisenhofen, Germany
Hydrochloric acid HCl	Sigma-Aldrich, Seelze, Germany
Magnesium chloride $MgCl_2$	Merck, Darmstadt, Germany
Methanol	J.T. Baker, Deventer, Holland
Phosphate buffered saline (PBS) 10x	Invitrogen, Karlsruhe, Germany
Phenol	Merck, Darmstadt, Germany
Sodium acetate CH_3COONa	Merck, Darmstadt, Germany
Sodium bicarbonate $NaHCO_3$	Merck, Darmstadt, Germany

Sodium carbonate Na_2CO_3	Merck, Darmstadt, Germany
Sodium citrate dihydrate $C_6H_8O_7Na_3 \cdot 2H_2O$	Merck, Darmstadt, Germany
Sodium chloride NaCl	J.T. Baker, Deventer, Holland
Sodium fluoride NaF	Merck, Darmstadt, Germany
Sodium hydroxide NaOH	Merck, Darmstadt, Germany
Sodium orthovanadate $NaVPO_4$	Merck, Darmstadt, Germany
Sodium phosphate, monobasic NaH_2PO_4	Merck, Darmstadt, Germany
Sodium phosphate, dibasic Na_2HPO_4	Merck, Darmstadt, Germany
Sucrose	Merck, Darmstadt, Germany
Trishydroxymethylaminomethan (Tris)	Sigma-Aldrich, Taufkirchen, Germany

2.4 Software

Basic Local Alignment (BLAST)	National Center for Biotechnology Information, Bethesda, MD, USA
Cellquest Pro 4	Becton Dickinson, Heidelberg, Germany
ClustalW	Conway Institute UCD, Dublin, Ireland
ImageQuant 5.0	Molecular Dynamics, Sunnywale, CA, USA
OligoAnalyzer 3.1.	Integrated DNA Technologies, Leuven, Belgium

2.5 Commercial kits

Kit	Used for	Company
BrdU Immunohistochemistry System	Immunohistochemistry staining of cells that incorporated BrdU.	Merck, Darmstadt, Germany
Cytofix/Cytoperm™	Fixation and permeabilization of FACS samples.	BD Biosciences, Heidelberg, Germany

Keratinocyte Detach kit2-125	Trypsinization of primary keratinocytes.	Promocell, Heidelberg, Germany
JetQuick Gel Extraction Spin Kit/250	Purification of DNA from agarose gels.	Genomed GmbH, Löhne, Germany
JetQuick PCR Purification Spin Kit/250	Cleaning and purification of DNA after PCR or enzymatic digestion.	Genomed GmbH, Löhne, Germany
JetQuick Plasmid Miniprep Spin Kit/250	Small scale plasmid DNA purification from bacteria.	Genomed GmbH, Löhne, Germany
Dual-Luciferase® Reporter (DLR™) Assay System kit	Measurement of promoter activity by luciferase reporter gene.	Promega, Mannheim, Germany
RNeasy® mini kit 50	Purification of RNA from cell extracts.	Qiagen, Hilden, Germany
Qiagen Plasmid purification kit	Large scale plasmid DNA purification from bacteria.	Qiagen, Hilden, Germany
Vectastain®ABC *Elite*® kit	Immunohistochemistry Avidin-Biotintylated enzyme complex.	Vector Laboratories, Burlingame, CA, USA

2.6 Solutions

Nucleic acids preparation and manipulation		
Solution	**Final concentrations**	**Components**
DEPC-H_2O. Store at RT.	0,1% Dissolve in	DEPC ddH_2O, incubate o/n 37°C
DNA loading buffer 5x. Aliquot and store at -20°C.	40% (w/v) 20 mM 0,05% (w/v) 0,05% (w/v) Dissolve in	Sucrose EDTA Bromophenol blue Xylene cyanol dH_2O

Electrophoresis buffer 50x (EP buffer). Store at RT.	2 M	Tris base
	0,25 M	CH_3COONa
	0,05 M	EDTA
	Dissolve in	dH_2O
		Adjust pH 7,8
TE buffer 10x. Store at RT.	100 mM	Tris-HCl pH 8,0
	10 mM	EDTA
	Dissolve in	dH_2O
TE buffer 1x. Store at RT.	10%	TE buffer 10x
	Dissolve in	dH_2O

Protein extraction		
Solution	**Final concentrations**	**Components**
Organotypic culture protein extraction buffer. Store at 4°C.	50 mM	Tris
	5 mM	EDTA
	10 mM	NaCl
	10 mM	NaF
	0,5%	NP40
	Dissolve in	dH_2O
		Adjust pH 8,0, Store at 4°C
		Just before use add:
	1x	Protease inhibitor cocktail
	2 mM	DTT
	1 mM	$NaVPO_4$
Monolayer cell culture protein extraction buffer (RIPA). Store at 4°C.	100 mM	Tris-HCl pH 8,0
	150 mM	NaCl
	1 mM	EDTA
	1%	NP40
	0,1%	SDS
		Just before use add:
	1x	Protease inhibitor cocktail
	2mM	DTT
	1mM	Pefabloc AEBSF

Sodium orthovanadate 10 M. Aliquot and store at -20°C.	10 M Dissolve in	$NaVPO_4$ H_2O 1. Adjust pH 10 2. Boil and cool down Repeat steps 1-2 until the solution becomes colorless.
Urea 12 M/Mercaptoethanol 0,8% buffer Aliquot and store at -20°C.	12 M 0,8% (v/v) Dissolve in	Urea β-ME dH_2O

SDS-polyacrylamide gel electrophoresis buffers		
Solution	**Final concentrations**	**Components**
Blotting buffer 10x. Store at RT.	250 mM 2 M Dissolve in	Tris Glycine dH_2O Adjust pH 8,3-8,7
Blotting buffer 1x. Prepare fresh just before use.	10% 20% Dissolve in	Blotting buffer 10x Methanol dH_2O
Loading buffer 5x. Aliquot and store at -20°C.	10% (w/v) 0,3 M 50% (v/v) Dissolve in 0,5% (w/v) 5% (v/v) Dissolve in	SDS Tris-HCl pH 6,8 Glycerol dH_2O Heat 10 min 40-50°C Bromphenol blue ß-ME dH_2O
Running buffer 5x. Store at RT.	120 mM 1,25 M 5% (w/v) Dissolve in	Tris Glycine SDS dH_2O
Running buffer 1x. Prepare fresh just before use.	20% Dissolve in	Running buffer 5x dH_2O

TBS buffer 10x. Store at RT.	0,2 M 1,36 M Dissolve in	Tris NaCl H_2O Adjust pH 7,6-8,0
TBS-T buffer 1x. Prepare fresh just before use.	10% 0,1% Dissolve in	TBS buffer 10x Tween20 dH_2O

SDS-polyacrylamide gel		
Solution	**Final concentrations**	**Components**
Stacking gel. Prepare fresh just before use. Polyacrylamide concentration varies depending on the size of the protein of interest, ranging between 10-15%.	10-15% (v/v) 25% (v/v) 1% (v/v) 1% (v/v) 0,1% Dissolve in	Polyacrylamide Tris-HCl 0,5 M, pH 8,8 SDS 10% APS 10% TEMED dH_2O
Resolving gel. Prepare fresh just before use.	7,5% (v/v) 25% (v/v) 1% (v/v) 1% (v/v) 0,1% Dissolve in	Polyacrylamide Tris-HCl 0,5 M, pH 6,8 SDS 10% APS 10% TEMED dH_2O

Cell culture		
Solution	**Final concentrations**	**Components**
Adenine 18 mM. Filter sterilize, aliquot and store at -20°C.	18 mM Dissolve in	Adenine HCl 0,05 M Stir 1 h at RT
Cholera toxin stock 0,83 mg/ml. Store at 4°C.	0,083% (v/v) Dissolve in	Cholera toxin dH_2O
Cholera toxin 0,83 µg/ml. Filter sterilize, aliquot and store at 4°C.	0,1% (v/v) 0,1% (w/v) Dissolve in	Cholera toxin stock 0,83 mg/ml BSA Hepes-buffered Earl´s salt 25 mM

EGF stock solution 1 mg/ml. Store at -20°C.	0,1% (w/v) Dissolve in	EGF dH_2O
EGF solution 1 µg/ml. Filter sterilize, aliquot and store at -20°C.	0,1% (v/v) 0,1% (w/v) Dissolve in	EGF stock solution 1 mg/ml BSA Hepes-buffered Earl´s salt 25 mM
FCS. Aliquot and store at -20°C.	500 ml	Heat inactivate at 56°C, 30 min
Freezing medium for cell line storage in liquid nitrogen.	90% 10%	Corresponding cell medium DMSO
Hydrocortisone stock 5 mg/ml. Store at -20°C.	0,5% (w/v) Dissolve in	Hydrocortisone Ethanol 100%
Hydrocortisone 0,8 µg/ml. Filter sterilize, aliquot and store at -20°C.	0,8% (v/v) 5% (v/v) Dissolve in	Hydrocortisone stock 5 mg/ml Heat inactivated FCS Hepes-buffered Earl´s salt 25 mM
Insulin 0,5 mg/ml. Filter sterilize, aliquot and store at -20°C.	0,05% (w/v) Dissolve in	Insulin HCl 5 mM
Reconstitution buffer 10x. Filter sterilize, aliquot and store at -20°C.	260 mM 2 M Dissolve in	$NaHCO_3$ Hepes NaOH 50 mM

Immunohistochemistry/ immunofluorescence		
Solution	**Final concentrations**	**Components**
Citrate buffer. Prepare fresh just before use.	18% 82% Dissolve in	Citric acid 0,1 M $C_6H_5Na_3O_7 \cdot 2H_2O$ 0,1 M dH_2O Adjust pH 6,0
H_2O_2/methanol 3%. Store at 4°C.	3% Dissolve in	H_2O_2 Methanol
Oil red O stock solution. Store at RT.	0,5% (w/v) Dissolve in	oil red O Triethyl-phosphate 60%
Oil red O working solution. Prepare fresh just before use.	60% (v/v) Dissolve in	oil red O stock solution dH_2O

4% Paraformaldehyde. Prepare fresh just before use.	4% (w/v) Dissolve in	PFA dH_2O Stir at 60°C Adjust pH 7,2 with NaOH
PBS/0,5% Triton buffer. Store at 4°C.	0,5% Dissolve in	Triton X-100 PBS
Trypsin solution 10x. Store at 4°C for 14 days.	1% (w/v) 10 mM Dissolve in	Trypsin $CaCl_2$ Tris-HCl 50 mM pH 7,8

Lipid preparation		
Solution	**Volumes**	**Components**
Folch reagent	200 ml 100 ml	Chloroform Methanol
Trans-methylation reagent	39 ml 20 ml 5 ml 2 ml	Methanol Toluene Dimethoxypropane conc.H_2SO_4

2.7 Bacteria

2.7.1 Strain

Cell line	Genotype	Company
E.coli One Shot® TOP 10	F- *mcr*A Δ(*mrr-hsd*RMS-*mcr*BC) φ80*lac*ZΔM15 Δ*lac*X74 *rec*A1 *ara*D139 Δ(*araleu*) 7697 *gal*U *gal*K *rps*L (StrR) *end*A1 *nup*G	Invitrogen, Karlsruhe, Germany

2.7.2 Medium

Medium	Composition
LB medium (Luria Bertani)	1% trypton 1% NaCl 0,5% yeast extract Dissolve in dH_2O and autoclave.
LB agar plates	1% trypton 1% NaCl 0,5% yeast extract 1,5% bacto-agar Dissolve in dH_2O, autoclave and pour in bacterial culture plates.
Ampicillin	Stock solution: 100 mg/ml. Filter sterilize aliquot and store at -20°C. Final concentration: 100 µg/ml LB-medium.

2.8 Mammalian cell lines

2.8.1 Cell lines and mediums

Cell line	Properties	Medium
H1299	Non small-cell lung carcinoma cell line (Ji *et al.*, 1999). ATCC Nr: 5803™	500 ml RPMI medium 10% heat inactivated (56°C) FCS 100 U/ml penicillin, 10 µg/ml streptomycin
HFK	Primary human foreskin keratinocytes. Cascade Biologics, Mansfield, UK.	500 ml Epilife medium 5 ml HKGS supplements 100 U/ml penicillin, 10 µg/ml streptomycin

Oral KER16	Oral keratinocyte cell line immortalized with HPV16. Kindly provided by Prof. Dr. Steinberg (Department of Operative Dentistry and Periodontology, Dental School, University of Heidelberg, Germany).	500 ml Keratinocyte medium 2 10% heat inactivated (56%) FCS Keratinocyte medium supplements 2 100 U/ml penicillin, 10 µg/ml streptomycin
J23T3	Primary murine fibroblasts. Kindly provided by Prof. Dr. Laimins (Department of Microbiology-Immunology, Feinberg School of Medicine, Chicago, USA).	500 ml DMEM medium 10% heat inactivated (56%) FCS 100 U/ml penicillin, 10 µg/ml streptomycin
Phoenix	Human embryonic kidney 293T-based amphotrophic packaging cell line. Kindly provided by Prof. Dr. Alonso (Department of cell differentiation, DKFZ, Heidelberg, Germany).	500 ml DMEM medium 10% heat inactivated (56°C) FCS 100 U/ml penicillin, 10 µg/ml streptomycin
NIKS	Spontaneous immortalized near-diplod human foreskin keratinocyte cell line (Allen-Hoffmann *et al.*, 2000).	For INCOMPLETE MEDIUM: 270 ml Ham´s F-12 medium 90 ml DMEM 5% heat inactivated (56°C) FCS 4 ml of 0,8 µg/ml hydrocortisone 4 ml of 0,83 µg/ml cholera toxin 4 ml of 0,5 mg/ml insulin 4 ml of 18 mM adenine 100 U/ml penicillin, 10 µg/ml streptomycin For COMPLETE MEDIUM: Add freshly 4 ml of 1 µg/ml EGF

2.9 Plasmids

Plasmid	Properties	Source
pcDNA3.1.(+)	Cloning vector.	Invitrogen, Karlsruhe, Germany.
pcDNA3.1.(+)-HPV20 E6-flag	Expresses HPV20 N-terminal flag-tagged E6.	Gift from Dr. Fei (Division of tumor virus characterization, DKFZ, Heidelberg, Germany).
pcDNA3.1.(+)-HPV20 E7-flag	Expresses HPV20 N-terminal flag-tagged E7.	Gift from Dr. Fei (Division of tumor virus characterization, DKFZ, Heidelberg, Germany).
pcDNA3.1.(+)-wtp53	Expresses wtp53.	Gift from Dr. Fei (Division of tumor virus characterization, DKFZ, Heidelberg, Germany).
pcDNA3.1.(+)-p53R248W	Expresses p53R248W.	Gift from Dr. Fei (Division of tumor virus characterization, DKFZ, Heidelberg, Germany).
pcDNA3.1.(+)-TAp63α	Expresses TAp63α.	Gift from Prof. Dr. G. Melino (Biochemistry IDI-IRCCS laboratory, University of Rome, Italy).
pcDNA3.1.(+)-ΔNp63α	Expresses ΔNp63α.	Gift from Prof. Dr. G. Melino (Biochemistry IDI-IRCCS laboratory, University of Rome, Italy).
pGL3 basic	Basic firefly luciferase reporter cloning vector.	Promega, Mannheim, Germany.
pGL3 basic-HPV20URR	Contains HPV20URR.	Gift from Dr. Fei (Division of tumor virus characterization, DKFZ, Heidelberg, Germany).
pRL-β-actin	Renilla luciferase reporter plasmid. Contains the minimal β-actin promoter.	Promega, Mannheim, Germany.
pLXSN	Retroviral vector.	Gift from Prof. Dr. A. Alonso (Department of cell differentiation, DKFZ, Heidelberg, Germany).
pLXSN16 E6/E7	Expresses HPV16 E6 and E7 proteins.	Gift from Prof. Dr. A. Alonso (Department of cell differentiation, DKFZ, Heidelberg, Germany).

pLXSN-GFP	Expresses GFP protein.	Gift from Prof. Dr. A. Alonso (Department of cell differentiation, DKFZ, Heidelberg, Germany).

2.10 Primers

DNA primers were purchased from Sigma-Aldrich (Taufkirchen, Germany) or DKFZ oligonucleotide synthesis core facility (Dr. Hunziker). PCR primers were obtained in desalted, lyophilised form and were dissolved in water. After cloning, all constructs were sequenced in the DKFZ sequencing core facility and verified by multiple alignment against the corresponding GeneBank sequence using the program ClustalW (EMBL-EBI**,** Heidelberg, Germany).

Primer	Melting T°
Primers for pcDNA3.1.(+) vector.	
HPV20 E6 Forward (Kozak sequence) *Bam HI* 5'- AA*G GAT CC*A CCA TGG CTA CAC CTC CTT CTT CAG AAG ACA G -3'	67°C
HPV20 E6Flag Forward (Kozak sequence) *Bam HI* *Flag* 5'- AA*G GAT CC*A CCA TG*G ACT ACA AGG ACG ACG ACG ACA AG*G CTA CAC CTC -3'	69°C
HPV20 E6 Reverse *Xba I* 5'- GC*T CTA GA*G CTT ATT GAA AAT GCT TAC ACA GCC -3'	60°C
HPV20 E7 Forward (Kozak sequence) *Bam HI* 5'- AA*G GAT CC*A CCA TGA TTG GTA AAG AGG CTA CAT TGC AAG-3'	65°c
HPV20 E7Flag Forward (Kozak sequence) *Bam HI* *Flag* 5'- AA*G GAT CC*A CCA TG*G ACT ACA AGG ACG ACG ACG ACA AG*A TTG GTA AAG-3'	67°C
HPV20 E7 Reverse *Xba I* 5'- TGC *TCT AGA* GCA TTA GGA TCC GCC ATG TTT GCA G -3'	65°C

Primers for pLXSN vector.	
HPV20 E6 Forward (Kozak sequence) *Eco RI* 5´TTA *GAA TTC* ACC ATG GCT ACA CCT CCT TCT TCA GAA GAC AG- 3´	67°C
HPV20 E6Flag Forward (Kozak sequence) *Eco RI* *Flag* 5´TTA *GAA TTC* ACC ATG *GAC TAC AAG GAC GAC GAC GAC AAG* GCT ACA C- 3´	64°C
HPV20 E6 Reverse *Bam HI* * 5´TTA *GGA TCC* TTA TTG AAA ATG CTT ACA CAG CCT ACA G 3´	60°C

RT-PCR primers.	
GAPDH forward 5'- GAA GGT GAA GGT CGG AGT -3'	53°C
GAPDH reverse 5'- GAA GAT GGT GAT GGG A -3'	47°C

Constructs:

(a) pcDNA3.1.(+)-HPV20 E6: containing the Kozak sequence. It was amplified by PCR from pcDNA3.1.(+)-HPV20 E6 and cloned into the multiple cloning site at *Bam HI* and *Xba I* restriction sites of pcDNA3.1.(+) vector.

(b) pcDNA3.1.(+)-HPV20 E6-flag: containing the Kozak sequence and a Flag-tag in N-terminal. It was amplified by PCR from pcDNA3.1.(+)-HPV20 E6 and cloned into the multiple cloning site at *Bam HI* and *Xba I* restriction sites of pcDNA3.1.(+) vector.

(c) pcDNA3.1.(+)-HPV20 E7: containing the Kozak sequence. It was amplified by PCR from pcDNA3.1.(+)-HPV20 E7 and cloned into the multiple cloning site at *Bam HI* and *Xba I* restriction sites of pcDNA3.1.(+) vector.

(d) pcDNA3.1.(+)-HPV20 E7-flag: containing the Kozak sequence and a Flag-tag in N-terminal. It was amplified by PCR from pcDNA3.1.(+)-HPV20 E7 and cloned into the multiple cloning site at *Bam HI* and *Xba I* restriction sites of pcDNA3.1.(+) vector.

(e) pLXSN-HPV20 E6: containing the Kozak sequence. It was amplified by PCR from pcDNA3.1.(+)-HPV20 E6 and cloned into the multiple cloning site at *Eco RI* and *Bam HI* restriction sites of pLXSN vector.

(f) pLXSN-HPV20 E6-flag: containing the Kozak sequence and a Flag-tag in N-terminal. It was amplified by PCR from pcDNA3.1.(+)-HPV20 E6 and cloned into the multiple cloning site at *Eco RI* and *Bam HI* restriction sites of pLXSN vector.

2.11 Enzymes

Antibody	Company	Buffer
Antarctic alkaline phosphatase	New England Biolabs, Ipswich, USA	10x AP buffer
Bam HI	Invitrogen, Karlsruhe, Germany	10x Buffer 2
Cla I	Fermentas, St. Leon-Rot, Germany	10x Buffer 1
DNase I RNase-free RQ1	Promega, Mannheim, Germany	10x DNase buffer
Eco RI	Invitrogen, Karlsruhe, Germany	10x Buffer 3
Proof start Taq DNA polymerase	Qiagen, Hilden, Germany	10x Taq buffer
Superscript II reverse transcriptase	Invitrogen, Karlsruhe, Germany	5x Superscript II RT buffer
T4 DNA-ligase	Invitrogen, Karlsruhe, Germany	5x DNA ligase buffer
Xba I	Invitrogen, Karlsruhe, Germany	10x Buffer 2
Xho I	Invitrogen, Karlsruhe, Germany	10x Buffer 1

2.12 Antibodies

Antibody against	Company	Dilution used		
		Western blot	IHC Paraffin	IHC Cryo
β-actin	MP biomedicals, Eschwege, Germany	1:10000		
Cingulin	Progen, Heidelberg, Germany			1:100
Cytokeratin 4	Progen, Heidelberg, Germany			1:2000
Cytokeratin 10	Progen, Heidelberg, Germany	1:5000		
Cytokeratin 13	Progen, Heidelberg, Germany		1:3000	
Cytokeratin 14	Progen, Heidelberg, Germany	1:80000	1:2000	

Cytokeratin 77	Prof. Langbein (DKFZ)		1:2000	
Desmoplakin I/II	Prof. Langbein (DKFZ)			1:50
Flag M2	Stratagene, CA, USA	1:500		
GFP (JL-8)	BD Biosciences, Heidelberg, Germany	1:1000		
Guinea pig-Cy3	Jackson ImmunoResearch, PA, USA		1:500	1:500
Involucrin	Sigma-Aldrich, Taufkirchen, Germany	1:500	1:100	
Loricrin	Covance, Münster, Germany		1:500	
Mouse-Cy3	Jackson ImmunoResearch, PA, USA		1:500	1:500
Mouse-Horseradish peroxidase (HRP)	Promega, Mannheim, Germany	1:5000		
p16 (50.1)	Santa Cruz Biotechnology, CA, USA	1:500		
p21 OP 64	Calbiochem, Darmstadt, Germany	1:500		
p21 (WA-1)	Progen, Heidelberg, Germany		1:500	
p53 (DO-1)	Santa Cruz Biotechnology, CA, USA	1:500		
p53 (Bp53-11)	Progen, Heidelberg, Germany		1:500	
p63 (4A4)	Santa Cruz Biotechnology, CA, USA	1:1000	1:100	
p63α (H-129)	Santa Cruz Biotechnology, CA, USA	1:1000		
PCNA (PC-10)	Santa Cruz Biotechnology, CA, USA	1:1000	1:500	
Rabbit- HRP	Promega, Mannheim, Germany	1:5000		
Rabbit-alexa 488	Molecular Probes Inc., USA		1:1000	1:1000

2.13 Markers

Markers were purchased from Fermentas GmbH (St. Leon-Rot, Germany).

Marker	Size range
GeneRuler™ DNA Ladder mix	100-10000 bp
PageRuler™ Prestained Protein Ladder	170-10 kDa
RiboRuler™ High Range RNA Ladder	200-6000 bp

3 Methods

3.1 Bacterial manipulation

3.1.1 Bacterial culture

Plasmid DNA preparation was performed in *E. coli* TOP 10 bacteria strain. Cells were grown in LB media liquid or on LB agar plates at 37°C (Sambrook, 1989). Bacteria were selected by ampicillin resistance in medium/agar containing 100 µg/ml ampillicin for all the plasmids used. The inoculation of bacterial cultures as well as the plating was carried out under semi sterile conditions using a Bunsen burner.

3.1.2 Bacterial stocks

Clones of interest were stored by freezing plasmid-containing bacterial culture. Exponent growing bacterial culture were pelleted by centrifugation at 1,000 rpm for 5 min at RT and resuspended in 1 ml LB media containing 15% glycerol, keeping them at -70°C.

3.1.3 Bacterial transformation

Ligated DNA (2 µl) (see 3.2.6.3) was transformed into 50 µl competent bacteria (*E. coli,* One Shot®, Top 10, Invitrogen) and kept 30 min on ice. After pipeting the ligated DNA, bacteria were exposed to heat shock at 42°C during 30 seconds and kept on ice for 2 min. Subsequently, pre-warmed SOC media (250 µl) was added to the cells and they were incubated at 37°C by shaking at 200 rpm for 1 h. Transformed bacteria were plated in agar plates containing 100 µg/ml ampicillin and incubated overnight at 37°C. Colonies were picked and bacteria were grown overnight at 37ºC by shaking for small scale preparations of plasmid DNA (see 3.2.1).

3.2 DNA

3.2.1 Small scale preparation

DNA mini plasmid preparation was performed with the JetQuick Plasmid Miniprep Spin Kit (Genomed) according to manufacturer´s instructions. Bacterial cultures (4 ml) were pelleted at 12,000 x g for 3 min and resuspend in 250 µl G1 solution (50 mM Tris-HCl pH 8,0, 10 mM EDTA, 100 µg/ml RNase A). Cells were lysated by adding G2 solution (250 µl) (200 mM NaOH, 1% SDS). After 5 min incubation at RT, neutralization was induced by adding G3 solution (350 µl) (contains acetate and guanididine hydrochloride) and homogenized by inverting the tube. Lysated cells were centrifuged and supernatant containing plasmid DNA was loaded in a spin column, centrifuged at 12,000 x g for 1 min, discarding the flow-through. Sample reconstitution was achieved by addition of G4 solution (500 µl) (contains ethanol, NaCl, EDTA and Tris-HCl) and centrifugation at 12,000 x g for 1 min, discarding the flow-through. Samples were centrifuged at 12,000 x g for 1 min and DNA was eluted from the column by addition of 50 µl of pre-warmed (37°C) TE buffer pH 8,0 and centrifugation at 12,000 x g for 2 min.

3.2.2 Large scale preparation

DNA maxi plasmid preparation was performed according to manufacturer´s instructions (Qiagen Plasmid Maxi Purification). Bacteria were grown for 12-16 h in 400 ml medium containing 100 µg/ml ampicillin and incubated on agitation at 220 rpm at 37°C. Bacteria were pelleted by centrifugation at 6,000 x g for 15 min at 4°C and resuspended in P1 buffer (10 ml) (50 mM Tris-HCl pH 8,0, 10 mM EDTA, 100 µg/ml RNase A) by pipetting up and down. Cells were lysed by addition of P2 buffer (200 mM NaOH, 1% SDS), mixed and incubated 15-25 min at RT. The lysis was neutralized with chilled P3 buffer (10 ml) (3 M potassium acetate, pH 5,5), vigorously inverted 4-6 times and incubated on ice for 20 min. Samples were centrifuged at 20,000 x g for 30 min at 4°C and supernatant was promptly removed and centrifuged again at 20,000 x g for 15 min at 4°C. Qiagen-tip columns were equilibrated with Buffer QBT (10 ml) (750 mM NaCl, 50 mM MOPS pH 7, 15% isopropanol, 0,15% triton X-100) and allowed to empty by gravity flow. Lysates were applied to the Qiagen-tip columns and cleared by filtration. Columns were washed twice with Buffer QC (30 ml) (1 M NaCl, 50 mM Tris-HCl pH 8,5, 15% isopropanol) and DNA was eluted by addition of Buffer QF (15 ml) (1,25 M NaCl, 50 mM Tris-HCl pH 8,5, 15% isopropanol).

DNA precipitation was performed by adding 10,5 ml isopropanol to the eluted DNA and centrifugation at 15,000 x g for 30 min at 4°C. DNA was washed with 70% ethanol (5 ml) and centrifuged at 15,000 x g for 15 min at 4°C. Pelleted DNA was air dried in a SpeedVac concentrator and allowed to dissolve overnight at 4°C in TE buffer, pH 8,0.

3.2.3 Determination of nucleic acid concentration

The DNA or RNA concentration was determined photometrically by measuring the absorbance at 260 nm. The spectrophotometer was calibrated using the same solution as the solvent for the correspondent nucleic acid. The concentration was calculated as follows:

Single-stranded DNA (µg/ml) = 33 x OD_{260} x dilution factor
Double-stranded DNA (µg/ml) = 50 x OD_{260} x dilution factor
RNA (µg/ml) = 40 x OD_{260} x dilution factor

The purity of the preparation was determined by calculating the ratio OD_{260nm}/OD_{280nm}. DNA was considered free of protein contamination when the range was between 1,7-2,0. Pure RNA ratio should be in the range of 1,9-2,1.

3.2.4 Agarose gel electrophoresis

For a 1 % (w/v) gel, 1 g agarose was dissolved in 100 ml EP buffer and was brought to boil in a microwave oven. The solution was allowed to cool down and was poured into the casting gel. Once agarose gel had solidified, the electrophoresis tray was filled with EP buffer and the casting gel was placed in it. DNA loading buffer was added to the samples, loaded into wells and runned at 100 V. The DNA was stained with ethidium bromide solution (0,5 µg/ml) for 10 min and visualized under UV light.

3.2.4.1 DNA isolation from agarose gels

DNA fragments generated by PCR or by restriction digestion were separated by electrophoresis depending on their sizes on 0.8-1.5% agarose gels at 100V. Subsequently, the agarose gel was incubated in ethidium bromide solution (0,5 µg/ml) for 10 min, analyzed under UV light (366 nm) and the fragment of interest cut from the gel.

The DNA extraction from the agarose fragment was performed using the JetQuick Gel Extraction Spin Kit from Genomed according to manufacturer´s instructions. Agarose fragment was dissolved in L1 buffer (contains $NaClO_4$, sodium acetate and TBE solubilizer), with 300 µl L1/100 mg gel slice. Samples were incubated 15 min at 50°C in a water bath, inverting the tubes every 3 min to ensure agarose solubilization. Samples were placed in a JetQuick spin column and centrifuged at 12,000 x g for 1 min. Supernatant was discarded and silica filter was washed twice with 500 µl of L2 buffer (contains ethanol, NaCl, EDTA and Tris-HCl), discarding the flow-through. DNA was eluted by adding 50 µl 10 mM Tris-HCl pH 8,0 and centrifugation at 12,000 x g for 2 min.

3.2.5 Polymerase Chain Reaction (PCR)

For cloning, suitable primer pairs were designed to incorporate appropriate restriction enzyme sites followed by sequences that were complementary to the ends of the desired insert. Primers were designed with the presence of two bases preceding the restriction enzyme site to improve the efficiency of restriction enzyme digestion of the fragment (Dieffenbach *et al.*, 1993).

Final concentrations of the reagents in an example reaction contained 100 ng of template DNA, 0,5 µM forward and reverse primers, 200 µM of dNTPs, 2,5 units of Proof Start Taq Polymerase and the correspondent enzyme buffer in a final volume of 50 µl.

Annealing temperatures were adapted for each reaction, depending on the primers used and were calculated with computer analysis using the program OligoAnalyzer 3.1 (see appropriate melting temperature (Tm) in section 2.9). Elongation time was different for each reaction and was calculated depending on the lengh of the amplified fragment (1 kb/min). An example PCR thermocycle protocol was:

Cycles	Time	Temperature	Step
1 x	4 min	94 °C	Denaturation
30 x	30 sec	94° C	Denaturation
	45 sec	Temperature depending on primer´s Tm	Annealing
	variable	72°C (time depending on fragment´s lengh, 1kb/min)	Elongation
1 x	10 min	72°C	Elongation
	∞	4°C	

3.2.6 Cloning

3.2.6.1 Digestion of DNA using restriction enzymes

Vector (10 µg) or PCR product (200 ng) was cut with 10 U enzyme/µg DNA for 1 h at 37°C in the corresponding buffer. Enzyme was inactivated by incubation at 65°C during 20 min.

DNA was purified using the JetQuick PCR Purification Spin Kit according to manufacturer´s instructions. H1 buffer (400 µl) (contains guanidine hydrochloride and isopropanol) was added to 100 µl PCR product. Spin column was loaded with the H1 buffer-PCR product mixture and centrifuged at 12,000 x g for 1 min. Flow-through was discarded and column was washed twice by adding 500 µl H2 buffer (contains ethanol, NaCl, EDTA and Tris-HCl) and centrifugation at 12,000 x g for 1 min. DNA was eluted by adding 10 mM Tris-HCl pH 8,0 and centrifugation at 12,000 x g for 2 min.

Restricted fragments volumes were too low to be quantified espectrophotometrycally. Instead, quantification was performed by agarose gel electrophoresis, comparing the intensity of the bands to the known concentration of the marker bands.

3.2.6.2 Dephosphorylation of DNA

In order to avoid vector recircularization, phosphate groups were removed by phosphatase treatment. After restriction and purification, 1 µg of digested plasmidic DNA was incubated with 5 U of antartic alkaline phosphatase and its corresponding buffer for 1 h at 37°C. The solution was incubated 10 min at 65°C for inactivating the enzyme. After purification with the JetQuick PCR Purification Spin Kit (see 3.2.6.1), the vector was quantified by electrophoresis.

3.2.6.3 Ligation

The ratio between the molarity of the vector and fragment was calculated according to the size of the insert. The ligation reaction was prepared by mixing 20 fmoles of linearized and dephosphorylated plasmid with 60 fmoles of the cut DNA fragment with compatible ends, 5 U of T4-ligase and 1x T4-ligase buffer in a final volume of 20 µl. The ligation was carried out overnight at 14°C and ligase was inactivated by incubation at 65°C during 10 min. The DNA molarity was calculated as follows:

$$\text{Fmoles} = \text{ng}/\mu\text{l} : \text{kb} \times 0.66$$

Efficiency of ligation was controlled by electrophoresis of the reaction mixture before and after T4-ligase incubation, comparing the amount of linearized vector and fragment before and after ligation. Ligation mix was used for bacterial transformation (see 3.1.3).

3.2.6.4 Analysis of transformed clones

After transformation (see 3.1.3) colonies were selected and plasmid DNA was extracted. Small scale DNA preparation (20 µl) was restricted with the appropriate enzymes in a volume of 50 µl as described (see 3.2.6.1). Clones harbouring the insert of correct size were sequenced and large scale DNA preparations were performed (see 3.2.2).

3.3 RNA

3.3.1 RNA isolation from cultured cells

Prior to extraction, surfaces and equipment were extensively cleaned with ethanol and rinsed with DEPC-treated water. RNA isolation from 145 mm diameter cell culture plates was performed using the Qiagen RNeasy® mini kit, following manufacturer´s instructions. Briefly, cells were washed and lysed directly in the cell culture plate with 600 µl RLT buffer. Lysates were homogenized by pipetting into a QIAshredder™ spin column and centrifugation at 12,000 x g for 2 min. Homogenized lysate (corresponding to the flow-through) was combined with 1 vol 70% ethanol and the samples were mixed by inverting the tubes several times. Samples were transferred to an RNeasy spin column and centrifuged at 8,000 x g for 15 sec. Flow-through was discarded. Column was washed by addition of 700 µl RW1 buffer and centrifugation at 8,000 x g for 15 sec, discarding the flow-through. RPE buffer (500 µl) was added to the column and centrifugated at 8,000 x g for 15 sec. Flow-through was discarded and again 500 µl RPE buffer were added, followed by centrifugation at 8,000 x g for 2 min. Column was centrifuged at 10,000 x g for 1 min to eliminate any possible carryover of the buffers. Total RNA was eluted in 50 µl RNase-free water. Each sample (2 µl) was separated by electrophoresis in 1% agarose gel (see 3.2.4) and possible RNA degradation was controlled by visualizing intact 28S, 18S and 5S rRNA bands.

3.3.2 DNAse I treatment

DNAse I treatment was performed to prevent cellular DNA contamination in the PCR reaction. Total RNA (2 µg) was incubated for 30 min at 37°C with 2 units of DNAse I (RQ1 RNase-Free DNase I, Promega, Mannheim, Germany) and its corresponding DNase I buffer in a final volume of 10 µl. Reaction was stopped by adding 1 µl of DNAse I stop solution provided with the enzyme and 10 min incubation at 65°C.

3.3.3 cDNA synthesis by Reverse Transcriptase-Polymerase Chain Reaction (RT-PCR)

Total RNA was used as substrate for single strand cDNA synthesis. RNA (2 µg) was mixed with 2 µl of 50 µM random hexamers, 0,4 µl of 25 mM dNTPs in 12 µl final volume. Samples were incubated at 70°C for 10 min to minimize RNA secondary structure, shortly spinned and placed 1 min on ice. Subsequently, 4 µl 5x Superscript II RT buffer, 0,5 µl RNase inhibitor RNasin® and 2 µl 0,1 M DTT were added to each tube. Mix was placed 2 min at 25°C and 1 µl Superscript II reverse transcriptase was added. Samples were incubated 10 min at 25°C (necessary for pre-incubation of random hexamers). Retrotranscription was performed for 50 min at 42°C followed by heat inactivation for 15 min at 70°C. Genes of interest were amplified by PCR as previously described (see 3.2.5). Control of DNA contaminations was done by performing RT-PCR reactions without reverse transcriptase, where retrotranscription from mRNA to cDNA does not happen and, therefore, DNA amplification after PCR must correspond to DNA contamination.

3.4 Protein

3.4.1 Protein extraction

3.4.1.1 Passive lysis buffer

For HPV20 promoter activity studies, cells were lysed with passive lysis buffer contained in the Dual-Luciferase® Reporter (DLR™) Assay System kit. Cells growing in six-well plates were washed twice with ice cold PBS. Pre-chilled passive lysis buffer (200 µl) was applied in the wells, gently rotated at 4°C, and cells were scraped while kept on ice.

Subsequently, the samples were centrifuged at 10,000 rpm for 10 min at 4 ºC to pellet the undissolved material. Samples were stored at -70 ºC until use.

3.4.1.2 RIPA buffer

For protein isolation from monolayer cultured cells, medium was removed from the cell culture plates and centrifuged for 2 min at 1,000 rpm and 4°C, discarding the supernatant. Cells were washed twice with ice cold PBS and 150 µl fresh RIPA buffer (see 2.6) was applied per 10^6 cells.

Cells were scraped from the cell culture plate while kept on ice and samples were incubated in severe agitation for 5 min at 4°C. Sonicator was filled with ice and water, tubes were submerged and sonicated during 5 min (30 sec cycles). Extracts were centrifuged at 10,000 rpm for 10 min at 4°C to pellet undissolved material and stored at -70°C.

3.4.1.3 Organotypic culture protein isolation

Epithelial cell cultures were isolated by loosen the keratinocyte culture from the surrounding transwell with the help of a scalpel. Then, the epidermal layer was separated from the collagen matrix, mixed with 150 µl of organotypic culture protein extraction buffer (see 2.5) and lysed manually in a chilled glass tissue grinder (Dounce). Lysates were cleared by centrifuging at 10,000 rpm for 10 min at 4°C and proteins were stored at -70°C.

3.4.2 Protein quantification

Protein concentration was measured using a protein quantification reagent (BioRad Protein Assay), following the Bradford method (Bradford, 1976). This is a colorimetric assay method based on the change in absorbance of the Coomassie Brilliant Blue G-250 dye, which shifts from 465 nm to 595 nm when it binds to proteins. The increase of absorbance at 595 nm is proportional to the amount of dye coupled to proteins.

Protein samples (2 µl) were mixed with 20 µl of urea-β mercaptoethanol buffer and boiled at 95°C for 5 min. The BioRad Protein Assay reagent was prepared by diluting it 1:5 with dH_2O and added to the protein mixture. Absorbance was measured at 595 nm. BSA at given concentration was used as reference.

3.4.3 SDS-polyacrilamide gel electrophoresis

Proteins were separated by SDS-polyacrylamide gel electrophoresis (SDS-PAGE). SDS denatures the proteins and covers them with equal negative charges, allowing them to migrate in an electric field. Proteins were mixed with SDS-loading buffer (1x final concentration) and heated for 5 min at 95 ºC before loading.

Polyacrylamide gels contained an upper stacking gel that concentrates the samples in the gel, ensuring that all proteins in the sample enter the lower resolving gel simultaneously. The lower resolving gel had a 10-15% polyacrilamyde concentration, depending on the size of the proteins of interest.

The electrophoresis was run at 100 V in 1x protein running buffer (see 2.6) until the bromophenol blue dye of the sample buffer (corresponding to 6,7 kDa) had run out of the gel.

3.4.4 Western blot

3.4.4.1 Transfer of proteins onto nitrocellulose membrane

To transfer proteins from a polyacrylamide gel onto a nitrocellulose membrane a Protein Minigel Wet Transfer System (BioRad) was used. All the components of the blotting sandwich were soaked in 1x blotting buffer (see 2.6) and placed avoiding the formation of air bubbles as follows: a sponge pad, two sheets of Whatman filter, the nitrocellulose membrane, the polyacrylamide gel, two sheets of Whatman filter paper and a sponge pad. This sandwich was placed in the anode part of the cassette, the cuvette was filled with 1x blotting buffer and the proteins were allowed to transfer at 4°C at 100 V for 1.30 h or 30 V overnight.

3.4.4.2 Immunoprobing of nitrocellulose membranes

After the transfer, the membrane was washed in TBS-T buffer (see 2.5) and incubated on a platform shaker for 1 h in blocking buffer (5 % w/v non-fat milk powder in TBS-T). Primary antibody was added to blocking buffer at the appropriate concentration (see listed antibodies 2.12) and incubated overnight at 4°C on a platform shaker. The membrane was subsequently washed in TBS-T (3 x 15 min) and then exposed to a secondary antibody diluted in blocking buffer for 1 h at RT. After membrane washing in TBS-T (3 x 15 min), proteins were detected using a Western blotting detection reagent (ECL system, Amersham Biotech) following manufacturer´s instructions. Signals were visualized on autoradiograph ECL film.

For anti-Flag antibody, all steps were carried out in TBS buffer and the blocking buffer composition consisted in 3% non-fat powder milk in TBS.

3.4.4.3 Densitometric analysis

After Western blot, X-ray films were quantified by using the ImageQuant 5.0 software.

3.5 Cell culture

3.5.1 Culturing of cell lines

Cells were grown in an incubator at 37 °C in a 5 % carbon dioxide / 95 % humidity atmosphere. For cell detachment, medium was removed, cells were washed with PBS/EDTA and incubate in trypsin/EDTA solution. Trypsin was inactivated by adding cell culture media containing FCS. Cells were centrifuged at 1,000 rpm for 10 min at RT, counted and seeded onto new plates. Primary foreskin keratinocytes are too sensitive to normal trypsin/EDTA; instead, Keratinocyte Detach Kit2-125 (Promocell) was used. Cells were washed with Hepes solution, trypsinized and reaction was blocked by adding a trypsin neutralizer following the protocol provided by the supplier (Hepes solution, trypsin and trypsin neutralizer contained in the kit).

H1299 cells were split 1:5 and medium was changed every 3 days. One vial of primary foreskin keratinocytes was initially plated in 3 T-75 flasks and cells were refed every 3 days and split 1:2. Phoenix cells were split 1:10 and medium was change every second day. Oral keratinocytes immortalized with HPV16 (oral KER16) were split 1:3 and medium was replaced every 3 days. NIKS were maintained as subconfluent cultures on a mitomycin C-treated J23T3 fibroblast feeder layer in NIKS medium. Mitomycin C irreversibly damages DNA, arresting the fibroblast cell cycle. J23T3 fibroblasts were treated with 8 µg/ml mitomycin C for 2-4 h at 37°C. Cells were then washed with PBS/EDTA, trypsinized and split 1:3 in incomplete NIKS medium. Next day, NIKS cells were plated over the treated J23T3 cells. After one day, medium was changed to complete NIKS medium and cells were refed every 3 days.

3.5.2 Cell lines cryopreservation

Cells (10^6-10^7) were pelleted by centrifugation at 1,000 rpm for 10 min at RT and resuspended in 0,5 ml medium containing 10% DMSO. Cryotubes were placed immediately in a -80 °C freezer. After one week, the cells were transferred to liquid nitrogen containers. Cells were thawed by warming them in at 37 °C, centrifugated at 1,000 rpm for 5 min at RT and seeded in fresh medium.

3.5.3 Determination of cell number and viability

Cells were counted with the help of a hemocytometer (Neubauer cell counting chamber, depth 0,1 µl) and an optical microscope Wilovert S.

Trypan blue dye (0,02%) was used to distinguish dead cells and calculating cell viability. This vital dye is negatively charged and does not interact with the cell unless the membrane is damaged. Therefore, all the cells which exclude the dye are viable whereas stained ones correspond to dead cells.

3.5.4 Transient transfection

H1299, Phoenix and oral KER16 cell lines were plated one day prior transfection at $2{,}5x10^4$ cells/cm^2, $2x10^4$ cells/cm^2 and $3x10^4$ cells/cm^2 respectively. Transfection was performed using Plus Reagent- Lipofectamine following manufacturer´s instructions. Plus Reagent enhances the transfection efficiency while lipofectamine is a mixture of 2,3-dioleyloxy- N- [2(spermine-carboxamido)ethyl]- N,N- dimethyl-1 - propanaminiumtrifluoro-acetate (DOSPA) -a polycationic synthetic lipid- and phosphatidyl-ethanolamine -a fusogenic lipid. This lipid mixture spontaneously associates with nucleic acids (negatively charged), forming lipoplexes. Mixture lipid-DNA results in the formation of structures that fuse and pass through the plasma membrane, delivering the DNA into the cell.

DNA was dissolved in OPTI-MEM medium (10 µl/cm^2) and combined with Plus Reagent (1,2 µl/cm^2), following by incubation for 15 min at RT. Lipofectamine (0,8 µl/cm^2) was added to the this preparation, mixed and incubated for 15 min at RT. Medium was removed from the cells and the complexed DNA mixture was carefully spread drop-wise over the cells. After 3 h, normal cell culture medium without penicillin/streptomycin was added and cells were returned to the incubator for 24 h. Moreover, oral KER16 were treated in two different forms in order to compare best protocol for Lipofectamine reagent: in a subset of the

cells the medium was removed and replaced for OPTI-MEM 3 h prior transfection whereas in the other subset the medium was not replace before the transfection procedure.

Oral KER16 were also transfected with Lipofectamine 2000 and FuGENE HD reagent in order to choose the method with highest transfection efficiency. Cells were plated one day prior transfection at a density of $3x10^5$ cells per 35 mm diameter cell culture plate. For Lipofectamine 2000, 2 µg DNA were diluted in 250 µl OPTI-MEM, gently mixed and incubated for 5 min at RT. Then, diluted DNA was combined with 10 µl Lipofectamine 2000 plus 250 µl OPTI-MEM and incubated for 20 min at RT. Medium was removed from the cells and the complexed DNA mixture was carefully spread drop-wise over the cells. After 3 h, normal cell culture medium without penicillin/streptomycin was added and cells were returned to the incubator for 24 h. Similarly to the Lipofectamine protocol, two variants of the protocol were done; one where medium was replaced by OPTI-MEM 3 h prior transfection and other with no medium replacement until the transfection was performed. For FuGENE HD transfection, 2 µg DNA were diluted in 100 µl OPTI-MEM and incubated for 15 min with FuGENE HD reagent. Different FuGENE HD reagent (µl):DNA (µg) ratios were used (3:2, 4:2, 5:2, 6:2, 7:2) in order to optimize the protocol for best transfection efficiency. The mix was added drop-wise over the cells fed with 2 ml normal cell culture medium without penicillin/streptomycin. Proteins were extracted 24 h after transfection.

3.5.5 Luciferase assay

The luciferase dual reporter assay was used to investigate the promoter activity of the HPV20, cloned upstream of the reporter gene Firefly Luciferase. One day prior transfection, $2{,}5x10^5$ H1299 cells or $2{,}5x10^5$ oral KER16 cells were plated in 6-well plates.

H1299 cells were co-transfected with the Firefly reporter construct pGL3-HPV20 URR (1 µg/well), together with the pRL-β-actin *Renilla* reporter plasmid (0,1 µg/well) and with or without wtp53, mutp53R248W, TAp63α ΔNp63α plasmids (1 µg/well), or HPV20 E6 (2 µg/well).

Oral KER16 were co-transfected with the Firefly reporter construct pGL3-HPV20 URR (1 µg/well), together with the pRL-β-actin *Renilla* reporter plasmid (0,1 µg/well) and HPV20 E6 (2 µg/well) and/or HPV20 E7 (2 µg/well). After 24 h cells were lysed and stored at -70°C (see 3.4.1.1). Promoter activity was quantified by adding the Firefly Luciferase substract Luciferase Assay Reagent II (LAR II) (100 µl) to 20 µl of lysed extract generating a luminescent signal. After quantifying the Firefly luminescence, the reaction is quenched and

the *Renilla* luciferase reaction was initiated simultaneously by adding Stop & Glo® Reagent (contains coelenterazine, the substract for *Renilla* luciferase) (100 µl) to the same sample. All experiments were performed in triplicates.

3.5.6 Retroviral production

Retroviruses were used to create stable cells expressing the gene of interest. These vectors integrate in the host cell genome, ensuring continuous gene expression. Phoenix™ amphotrophic cell line (Orbigen Inc., San Diego, Ca, USA) is a helper free packaging cell line derived from human embryonic kidney cell line 293-T transformed with adenovirus type 5 (Ad5) and polyomavirus SV40. Phoenix™ cells contain the retroviral genes gag, pol and env, the retroviral origin of replication and the RNA Ψ packaging signal necessary for producing retroviral particles. Retroviruses produced from these cells can infect the target cells and integrate into the host genome. However, they are replication deficient because they lack the corresponding viral machinery.

High titers of recombinant retroviruses were produced by transfecting subconfluent Phoenix™ with 21 µg retroviral DNA using Lipofectamine reagent (see 3.5.4). One day prior transfection $29x10^5$ cells were plate in a 145 cm^2 cell culture plate. Maximal retroviral production is achieved 30 h post-transfection (Pear, 1997). Therefore, 24 h post-transfection the medium containing retroviruses was collected (named *supernadant 1*), new medium was added and collected again 48 h after transfection (named *supernadant 2*). Viral supernatants were kept at -70°C until used.

3.5.6.1 Transduction of target cells

HFK and NIKS target cells were subconfluent at the time of infection. Polybrene was added at a final concentration of 6 µg/ml to the viral supernatant to increase retroviral gene transfer (Davis *et al.*, 2002). Viral supernatant collected 48 h after transfection (*supernadant 2)* was filtered (Whatman Puradisc filter, 0,45 µm) to remove any cell debris and added to the cells, replacing the medium after 3 h. After 24 h, *supernadant 1* was filtered and applied to the cells. Medium was replaced after 3 h and cells were incubated overnight. Cells that incorporated the retrovirus in their genome were selected by antibiotic resistance contained in the retroviral vector. The cells were trypsinized and plated in medium containing geneticin sulphate (G418) (100 µg/ml). Uninfected cells were exposed to the antibiotic to determine the end point of selection: when all uninfected cells were dead we assumed that all surviving cells

in the transduced sample corresponded to cells that had incorporated the retrovirus in the genome (5-7 days).

Retroviral transduction into NIKS was done in subconfluent cells without feeder layer. Stable clones were propagated on fresh mytomicin C-treated feeder layer in NIKS medium, expanded (4 to 8 passages) and used for organotypic raft cultures.

3.5.6.2 Study of life span

Growth of primary keratinocytes retrovirally transduced was monitored. Cells were passaged when the confluency was approximately 80%. The population doubling (PD) corresponds to a two-fold increase in the total number of cells in a culture and it is used to study the growth rate and life span of cells. PD was calculated considering the split ratio and the number of cells until they died.

3.5.7 Organotypic raft cultures

HPV life cycle is linked to the differentiation of stratified squamous epithelia (reviewed in Longworth and Laimins, 2004). Organotypic culture is a three-dimensional system that develops well-ordered epithelia, thus offering an opportunity to analyze the cellular mechanisms of tissue formation, such as cell-cell interactions and the regulation of proliferation and differentiation. It is a very useful tool to investigate the role of individual viral genes or full viral life cycle (reviewed in Stark *et al.*, 2004). In this model, cells are nourished by diffusion from below. Keratinocytes are plated on a matrix of collagen type I, extracted from rat tail tendon. To serve as functional dermal equivalents, the collagen gels contain viable fibroblasts which produce extracellular matrix components comparable with the *in vivo* situation (**Fig. 9**).

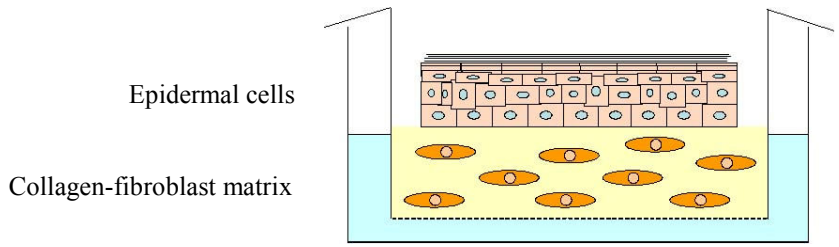

Figure 9. Schematic illustration of the organotypic culture system.

When using HFK it is necessary that the HPV used extend the life span of the cells in order to have sufficient cell generations to form differenting epithelia. In our studies we used NIKS cells that display normal differentiation properties in organotypic cultures, mimicing the natural host of HPV.

3.5.7.1 Preparation of dermal equivalent matrix

Collagen mix (in a proportion 8:1:1 rat tail collagen type 1, reconstitution buffer and 10x DMEM) was prepared on ice by resuspending $3x10^5$ fibroblast in 10x DMEM followed by adding the reconstitution buffer (see composition in section 2.6) and finally mixing by pipetting with rat tail collagen type I with the help of a disposable pipet. Collagen mix (2 ml) was placed in a filter insert and allowed to solidify by incubation at 37°C for 1 h in a humified incubator. Collagen dermal equivalents composed of collagen mix and embedded J23T3 fibroblasts (Davy, 2005) were maintained in complete immersion in NIKS medium without EGF in 6-well-deep plates for four days.

3.5.7.2 Raft cultures

Stably transduced pLXSN-, pLXSN- HPV20 E6-Flag or pLXSN-HPV16 E6/E7 NIKS cells were seeded onto collagen dermal equivalents ($1x10^6$ cells/ transwell). Medium was replaced with complete NIKS medium 24 h later and cells were cultured for 5 days. Medium was added to the level of the collagen matrix, thus restricting nourishment to diffusion from below. This air-lift procedure was defined as the start of the culture time. From this moment, incomplete NIKS medium was replaced every second day. BrdU (50 µg/ml) was added 12 h prior to harvest on day 14 in all the samples. Rafts were either fixed overnight in 4% formalin followed by embedding in paraffin (for immunohistochemistry and immunofluorescence), or embedded in Tissue Tek-OTC and subsequently snap frozen in liquid nitrogen vapour (for barrier function studies), or fixed in resin (for electron microscopy analyses). Organotypic raft cultures were repeated at least 3 times for each stable cell line.

3.5.7.3 Barrier function analyses

Lucifer yellow penetration assay

To assess the functionality of the stratum corneum in the epidermal equivalents, outside-in epidermal barrier was investigated. Lucifer Yellow (1mM) dissolved in PBS (pH 7,4) was placed over the epidermal surface of the organotypic raft cultures for 1 h as previously described (Koch *et al.*, 2000). Raft cultures were subsequently embedded in Tissue Tek-OCT and snap frozen in liquid nitrogen. Serial sections were cut at -20°C using a cryostat Leica CM3050S at a thickness of 5 µm and air dried for 15 min before storage at -70°C. Cryosections were counterstained with Hoechst dye 33258 and penetration of the dye was assessed by immunofluorescence microscopy observation (microscope Leitz DM RBF and firewire fluorescence camera F-View II).

Biotin uptake assay

To examine whether the viral-containing organotypic rafts had an increased inside-out permeability due to alterations in tight junctions (present in the stratum granulosum), Biotin uptake was examined. Biotin was added at a final concentration of 2 mg/ml to the raft culture media as previously described (Furuse *et al.*, 2002). After 30 min, epidermal equivalents were washed with PBS, embedded in Tissue Tek-OCT, snap frozen in liquid nitrogen and stored at -70°C. Serial sections were cut at -20°C using a cryostat Leica CM3050S and air dried for 15 min before storage at -70°C. Sections were defrosted at RT for 15 minutes and then rehydrated with PBS for another 15 minutes. To follow the penetration of the Biotin, sections were stained with Alexa 488- labelled streptavidin and nuclei were counterstained with Hoechst 33258 dye. Samples were analyzed using a Leitz DM RBF microscope and fluorescent staining was visualized using a F-View II firewire fluorescence camera.

3.6 Immunohistochemistry

Embedding in paraffin (Paraffin Paraplast® Plus) and cutting of organotypic cultures was performed in the Department of Cellular and Molecular Pathology (Prof. Dr. H.-J. Gröne).

Samples were fixed overnight in 4% formalin, dehydratated in increasing ethanol solutions and embedded in paraffin for 1 h at 60°C. Blocks were cut by sequential sections of 5 µm thickness using a microtome (Leica RM2235), placed on microscope slides Super-

frost® Plus, and allowed to dry for 1 h at 65°C. Slides were kept at RT until use. Sections of rafts were deparaffinized 3x 5 min in xylene. Rehydratation was performed by incubation in a serial grade of ethanol solutions 100%, 95%, 80%, 70% and 50% for 5 min each. All the incubation steps were performed placing the slides in a wet chamber in order to avoid the drying of the samples. Leaking of the solutions was prevented by encircling the tissue samples using a Pap Pen Liquid Blocker creating a water repellent barrier around the tissue.

3.6.1 Haematoxylin-eosin staining

Morphological study of the organotypic culture sections was done by haematoxylin-eosin staining visualization. The staining was performed in the Department of Cellular and Molecular Pathology (Prof. Dr. H.-J. Gröne).

Haematoxlyin is a basic dye which colours basophilic structure in blue (nucleic acid-containing structures, such as cell nucleus and ribosomes). Acidic eosin Y colours proteins and most of the cytoplasm in pink.

Samples were fixed in formalin, embedded in paraffin, and sectioned as described (see 3.6). After deparaffinization and rehydratation, samples were dipped into hematoxylin for 10 sec and washed with tap water for 10 min. Eosinic staining was performed by quick dipping into eosin solution followed by washing 10 min in tap water. Samples were dehydrated through changes in ethanol solutions with increasing concentrations (95%-100%-100%, 5 min each), incubated 2x5 min in xylol, and mounted using Eukitt® solution. Immunohistochemical staining was documented using a digital colour camera Colorview II.

3.6.2 Fluorescence microscopy immunohistochemistry

Histological examination was performed on sections (5 µm) of paraffin-embedded raft cultures. Serial sections were stained for keratins 4, 10, 13, 14, 16 and 77, loricrin, involucrin, desmoplakin I/II, PCNA, BrdU, cingulin and p63. After deparaffinization and rehydratation, antigen retrieval was achieved by heating at 98ºC during 15 min in 10 mM citrate buffer (pH 6,0) (see 2.5). Slides were cooled and washed in H_2O and PBS. Samples were trypsinized (0,001% trypsin in 0,05 M Tris-HCl) for 15 min at 37ºC, followed by washing in PBS. Tissue sections were blocked in 1% BSA/PBS for 1 h. The respective primary antibody was added and incubated overnight in a humid chamber. The following day slides were washed 3x5 min in PBS. Mouse and guinea pig primary antibodies were detected using Cy3–conjugated-goat anti-mouse and Cy3-conjugated-goat anti-guinea pig, respectively. Rabbit primary antibody

was detected with Alexa 488 goat anti-rabbit. Secondary antibodies were incubated for 40 min in the dark and counterstained with Hoechst 33258 dye. Incorporated BrdU was detected using streptavidin-Alexa 488 and counterstained with Hoechst 33258 dye. Samples were washed in H_2O and mounted using Fluoromont G.

All slides were examined using a Leitz DM RBF microscope whereas fluorescent staining was visualized using an F-View II firewire fluorescence camera.

3.6.3 Light microscopy immunohistochemistry. Avidin-Biotin-peroxidase Complex

p53 and $p21^{CIP1}$ protein localization was visualized by light microscopy using the Vectastain®ABC *Elite*® system, were the avidin binds with high affinity to secondary antibody coupled to Biotintylated horseradish peroxidase. DAB is used as substrate for the peroxidase enzyme, giving a brownish color to positive cells.

Samples were treated as described for fluorescence microscopy immunohistochemistry (see 3.6.2) with the exception that before blocking, endogenous peroxidase activity was quenched by incubation with 3% hydrogen peroxide in methanol for 15 min at RT. Slides were incubated overnight with the primary antibody in a wet chamber, 3x5 min washed in PBS and incubated with Biotintylated anti-mouse secondary antibody for 30 min. After washing for 5 min in PBS, ABC reagent was added for 30 min. Samples were exposed to DAB as substrate for peroxidase until the desired colour intensity was obtained. Sections were counterstained with Meyers´ hemalaum, dehydrated through changes in ethanol solutions with increasing concentrations (95%- 100%- 100%, 5 min each), incubated 2x5 min in xylol, and mounted using Eukitt® solution. Immunohistochemical staining was documented using a digital colour camera Colorview II.

3.6.4 Lipid staining

Cryosections were stained for lipid visualization using oil red O (Koopman *et al.*, 2001). Tissue samples were fixed in 3,7% formaldehyde for 1 h, washed in PBS for 5 min and incubated with a oil red O working solution (see composition in section 2.6) for 30 min. Nuclei were counterstained with Meyers´ hemalaum, samples then dehydrated in aqueous solution with increasing alcohol content and slides mounted using Fluoromont G.

3.7 Electron microscopy

Electron microscopy was performed in the Department of Cellular and Molecular Pathology (Prof. Dr. H.-J. Gröne). Organotypic cultures were isolated from the transwell inserts and fixed in Karnovsky solution (2% paraformaldehyde and 0,5% glutaraldehyde) for 2 h at 4°C. Samples were rinsed in 1 M cacodylate buffer and subsequently fixed in 2% osmium tetroxide for 1 h. The specimens were dehydrated in increasing concentrations of ethanol and embedded in Araldite® epoxy resin. Ultrathin sections were performed in a ultramicrotome Leica Ultracut UCT and were stained with 0,7% lead citrate for 5 min and 1% uranyl acetate for 10 min. Samples were visualized by transmission electron microscopy (EM 900, Zeiss).

3.8 Gas chromatography- mass spectrometry

Lipid composition of the skin equivalents was studied by gas chromatography-mass spectrometry (GC-MS). Analysis was performed in the Deparment of Toxicology (Prof. Dr. R. Owen). Samples were mixed with the internal fatty acid standards for palmitic acid, stearic acid and oleic acid at 250 µg/ml in methanol. Then, 3 ml of Folch reagent (see 2.6) was added, whirly mix for 2 min and centrifuged at 2,000 x g for 10 min at 4°C. Supernatant was removed and samples dried under a stream of nitrogen gas. Pellet was resuspend with 900 µl heptane and 900 µl trans-methylation reagents (see 2.6) and incubated at 80°C for 60 min. Two phases could be distinguished in the samples and the upper heptane phase, corresponding to the fatty acids, was carefully removed for further analysis.

Analyses were performed using a HP 5973 mass selective detector coupled to a HP 5890 gas chromatograph. Sample volumes of 1 µl of the hexane phase were injected into the gas chromatograph. Separation was achieved using a HP 5MS capillary column (30 m × 0,25 mm I.D, 0,25 µm film thickness). Helium was used as carrier gas with a linear velocity of 0,9 ml/s. The oven temperature program was: initial temperature 100°C, 100-160 °C at 4 °C/min, 160-270°C at 2°C/min. The GC injector had a temperature of 250°C whereas the transfer line temperature was held at 280°C. The mass spectrometer parameters for EI mode were: ion source temperature: 230°C; electron energy: 70 eV; filament current: 34,6 µA; electron multiplier voltage: 1200 V. Standard curves of authentic standards were generated under similar conditions in the range of 5-100 µg/ml.

Three samples of each raft type were analyzed for lipid composition and comparisons between groups were performed by t-test. Multiplicity of testing was accounted by adjusting p-values according to stepdown Bonferroni method (significance at p<=0.05).

3.9 Flow cytometry

Flow activated cells sorting (FACS) distinguishes cells according to their size, structure, cell surface properties and internal composition. Aspirated cells from the sample move in a laminar flow and pass through a laser beam. The light is refracted by the cell depending on its size and granularity and the refraction can be used to determine the latter two properties of a cell. When the cells are stained, fluorescent is measured for every single cell and different populations can be established and isolated.

3.9.1 Determination of cell cycle profile

For cell cycle analysis, cells of interest were trypsinized, washed twice in PBS and pellet was fixed in 4 ml 80% ethanol at -20°C for at least 24 h. Cells were stained with 5 µM DAPI and 5 µM SR101 in 0,2 M Tris-HCl buffer as previously described (Stohr *et al.*, 1978). DAPI binds to the A-T bases of DNA and the intensity of the fluorescence emitted reflects the number of bonds and, therefore, the DNA content in labelled nuclei. For a typical DNA histogram, one peak represents the G1 and another (with twice the channel value due to double DNA content) represents the G2/M phase of the cell cycle. UV illumination was used for fluorescence excitation of DAPI and SR101 was used as protein counterstain for discriminating unspecific DAPI staining. Analysis was performed according to Dean and Jett (1974), with a cytofluorograph 30-L.

3.9.2 GFP measurement

After GFP retroviral transduction, HFK cells were trypsinized and centrifuged at 1,000 rpm for 5 min at 4°C. Pellet was washed with PBS and cells were fixed using the Cytofix/Cytoperm™ kit following manufacturer´s instructions. Cells were washed in PBS and analyzed on flow cytometer. Settings were adjusted with untransduced cells and the forward and side scatter were set for keeping the autofluorescence of the cells in the first decade.

4 Results

4.1 Characterization of HPV20 promoter activity in H1299 cells

Previous work in our group demonstrated the HPV20 promoter activation by p53 family members TAp63α and ΔNp63α through interaction with AP-1 c-Jun protein (Fei *et al.*, 2006; Fei *et al.*, 2005).

In order to study the influence of p53 family on HPV20 URR activity, luciferase reporter assays were performed. H1299 cells (a p63-null non-small cell lung cancer cell line) were transiently transfected with the corresponding vectors. wtp53, mutp53R248W, TAp63α and ΔNp63α cloned in pcDNA3.1.(+) vector were individually co-transfected with pGL3-HPV20 URR, that contains the luciferase gene under the control of the HPV20 promoter. In addition, pRL-β-actin reporter plasmid, which contains the gene for Renilla luciferase from the β-actin promoter, was co-transfected as control for normalizing the transfection efficiency. Protein expression was confirmed by Western Blot analysis.

4.1.1 Effect of wtp53 and mut p53R248W expression on HPV20 promoter

The p53 tumor suppressor gene is one of the most frequently mutated genes in human cancers (Hollstein *et al.*, 1991). It plays a critical role in activating genes involved in cell cycle arrest and apoptosis (see 1.3.1) and it is targeted for degradation by high risk HPV E6 (see 1.1.4.1). mutp53R248W is a common "hot spot" mutation in non-melanoma skin cancer (Ziegler *et al.*, 1993).

Under the context of wtp53 expression, HPV20 URR was 4-fold activated comparing to its basal activity in H1299 cells, suggesting that wtp53 up-regulation in the cell could promote protein viral gene expression. Interestingly, mutp53R248W expression did not influence HPV20 promoter activity. This is probably because the mutation in residue 248 enables p53 binding to the viral promoter and therefore it can not modify its activity (**Fig. 10**).

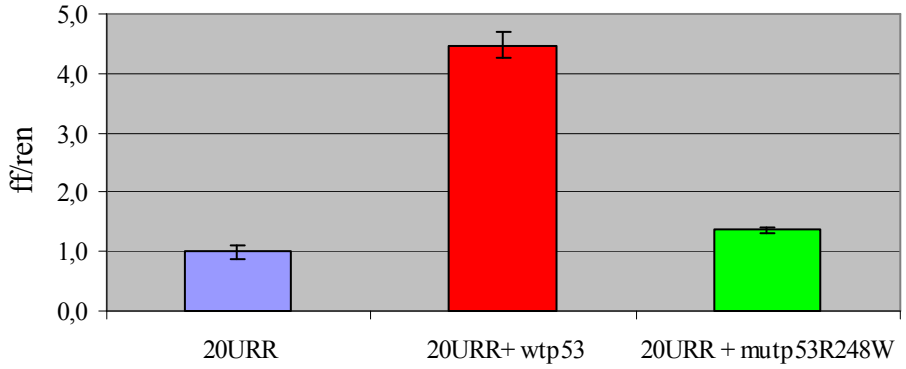

Figure 10. Luciferase reporter assays show that ectopically expressed wtp53 activates HPV20 promoter, whereas p53mutR248W over-expression does not significantly influence it.

4.1.2 Effect of TAp63α and ΔNp63α expression on HPV20 promoter

p63 protein is a member of the p53 family. Different protein isoforms have been described. TA isoforms contains a transactivation domain in N-terminus, whereas in ΔN isoforms it is partially deleted. C-terminal spliced proteins correspond to α, β and γ forms (reviewed in Candi *et al.*, 2007).

ΔNp63α has been shown to be over-expressed in SCC of skin, head and neck, cervix and lung, in transitional cell carcinomas as well as certain lymphomas and thymomas (Hall *et al.*, 2000; Hibi *et al.*, 2000; Irwin and Kaelin, 2001; Quade *et al.*, 2001; Wrone *et al.*, 2004; Yang *et al.*, 2004). In this study, we confirmed that HPV20 promoter is activated by ectopically expressed ΔNp63α (37 fold) as well as TAp63α (25 fold) proteins (**Fig. 11**), in accordance with previous reports from our group (Fei *et al.*, 2005; Fei *et al.*, 2006).

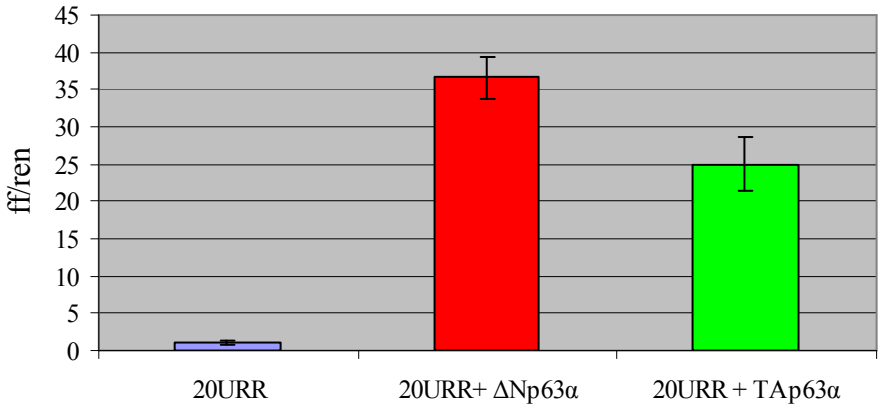

Figure 11. Luciferase reporter assays show that expression of ΔNp63α or TAp63α highly activates HPV20 promoter.

4.1.3 Effect of HPV20 E6 expression on HPV20 promoter

In order to study the influence of HPV20 E6 expression on its own viral promoter, co-transfection experiments with HPV20 E6 and HPV20 promoter were performed. pRL-β-actin reporter plasmid was co-transfected as control for transfection efficiency. Luciferase activity measurements demonstrated that Flag-tagged and non-Flag-tagged HPV20 E6 induce an up-regulation of HPV20 URR (1,5 fold) when compared with the promoter basal activity or with the empty vector pcDNA3.1.(+). Thus, we demonstrated that HPV20 promoter activity is directly or indirectly influenced by its own viral protein HPV20 E6. Additional simultaneous expression with a Flag-tag does not modify HPV20 E6 functionality in promoter activation (**Fig. 12**).

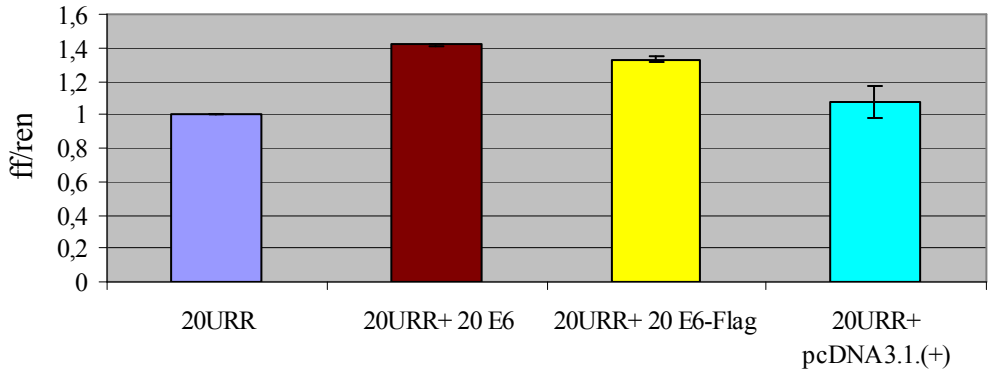

Figure 12. Luciferase reporter assays show that ectopically expressed HPV20 E6 protein directly activates HPV20 promoter activity.

4.1.3.1 E6 protein does not influence the activation of HPV20 promoter by wtp53

wtp53 and HPV20 E6 activate HPV20 promoter (see 4.1.1 and 4.1.3). However, when wtp53 was co-transfected together with HPV20 E6 and HPV20 URR, promoter activation levels were similar to those observed when wtp53 was co-transfected with the empty vector. Taken together, these results indicate that although HPV20 E6 activates HPV20 URR, it does not influence the HPV20 URR activation promoted by wtp53 (**Fig. 13 A**). That is probably because E6 protein from cutaneous HPV types does not directly interact with p53.

A

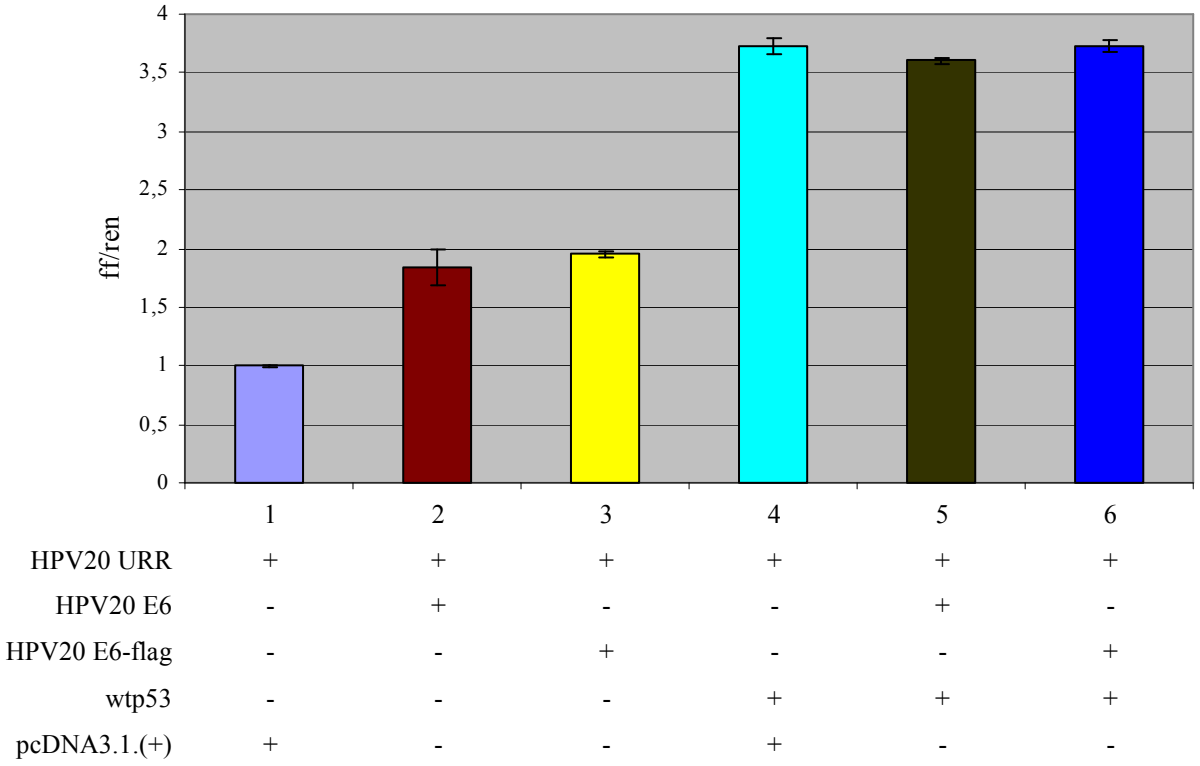

B

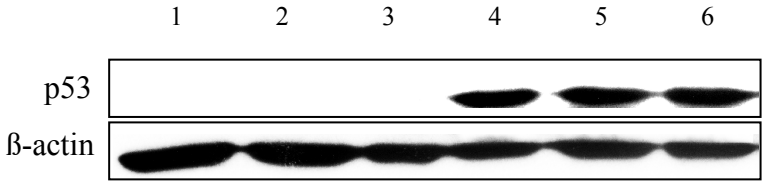

Figure 13. **A**. Luciferase reporter assays demonstrate that HPV20 promoter activitation by wtp53 it is not influenced by HPV20 E6 expression. **B**. Western blot from protein extracts after transient transfection in H1299 cells. wtp53 is not degraded when expressed together with HPV20 E6. ß-actin was used as loading control.

E6 protein of high risk HPV types binds to p53 and targets it for degradation (Munger *et al.*, 1992; Scheffner *et al.*, 1990). Cutaneous HPV20 E6 does not promote wtp53 degradation. When HPV20 E6 was co-transfected together with wtp53 and HPV20 URR, no difference in p53 expression was observed, indicating that HPV20 E6 does not degradate wtp53 (**Fig. 13 B**).

4.1.3.2 E6 protein does not influence the activation of HPV20 promoter by TAp63α

TAp63α highly up-regulates (15 fold) HPV20 promoter (see 4.1.2) and this effect is decreased when expressed together with HPV20 E6 (13 fold) and Flag-tagged HPV20 E6 (11,5 fold) (**Fig. 14 A**). However, TAp63α protein levels were not altered in the presence of HPV20 E6 (**Fig. 14 B**).

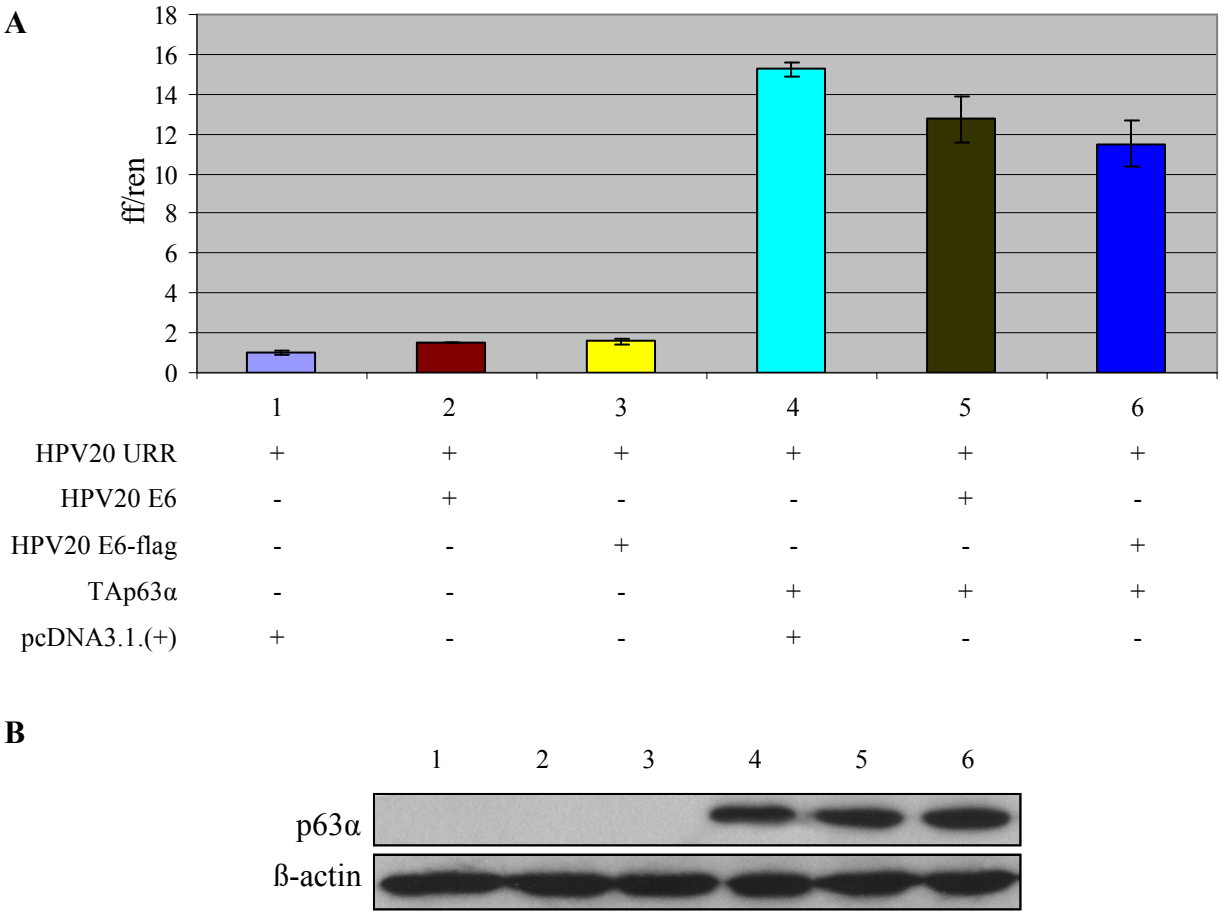

Figure 14. **A**. HPV20 E6 expression decreases the HPV20 promoter up-regulation by TAp63α as demonstrated by luciferase reporter assays. **B**. Western blot of protein extracts after transient transfection in H1299 cells shows that TAp63α levels are not modified when co-expressed together with HPV20 E6.

4.2 Effect of 4-NQO in immortalized oral keratinocytes

4.2.1 Standardization of transfection conditions

Keratinocytes were used in order to mimic the natural host cell infected by HPV. Primary foreskin keratinocytes were transiently transfected but the efficiency was too low to detect reliable luciferase reading and hence were not used for those experiments (data not

shown). HPV16 E6/E7 immortalized oral keratinocytes (oral KER16) were used for further characterization of HPV20 in cells treated with 4-NQO.

Efficiency of transfection was compared by GFP expression levels with different methods (lipofectamine, lipofectamine 2000 and FuGENE reagents) and protocols (depending on the cell culture medium used before transfection and the ratio reagent: DNA) (see 3.5.4). Fluorescence microscopy allowed quick evaluation of cell survival and morphology as well as determination of transfection efficiency by cell counting (**Fig. 15**).

The results showed that when medium was replaced by OPTI-MEM medium 3 h prior transfection using either Lipofectamine™ 2000 or Lipofectamine™ - Plus™ Reagent the efficiency was higher than when the medium was not replaced. However, both methods showed very low transfection efficiency (20%) and altered cell morphology (cells were increased in size and had an irregular shape).

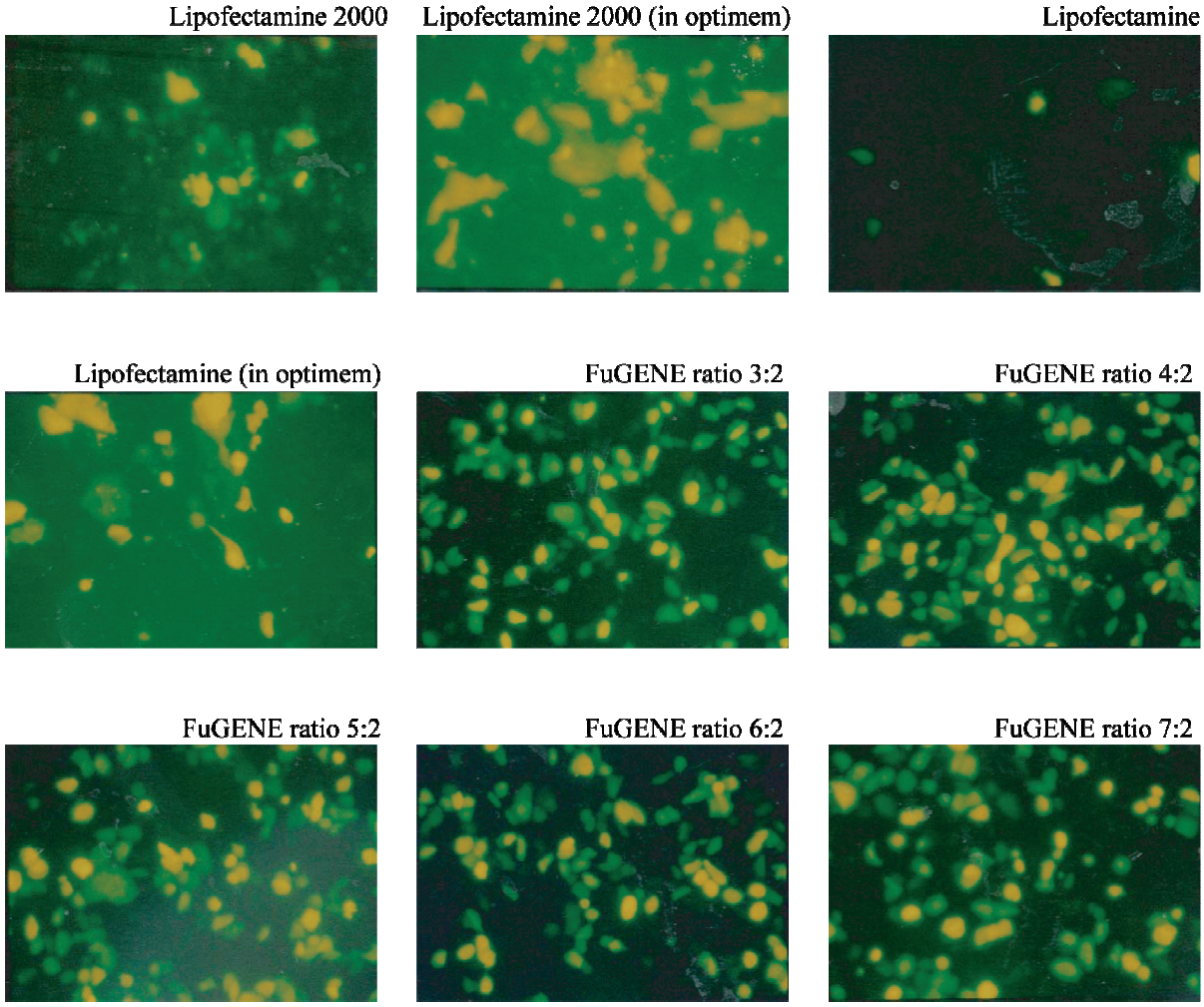

Figure 15. GFP expression levels in oral KER16 by different transfection methods.

When FuGENE HD was used, cell morphology remained intact and best efficiency (80%) was achieved when ratio FuGENE HD reagent (µl): DNA (µg) was 4:2, 5:2, 6:2 and 7:2. Following manufacturer´s instructions, we chose the ratio 4:2, where only 4 µl of FuGENE HD reagent pro 2 µg DNA were able to give 80% transfection efficiency.

Optimal DNA concentration for promoter activation studies was determined by transfection of different DNA amounts (1, 2, and 3 µg of pGL3-HPV20 URR) using the FuGENE HD reagent at ratio 4:2. When 2 µg of plasmid were transfected, a linear progression in the promoter activity was observed. Thus, this plasmid concentration was used for further luciferase reporter assays in oral KER16 (**Fig. 16**).

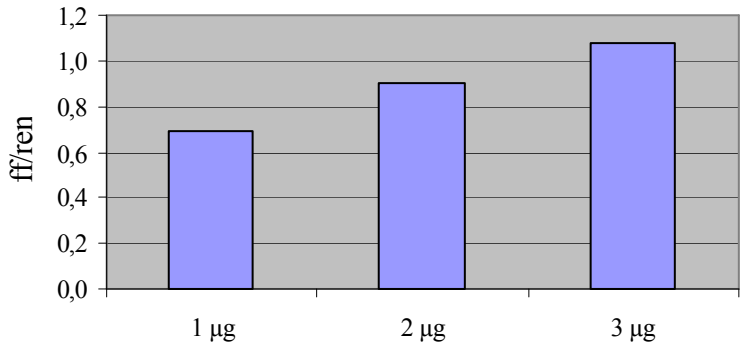

Figure 16. Luciferase reporter assay. Dose-dependent HPV20 URR activation in oral KER16.

4.2.2 Optimization of 4-NQO doses for treatment of keratinocytes

Optimal concentration of 4-NQO for treatment of keratinocyte cells needed to be established. 4-NQO is a synthetic chemical poorly soluble in water and organic solvents (DMSO or EtOH) have to be used for concentrated stocks. We dissolved the chemical following manufacturer´s instructions in a final concentration of 2 mM 4-NQO in 0,05% DMSO and treated the cells overnight with different concentrations of the chemical (**Fig. 17**). DMSO control was applied at a concentration of 0,015%, corresponding to the concentration of DMSO that the 30 µM 4-NQO sample contained. Viability was measured in triplicates by counting live cells (unstained) in comparison to dead cells (uptake trypan blue dye) in a Neuenbauer chamber.

Cells remained viable (96-98%) when treated with 0,015% DMSO, 2µM 4-NQO or 10µM 4-NQO. When 4-NQO was applied at 30 µM final concentration, cells changed to a rounded and shiny morphology and viability decreased to 85% (**Fig. 17**).

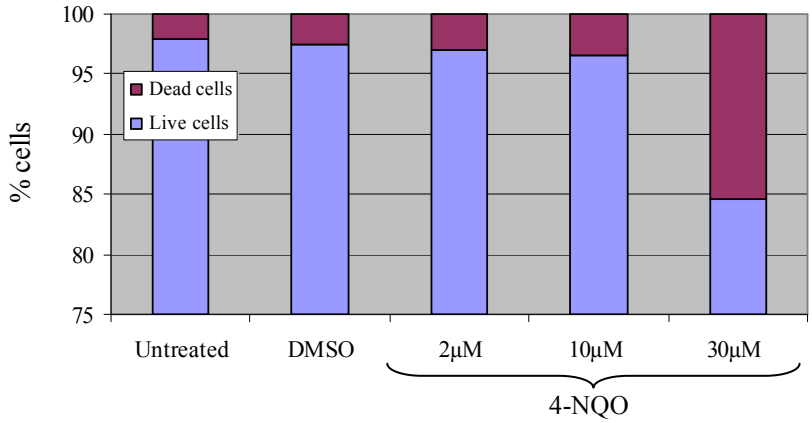

Figure 17. 4-NQO toxicity assay. Death cells were quantified by trypan blue uptake.

4.2.3 Effect of 4-NQO on cell cycle

Cell cycle profile was determined by measuring DNA content in samples treated overnight with varying concentrations of 4-NQO (**Fig. 18 A**). The first peak corresponds to G1 population, where cells have a haploid DNA content. Second peak represents cells in G2/M phase (with double DNA content). Populations with less than one copy of the genome (sub-G1) are considered apoptotic cells whereas populations between G1 and G2/M peaks correspond to cells in S phase. 4-NQO was applied at different concentrations and the results showed that low dose treatment (≤ 3 µM) promotes entry into S-phase and G2/M as previously observed (Heron-Milhavet *et al.*, 2001). 4-NQO induces G1 arrest and apoptosis when applied at high doses (Han *et al.*, 2007). In agreement with this report, we observed G1 arrest when 4-NQO was applied at 6, 9 and 12 µM. In addition, 4-NQO induced apoptosis at a concentration 12 µM, as observed in the cell cycle analysis by the appearance of a sub-G1 population (**Fig. 18 A and B**).

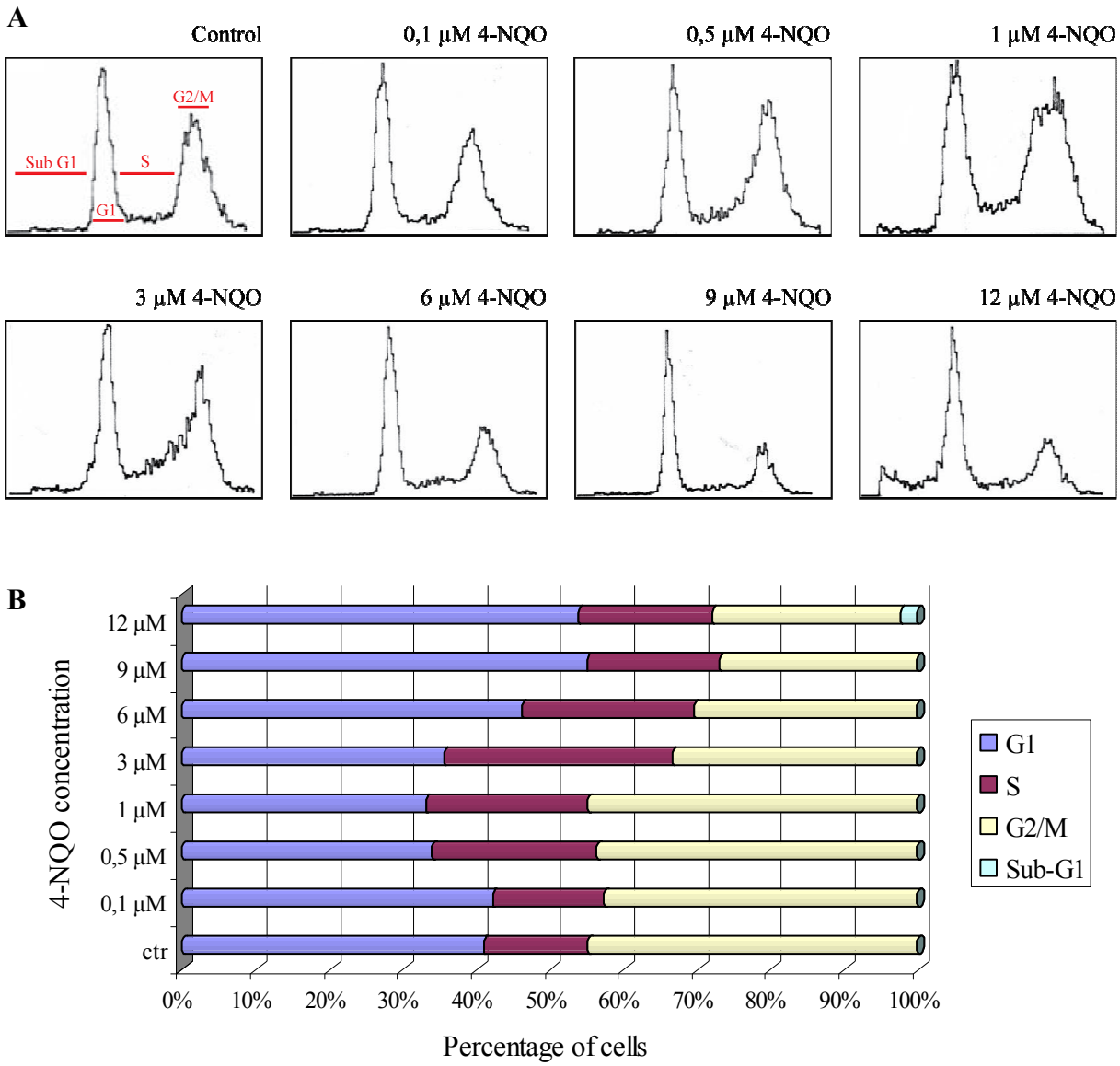

Figure 18. **A**. Cell cycle profile of 4-NQO treated oral KER16 measured by FACS analysis. **B**. Percentage of cells in G1, S and G2/M phases. Apoptotic cells correspond to sub-G1 population.

4.2.4 Influence of 4-NQO on HPV20 promoter activity

The viral promoter activity is often influenced by cellular factors, environmental factors and its own proteins. In order to study the promoter behavior of HPV20 when combined with 4-NQO, luciferase reporter experiments were performed. Oral KER16 were transiently transfected with either pGL3-HPV20 URR alone or in combination with Flag-tagged HPV20 E6 and/or E7 oncoproteins. 4-NQO was applied at a final concentration of 3 µM 4 h after transfection. Proteins were extracted 20 h after transfection using passive lysis buffer (see 3.4.1.1). Measurement of luciferase activity showed that DMSO alone does not

modify the HPV20 promoter activity whereas 4-NQO enhances it in cells transfected with the empty plasmid pcDNA3.1.(+) as well as cells expressing Flag-tagged HPV20 E6, Flag-tagged -E7 and Flag-tagged E6/E7, further contributing to the up-regulation induced by the respective viral proteins (**Fig. 19**).

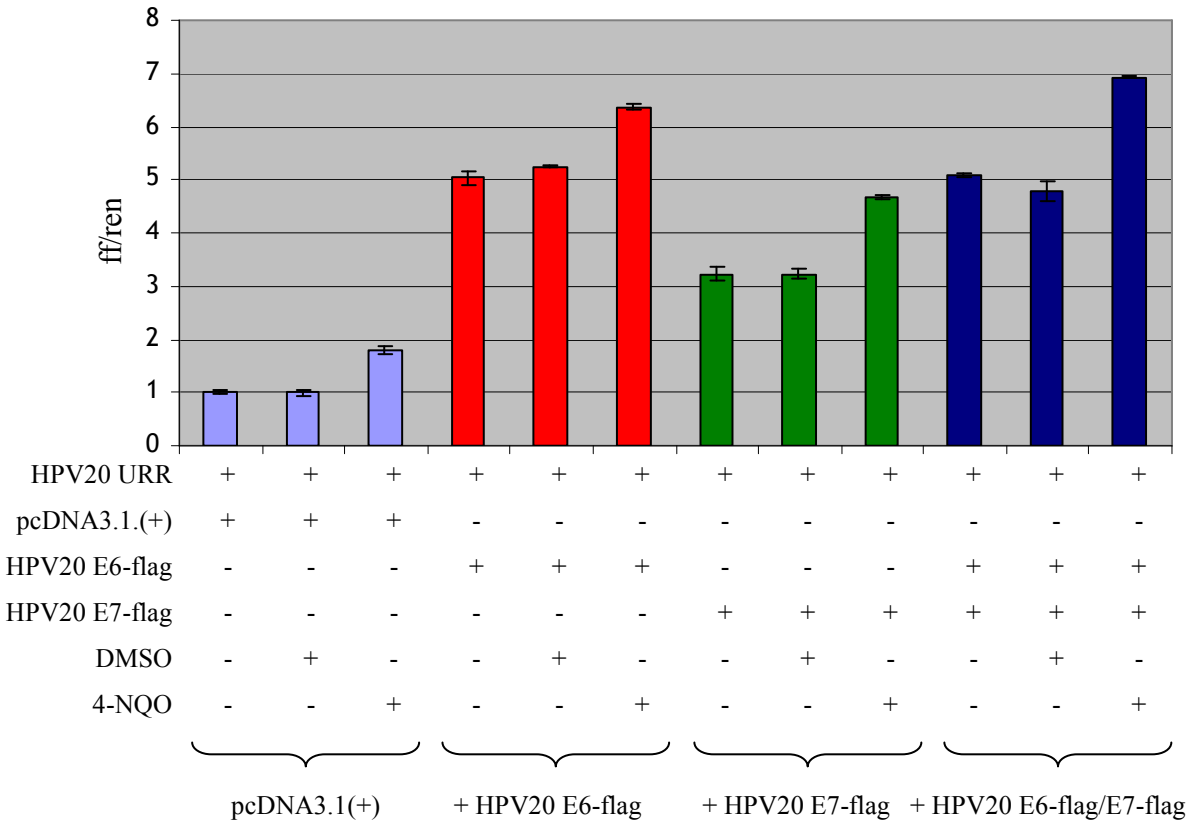

Figure 19. Luciferase activity assays show that 4-NQO enhances HPV20 promoter activity in oral KER16. 4-NQO further increases the promoter activation induced by HPV20 E6-flag, E7-flag and E6-flag/E7-flag proteins.

4.2.5 Influence of 4-NQO together with Flag-tagged HPV20 E6 on endogenous expression of ΔNp63α, p53, PCNA and p16

Oral KER16 were transiently transfected with Flag-tagged HPV20 E6 and subsequently treated with 4-NQO as described (see 3.2.5). Proteins of interest were demonstrated by Western Blot. Bands were quantified using the software program ImageQuant 5.0 (Molecular Dinamics, USA). Flag-tagged HPV20 E6 expression was demonstrated by antibody against Flag-tag (**Fig. 20 A**).

ΔNp63α protein was highly increased after Flag-tagged HPV20 E6 transfection. DMSO did not alter ΔNp63α levels whereas 4-NQO up-regulated ΔNp63α in both control vector and Flag-tagged HPV20 E6 samples. Interestingly, tumor suppressor gene p16 was

also similarly up-regulated when Flag-tagged HPV20 E6 expression was combined with 4-NQO treatment (**Fig. 20 B**).

Our group has previously demonstrated an up-regulation of p53 in transgenic mice expressing HPV20 E6/E7 when chronically exposed to UV (Michel *et al.*, 2006). In the present *in vitro* study p53 was over-expressed after Flag-tagged HPV20 E6 transfection and this effect was enhanced when incubated with the UV-mimetic 4-NQO.

It has been described that the transcription of the proliferation marker PCNA is increased after treatment with 4-NQO (Li *et al.*, 2005). However, no significant difference in PCNA expression was observed in 4-NQO treated samples after Western blot quantification (**Fig. 20 B**).

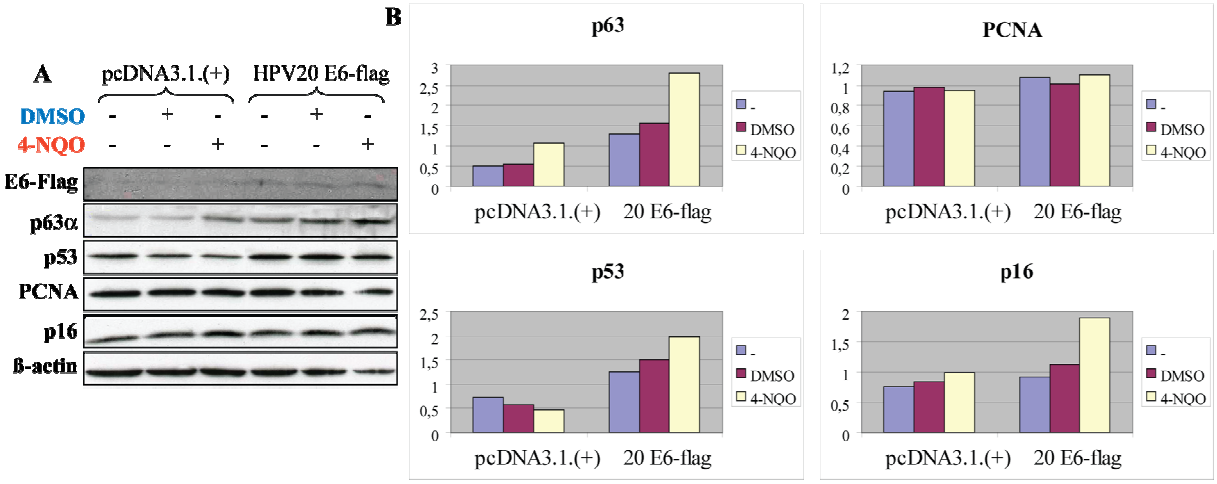

Figure 20. **A**. Western blot analysis of cellular proteins of oral KER16 after transfection with HPV20 E6-flag. **B**. Quantification of protein bands normalized to ß-actin using the densitometer software ImageQuant 5.0.

4.3 HPV20 E6 expression and/or 4-NQO treatment do not increase the life span of primary keratinocytes

HPV16 and 18 immortalize primary keratinocytes (Durst *et al.*, 1989; Kaur and McDougall, 1989). E6 or E7 from high risk genital HPV16 or 18 individually immortalize keratinocytes weakly whereas the effect is synergistic when E6 and E7 are co-expressed (Romanczuk *et al.*, 1991). However, low risk genital HPV and cutaneous HPV are not able to immortalize cells (reviewed in Munger and Howley, 2002), although an enhancement in life span after retroviral transduction of certain HPV types has been observed (Caldeira *et al.*, 2003; Schaper *et al.*, 2005). In this study, we characterize the effect of Flag-tagged HPV20 E6 and HPV16 E6/E7 proteins in the presence of 4-NQO in the keratinocytes life span.

Transfection efficiency is very low in primary keratinocytes (HFK). Therefore, cells were transduced with retroviral vectors that integrate in the host genome and ensure stable protein expression. HFK transduced with the empty pLXSN retroviral vector were used as control. Flag-tagged HPV20 E6 gene was cloned into pLXSN retroviral vector with a Kozak sequence upstream of the starting methionine and was Flag-tagged at N-terminus. Gene expression was controlled by the SV40 constitutive promoter contained in the pLXSN retroviral vector. Transduction efficiency was 28%, as determined by measurement of GFP fluorescence in FACS analysis (**Fig. 21 A**). Neomycin phosphotransferase expression (present in the pLXSN plasmid) was shown by RT-PCR and Western blot in the transduced cells (**Fig. 21 B and C**). Flag-tagged HPV20 E6 expression was demonstrated by RT-PCR (**Fig. 21 C**).

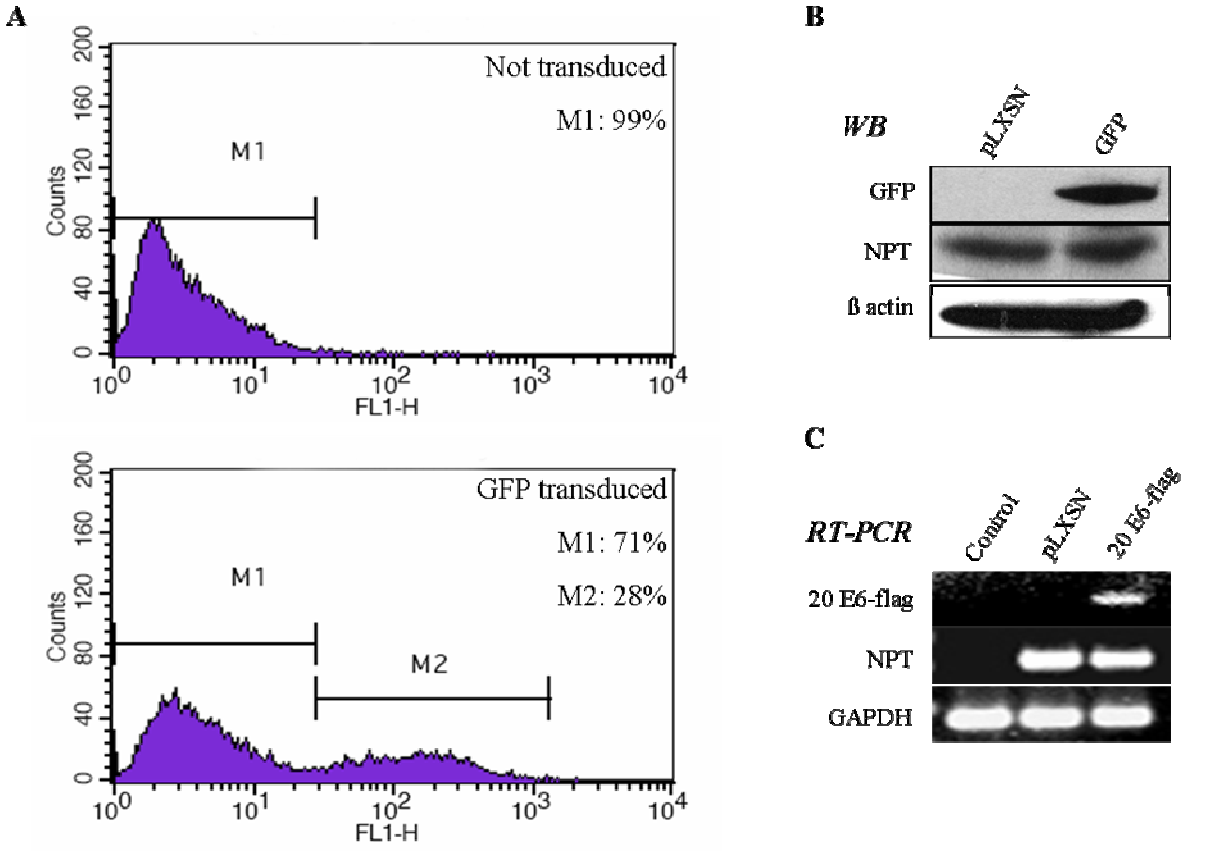

Figure 21. A. Measurement of GFP transduction efficiency. Cells were sorted by its fluorescence in a FACScalibur and population of transduced cells estimated in 28%. **B**. Western blot analyses of proteins from cells transduced with empty vector (pLXSN) or vector containing GFP (pLXSN-GFP). Cells containing pLXSN vector expressed the neomycin phosphotransferase (NPT) protein. β-actin was used as loading control. **C**. RT-PCR of normal HFK (control) and HFK stably transduced with empty vector (pLXSN) or pLXSN-HPV20 E6-flag. Cells containing pLXSN vector transcribed the NPT gene. GAPDH was used as housekeeping gene internal control.

After selection in geneticin (G418) antibiotic cells were exposed to 4-NQO. At 3 µM 4-NQO concentration all the cells died. We decided to reduce the chemical concentration to minimize cell death, choosing 1 µM as final concentration for long term chemical treatment in HFK cells. Stable clones containing the empty pLXSN vector, Flag-tagged HPV20 E6 or HPV16 E6/E7 were monitored in presence/absence of 1 µM 4-NQO. Cells were maintained for 5-6 passages. HPV16 E6/E7 transduced cells (used as positive control) had a higher growth rate and survived until they experiment was stopped at passage 15. When pLXSN and Flag-tagged HPV20 E6 transduced cells were treated with 1 µM 4-NQO, they died within the first 10 days. Interestingly, cells transduced with pLXSN-HPV16 E6/E7 and treated with 1 µM 4-NQO survived for only three days after the treatment started (**Fig. 22**). In summary, Flag-tagged HPV20 E6 expression did not extend the life span of HFK. Moreover, cell death was decreased in 4-NQO treated transduced cells.

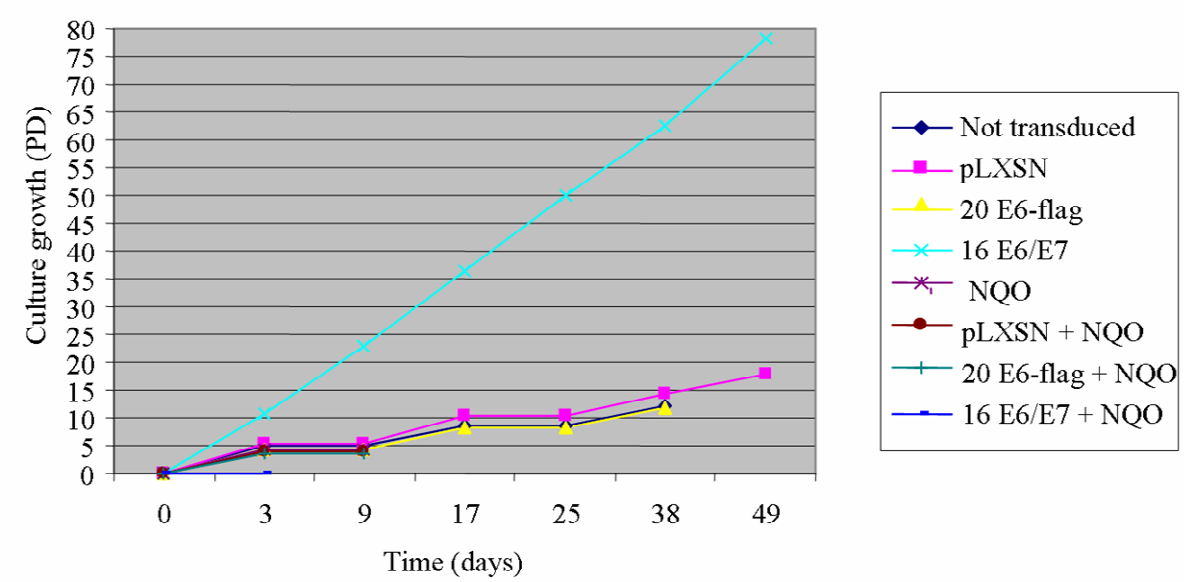

Figure 22. Life span of HFK stably transduced with pLXSN empty vector, HPV20 E6-flag or HPV16 E6/E7 alone or in combination with 1 µM 4-NQO treatment.

4.4 Organotypic cultures

The HPV life cycle is linked to the differentiation of the stratified squamous epithelium. NIKS is a near-diploid keratinocyte cell line that differentiates in culture similar to in *in vivo* situation, stratifies normally, presents the same expression profile of molecular markers as healthy skin and is non-tumorigenic in nude mice (Allen-Hoffmann *et al.*, 2000). These cells have been widely used in organotypic culturing techniques, which mimic the natural environment and conditions for HPV infection.

4.4.1 Epidermal morphology of organotypic cultures

Organotypic cultures of NIKS cells stably transduced with empty pLXSN vector, Flag-tagged HPV20 E6 or HPV16 E6/E7 were expanded and grown in the air-medium interphase. During the 14 days growth under these conditions, the epithelial surface became whiter and passed from a shiny and wet to a dry and mat appearance.

Sections from paraffin-embedded rafts were stained with haematoxylin/eosin (HE). Morphological examination by light microscopy revealed that NIKS cells transduced with the pLXSN empty vector developed into normal differentiating epithelia, containing the stratum basale, stratum spinosum, stratum granulosum and stratum corneum corresponding to normal skin layers (**Fig. 23**).

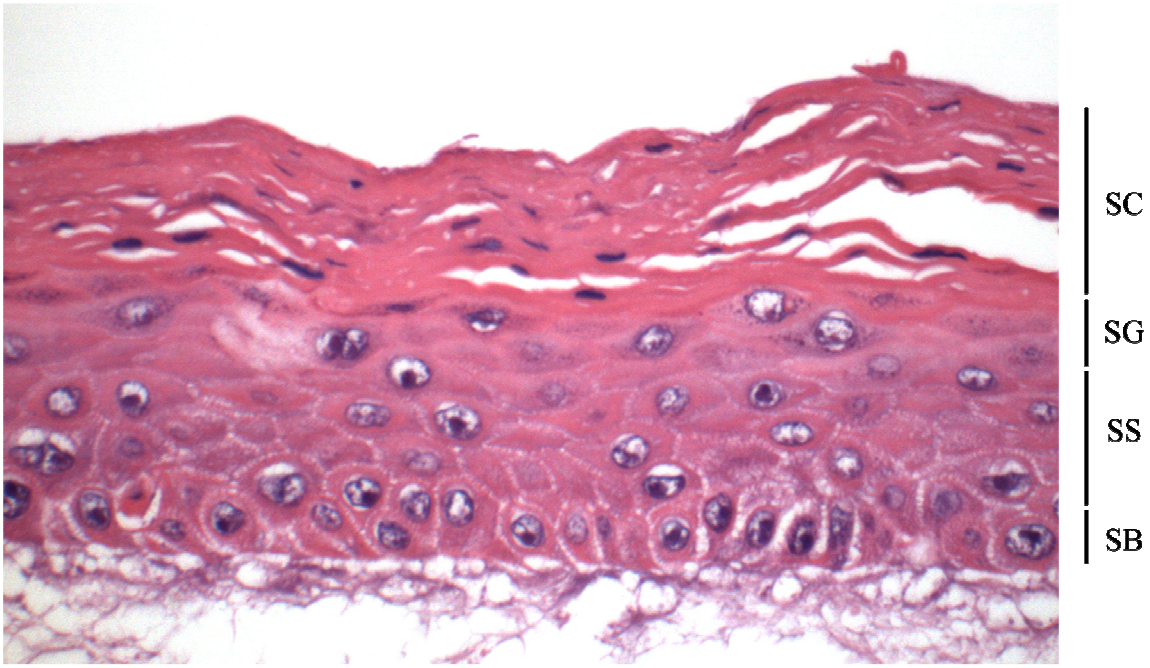

Figure 23. HE staining of organotypic raft culture based on NIKS cells stably transduced with pLXSN empty vector. Epidermal layers can be distinguished: stratum basale (SB), stratum spinosum (SS), stratum granulosum (SG) and stratum corneum (SC). Magnification 200x.

Flag-tagged HPV20 E6 expression resulted in unorganized epithelia with poorly differentiated parabasal layers of the stratified epithelia. The regular orientation and stratification of cells was disturbed (**Fig. 24**). The basal cell layer was present but was not as regular as in the control culture harboring the empty retroviral vector pLXSN (**Fig. 23**). Parabasal layers were poorly differentiated, the stratum spinous and stratum granulosum were poorly developed with an increase in apoptotic cells and fat droplets and, insofar, giving rise to morphological features of squamous epithelia. In contrast to control epidermis, the stratum corneum was thin and less compact. Foamy-cell-like structures were also found in the

uppermost differentiating layers (**Fig. 24 a**). The upper parts of Flag-tagged HPV20 E6 epidermis presented large vacuolated structures and unnucleated eosinophilic inclusions resembling dyskeratotic cells (**Fig. 24 b**). Basophilic flat oval and compact nuclei present in all parabasal layers indicate a high DNA content (**Fig. 24 c**). Bubble-like cavernae structures were evidenced in the considerable thinner cornified layers (**Fig. 24 d**), suggesting failures in adherence and cell junctions. Some areas of Flag-tagged HPV20 E6-expressing rafts formed circular basket-like cysts (**Fig. 24 e**). The increased number of apoptotic cell residues in the upper epidermis is interpreted as a consequence of the increased number of keratinocytes entering the disorganized stratum corneum.

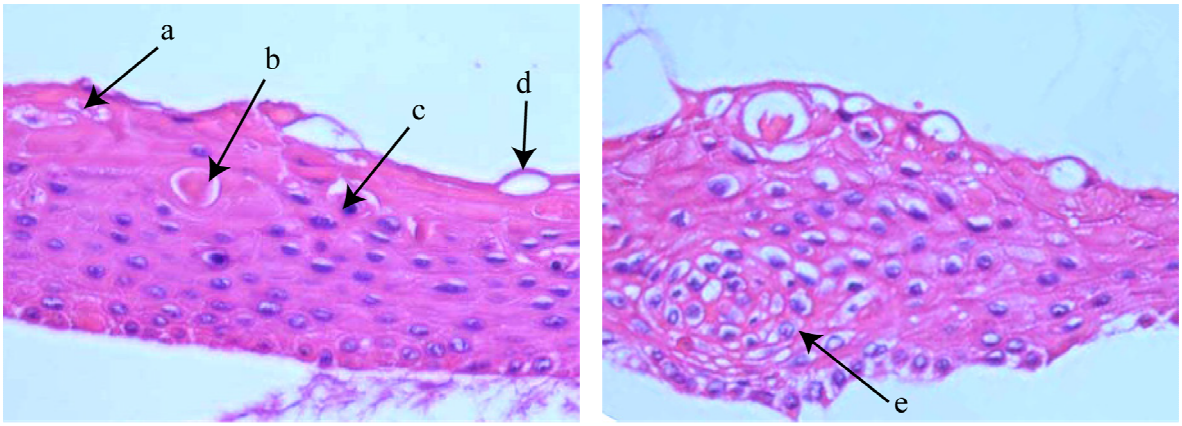

Figure 24. HE staining of HPV20 E6-flag expressing raft culture. It presents (a) foamy-like cells in the uppermost layers, (b) vacuolated structures with eosinophilic inclusions, (c) basophilic and compact nuclei, (d) cell bubbling in the cornified layer and (e) basket-like cysts. Magnification 200x.

Control HPV16 E6/E7 containing rafts showed a highly dysplastic and disorganized epidermal morphology. The stratum corneum was reduced in comparison to pLXSN control and only stratum basale could be distinguished. Abundant mitotic figures were found in suprabasal layers as described in cervical cancer (Babawale *et al.*, 2005) and organotypic raft cultures of HPV16 and HPV18-immortalized keratinocytes (Blanton *et al.*, 1991) (**Fig. 25**).

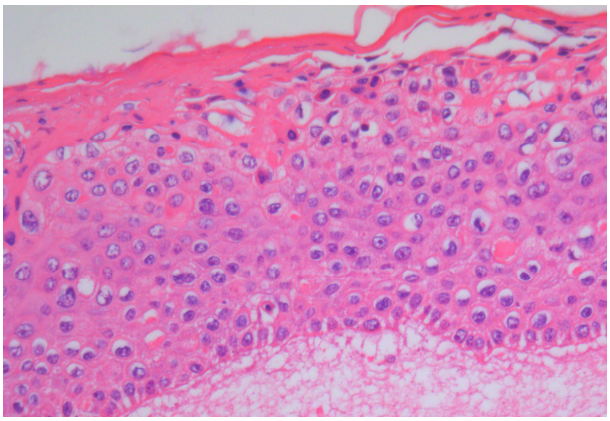

Figure 25. HE staining of HPV16 E6/E7 raft culture. Magnification 200x.

All three lines were additionally treated with 4-NQO. The chemical was dissolved in the NIKS medium at 3 µM final concentration and applied during the 14 days air-lifted organotypic culture growing. HE staining did not show any obvious difference in morphology and staining when compared to the untreated samples (**Fig. 26**). Prolonged treatment of these cultures with 4-NQO was not possible because of the limited life span of the organotypic raft cultures.

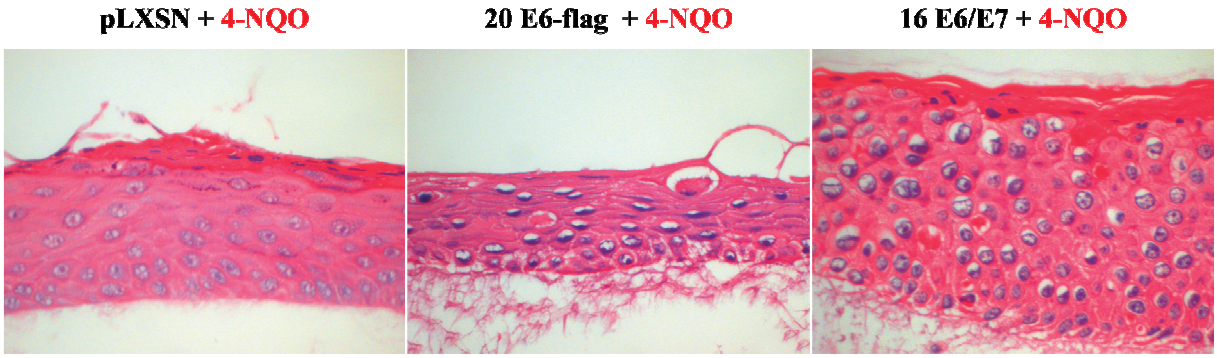

Figure 26. HE staining of pLXSN, HPV20 E6-flag and HPV16 E6/E7 organotypic cultures. 4-NQO was added to the medium at 3 µM final concentration for 14 days. Magnification 200x.

4.4.2 Verification of Flag-tagged HPV20 E6 expression in organotypic cultures

Flag-tagged HPV20 E6 gene transcription was demonstrated by RT-PCR of cDNA from monolayer cultures (**Fig. 27 A**). Moreover, Western blot analysis of proteins extracted from organotypic cultures showed Flag-tagged HPV20 E6 expression by anti-Flag immunodetection (**Fig. 27 B**). Interestingly, after 4-NQO treatment Flag-tagged HPV20 E6

protein was up-regulated as demonstrated by Western blot (**Fig. 27 B**); in this way, the addition of 4-NQO might enhance viral protein expression and/or stability.

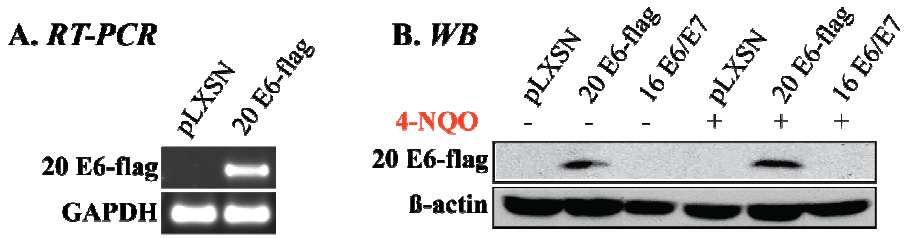

Figure 27. **A**. RT-PCR of transduced NIKS cells grown in monolayer. GAPDH was used as reference gene. **B**. Western blot of raft total lysates. HPV20 E6-flag protein was detected by anti-Flag antibody. ß-actin was used as loading control.

4.4.3 Flag-tagged HPV20 E6 alters the expression of p21^{CIP1}, p53 and ΔNp63α proteins

Our group has previously demonstrated the degradation of HPV20 E6 under simultaneous ectopic expression with wtp53 in the lung carcinoma cell line H1299 (Fei and de Villiers, 2008). In the organotypic culture system, we studied the effect of Flag-tagged HPV20 E6 expression on the endogenous p53 levels. Duplicate organotypic cultures were harvested for protein extraction and paraffin embedding. Protein expression levels and distribution were monitored by immunohistochemistry staining and Western blotting.

Expression of Flag-tagged HPV20 E6 in the organotypic cell cultures led to an increase of endogenous p53 as demonstrated by Western blot analyses (**Fig. 28 A and B**). HPV16 E6 mediates the degradation of p53 and it is therefore not detectable as shown in the immunohistochemistry and Western blot staining of HPV16 E6/E7 samples (**Fig. 28 A, B and C**). 4-NQO treatment induced the down-regulation of p53 protein levels in pLXSN control sample and the up-regulation of p53 protein levels in Flag-tagged HPV20 E6 when compared to its counterpart cultures not treated with 4-NQO (**Fig. 28 A and B**). Immunohistochemical staining of Flag-tagged HPV20 E6 cultures confirmed an up-regulation of endogenous p53 seen not only in the basal compartment, but extending into all suprabasal layers. Although differences in p53 levels were found between samples treated and untreated with 4-NQO, the protein distribution pattern was not altered in 4-NQO-treated samples as observed by immunohistochemistry staining (**Fig 28 C**).

p53 acts as tumor suppressor through up-regulation of the cyclin kinase inhibitor p21^{CIP1} (reviewed in Thomas and Laimins, 1998). p21^{CIP1} is degraded by proteosomes in normal

primary keratinocytes (Banerjee *et al.*, 2006). Our results showed an up-regulation in p53 levels in organotypic cultures expressing Flag-tagged HPV20 E6. Therefore, an up-regulation of the p53 downstream target $p21^{CIP1}$ in Flag-tagged HPV20 E6 rafts was expected.

In our system, $p21^{CIP1}$ expression in the pLXSN control rafts was not restricted to the basal cell layer only, but was evident through all strata (**Fig. 28 D**). This distribution is not surprising in view of the immortalized nature of the NIKS keratinocytes cells (Allen-Hoffmann *et al.*, 2000). $p21^{CIP1}$ expression was up-regulated in Flag-tagged HPV20 E6 cultures, as demonstrated in both Western blot analyses of the proteins extracted from the organotypic cultures and in the immunohistochemistry staining (**Fig. 28 A, B and D**). In HPV16 E6/E7 rafts, $p21^{CIP1}$ was up-regulated in comparison to pLXSN control. $p21^{CIP1}$ localization and expression levels were not altered when 4-NQO was applied to the medium of pLXSN, Flag-tagged HPV20 E6 and HPV16 E6/E7 organotypic cultures.

ΔNp63α is a p53 family member involved in skin proliferation and differentiation commonly over-expressed in SCC (Hibi *et al.*, 2000; Mills, 2006) that acts as a dominant negative of p53. Immunofluorescence staining of p63α indicated a moderate up-regulation of ΔNp63α protein levels by Flag-tagged HPV20 E6 (**Fig. 28 E**). This expression was, as in the pLXSN control organotypic cultures, not confined to the basal compartment, but extended through the suprabasal layers. Western blot analyses however indicated a clear up-regulation of the ΔNp63α protein level by Flag-tagged HPV20 E6 compared to the pLXSN control cultures. HPV16 E6/E7 also highly up-regulated p63α expression throughout the suprabasal layers (**Fig. 28 E**). pLXSN control culture treated with 4-NQO showed up-regulated levels of ΔNp63α protein by Western blot (**Fig. 28 A and B**) whereas no inffluence was found in Flag-tagged HPV20 E6 or HPV16 E6/E7. ΔNp63α protein expression pattern did not differed in 4-NQO treated versus 4-NQO untreated samples (**Fig. 28 E**).

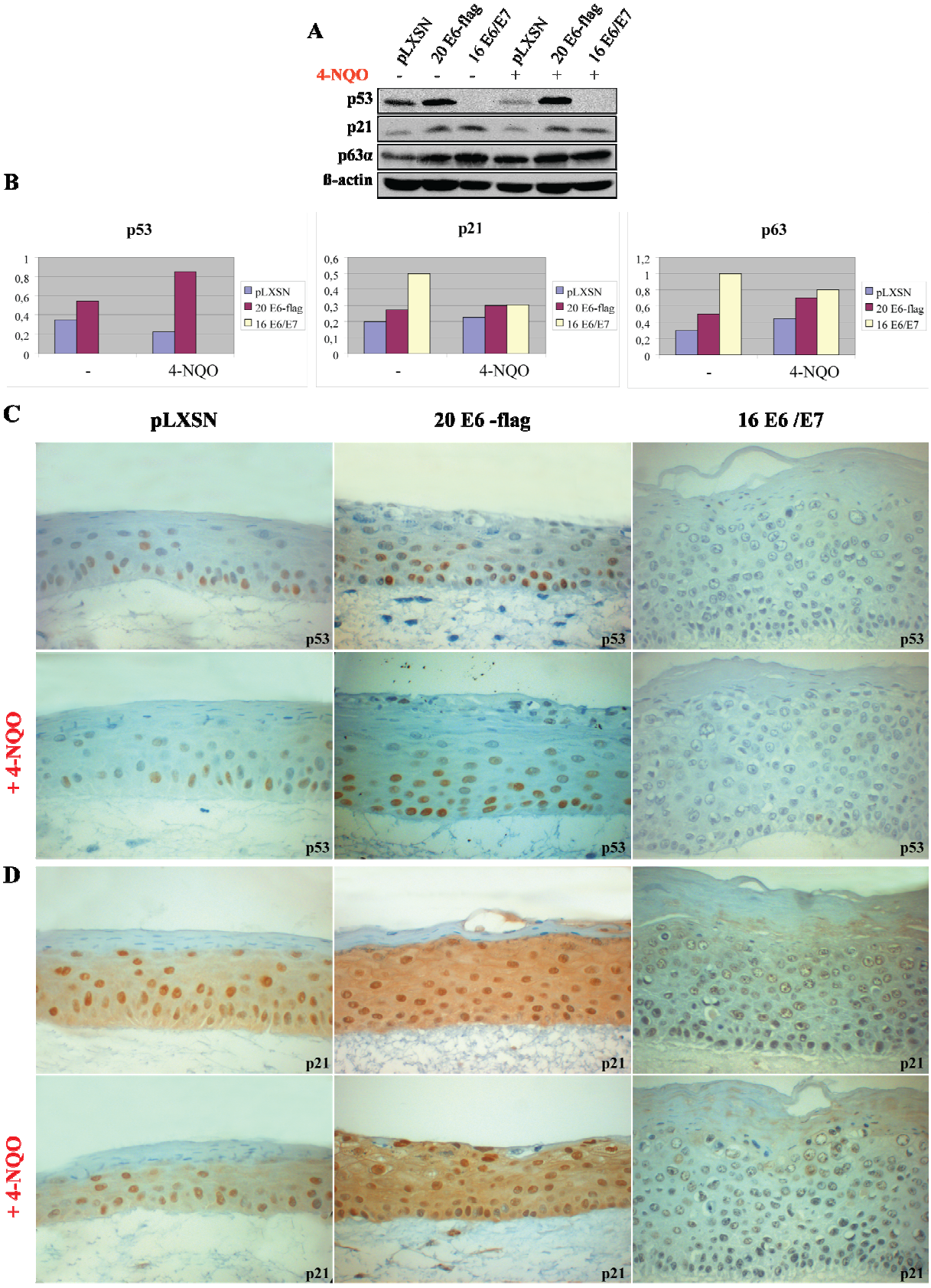

Figure 28. **A**. Western blot of proteins extracted from organotypic cultures. ß-actin was used as loading control. **B**. Quantification of protein bands normalized to ß-actin by densitometry. Immmunohistochemistry staining of p53 (**C**) and $p21^{CIP1}$ (**D**) revealed their up-regulation in HPV20 E6-flag rafts. Nuclei were counterstained with Meyers´hemalaum.

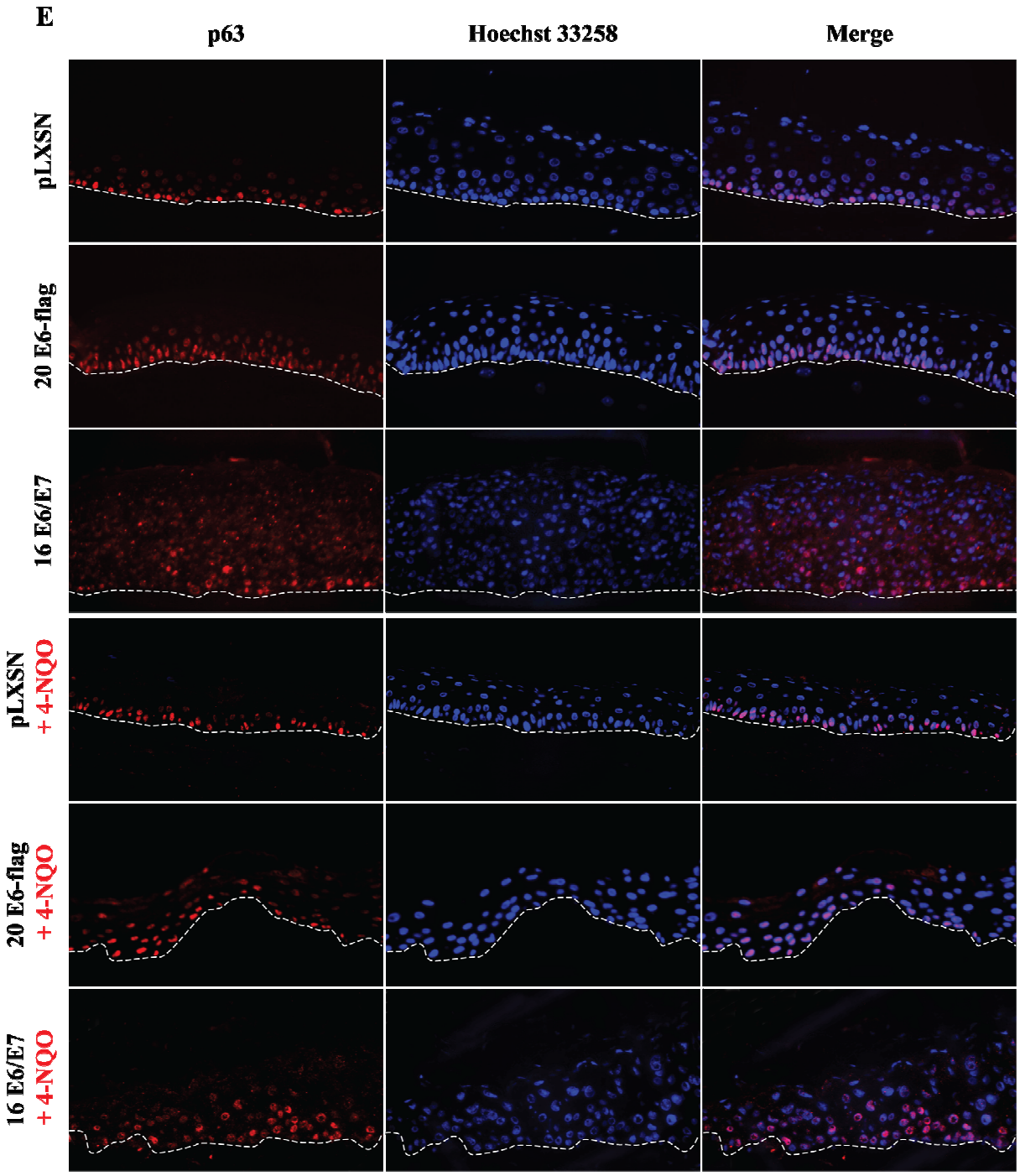

Figure 28. **E**. p63 immunofluorescence profile indicates expression in basal and parabasal layers, being slightly up-regulated in HPV20 E6-flag organotypic culture. Dotted lines indicate separation from collagen raft. Nuclei were counterstained with Hoechst 33258 dye. Magnification 200x.

4.4.4 Profiles of epidermal markers differ in Flag-tagged HPV20 E6 and HPV16 E6/E7-expressing organotypic cultures

4.4.4.1 Keratin pattern

Keratins are main components of the architecture of epithelial cells. These intermediate filaments present a characteristic profile in healthy epithelia that change during tumor development. Alterations in expression levels and profiles are useful tools for histological diagnosis and tumor classification (reviewed in Moll *et al.*, 2008). Since epidermal morphology was altered in Flag-tagged HPV20 E6 cultures, modified expression of keratins could be expected. Cytokeratin 10 and 14 were detected by immunofluorescence staining and Western blot.

Cytokeratin 14

Cytokeratin 14 expression is a marker for undifferenciated cells, strictly confined in healthy skin to the outer sheath of the hair follicle (reviewed in Stark *et al.*, 1987) and basal compartment (reviewed in Moll *et al.*, 2008), as found in the pLXSN control organotypic culture (**Fig. 29 C**). However, immunofluorescence staining showed extended cytokeratin 14 expression into all suprabasal layers in Flag-tagged HPV20 E6-expressing organotypic cultures, with a prominent staining of dyskeratotic cells. This expression was more restricted to the lower suprabasal layers in the HPV16 E6/E7-expressing cultures. 4-NQO treatment did not additionally alter the cytokeratin 14 expression and localization in any of the samples investigated (**Fig. 29 C**). Western blot analysis of organotypic cultures extracts confirmed the up-regulation of cytokeratin 14 in Flag-tagged HPV20 E6 compared with the pLXSN control in both samples treated and untreated with 4-NQO (**Fig. 29 A and B**).

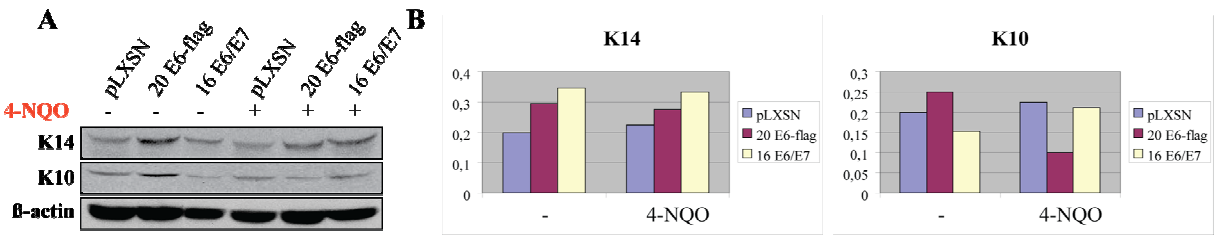

Figure 29. **A**. Western blot of proteins extracted from organotypic cultures. ß-actin was used as loading control. **B**. Quantification of protein bands normalized to ß-actin using the densitometer software ImageQuant 5.0.

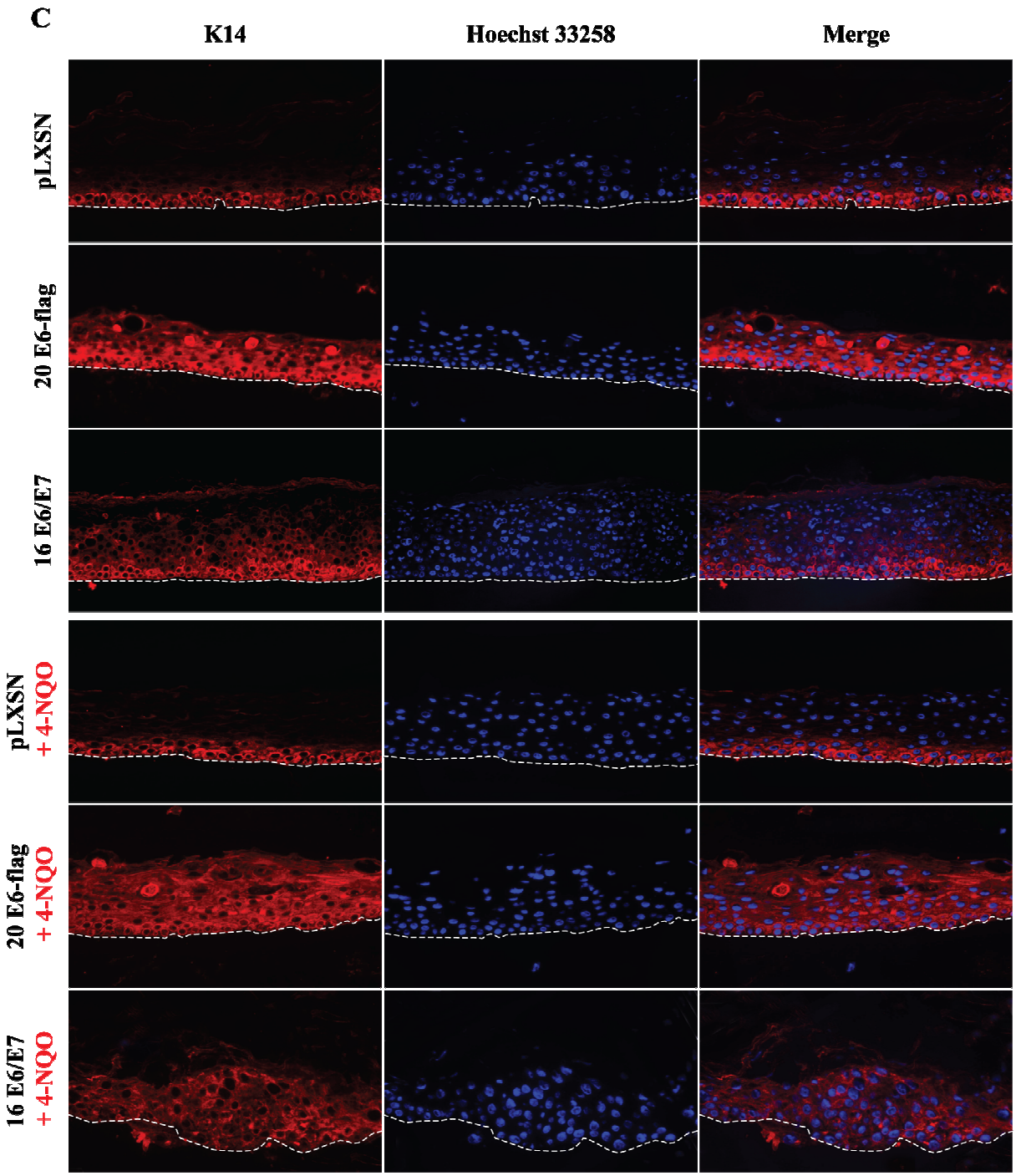

Figure 29. **C.** Immunofluorescence staining showed that Cytokeratin 14 was confined to the basal membrane in the pLXSN control raft whereas HPV20 E6-flag kept its expression along the epidermis, especially in the dyskeratotic cells. HPV16 E6/E7 cultures showed extended cytokeratin 14 expression into the suprabasal layers, becoming more pronounced after 4-NQO treatment. Dotted lines indicate separation from collagen raft. Nuclei were counterstained with Hoechst 33258 dye. Magnification 200x.

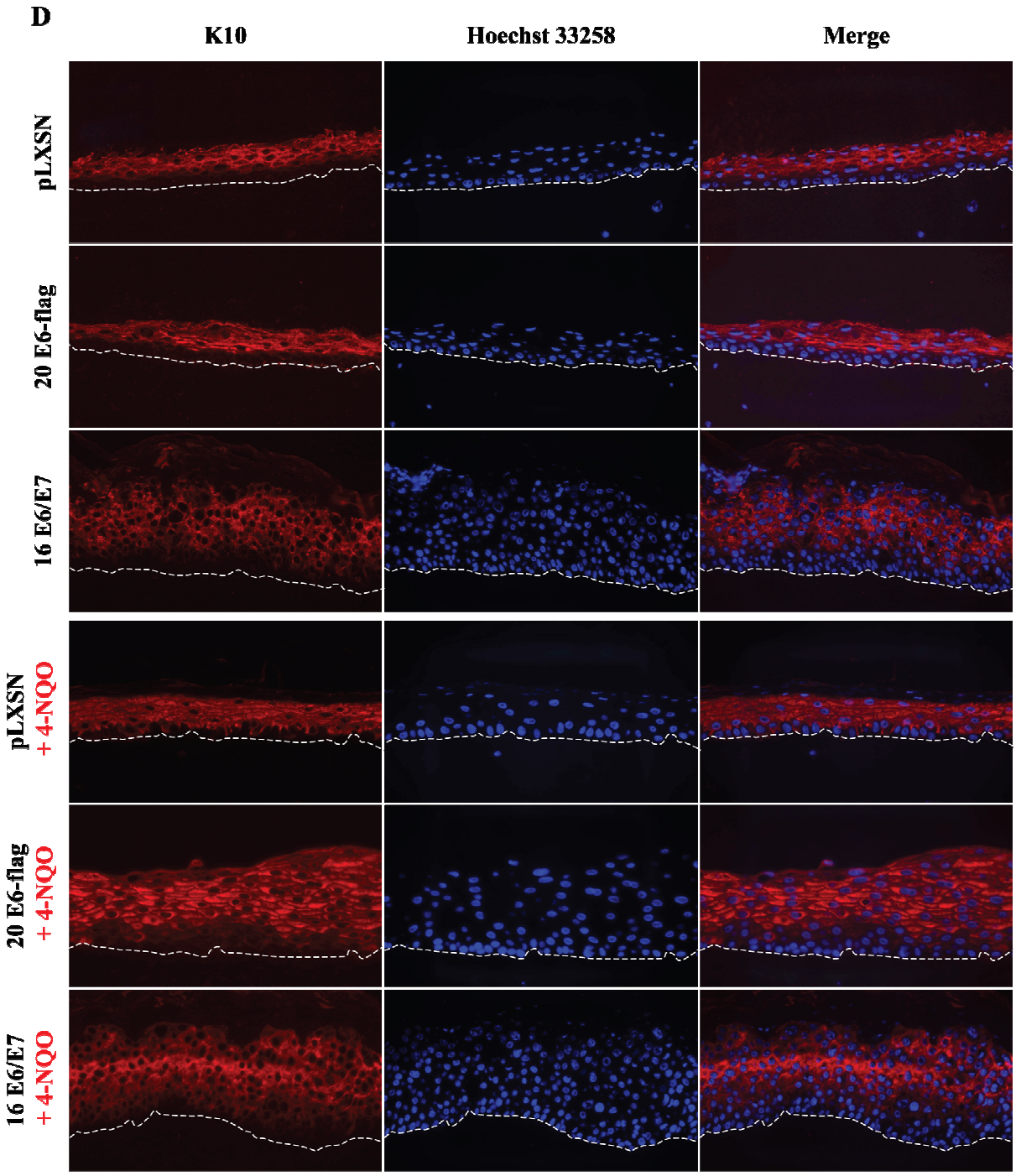

Figure 29. **D**. Immunofluorescence staining of cytokeratin 10 showed delayed expression in HPV20 E6-flag, HPV20 E6-flag treated with 4-NQO and more pronouncedly in HPV16 E6/E7 rafts. Dotted lines indicate separation from collagen raft. Nuclei were counterstained with Hoechst 33258 dye. Magnification 200x.

Cytokeratin 10

Cytokeratin 10 is expressed very early in differentiation, when keratinocytes leave the basal proliferative stratum and enter the suprabasal compartment, representing sensitive indicators for the onset of the epidermal differentiation program (reviewed in Moll *et al.*, 2008).

Cytokeratin 10 is localized in the suprabasal compartment beginning in the first suprabasal cell layer in normal epidermis, as observed in the pLXSN control raft (**Fig. 29 C**). In contrast to the pLXSN control, in HPV16 E6/E7 cytokeratin 10 expression pattern was delayed until the 5-6th suprabasal layer. Cytokeratin 10 expression was regularly delayed in rafts expressing Flag-tagged HPV20 E6, starting only from the second or third suprabasal layer. Interestingly, when 4-NQO was applied to the medium, a further delay in the expression pattern was observed in Flag-tagged HPV20 E6 rafts but not in pLXSN control or HPV16 E6/E7 samples (**Fig. 29 D**).

At Western blot level, cytokeratin 10 was up-regulated in Flag-tagged HPV20 E6 in comparison to pLXSN control and HPV16 E6/E7 (**Fig. 29 A and B**) whereas the cytokeratin 10 protein levels were reduced in the Flag-tagged HPV20 E6 samples treated with 4-NQO (**Fig. 29 A, B and D**).

Other cytokeratins

Keratins 4 and 13 are typically expressed in non-cornified mucosal stratified epithelium. Those keratins were not expressed in pLXSN, Flag-tagged HPV20 E6 or HPV16 E6/E7-expressing cultures irrespective of 4-NQO treament (data not shown), indicating that Flag-tagged HPV20 E6, HPV16 E6/E7 expression and/or 4-NQO treatment did not altered the cornifing nature of the NIKS raft cultures.

4.4.4.2 Late differentiation markers

To further confirm the defective development of the epidermis, expression of late differentiation markers was studied.

Involucrin and loricrin are important components of the epidermal barrier (reviewed in Steinert, 2000). In Flag-tagged HPV20 E6 cultures, involucrin expression was only slightly delayed whereas levels of loricrin were somewhat reduced and expression restricted to the uppermost epidermal layers. 4-NQO altered involucrin expression in Flag-tagged HPV20 E6 rafts, producing a further delay in its expression profile. Loricrin expression was markedly reduced in Flag-tagged HPV20 E6 samples when combined with the chemical treatment. Immunofluorescence staining of pLXSN control revealed the involucrin specific membrane-associated honeycomb texture and an expanded distribution commonly seen in regenerating epidermis (Watt *et al.*, 1987) (**Fig. 30 A**). Loricrin expression was concentrated strongly in the stratum granulosum of pLXSN control rafts (**Fig. 30 B**) as described in healthy skin (Hohl *et al.*, 1993).

Involucrin expression was highly decreased and delayed and loricrin was extremely faint or no longer visible in HPV16 E6/E7 expressing rafts (**Fig. 30 A and B**). No significant differences in involucrin and loricrin expression pattern were observed when the samples were treated with 4-NQO.

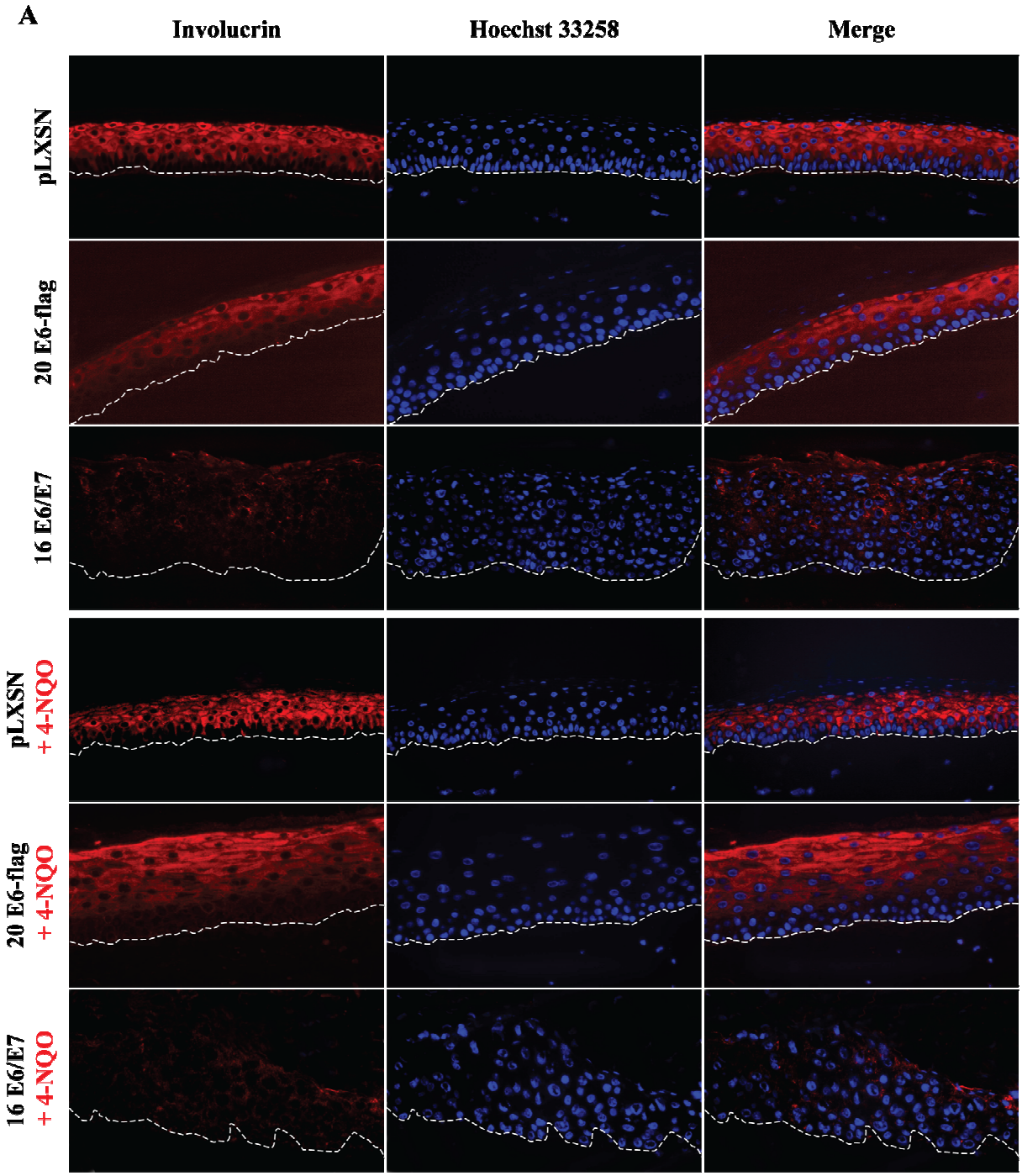

Figure 30. Immunofluorescence staining of late differentiation markers. **A.** Involucrin (red) expression was decreased in HPV20 E6-flag, HPV20 E6-flag treated with 4-NQO and much more pronouncedly in HPV16 E6/E7. Dotted lines indicate separation from collagen raft. Nuclei were counterstained with Hoechst 33258 dye. Magnification 200x.

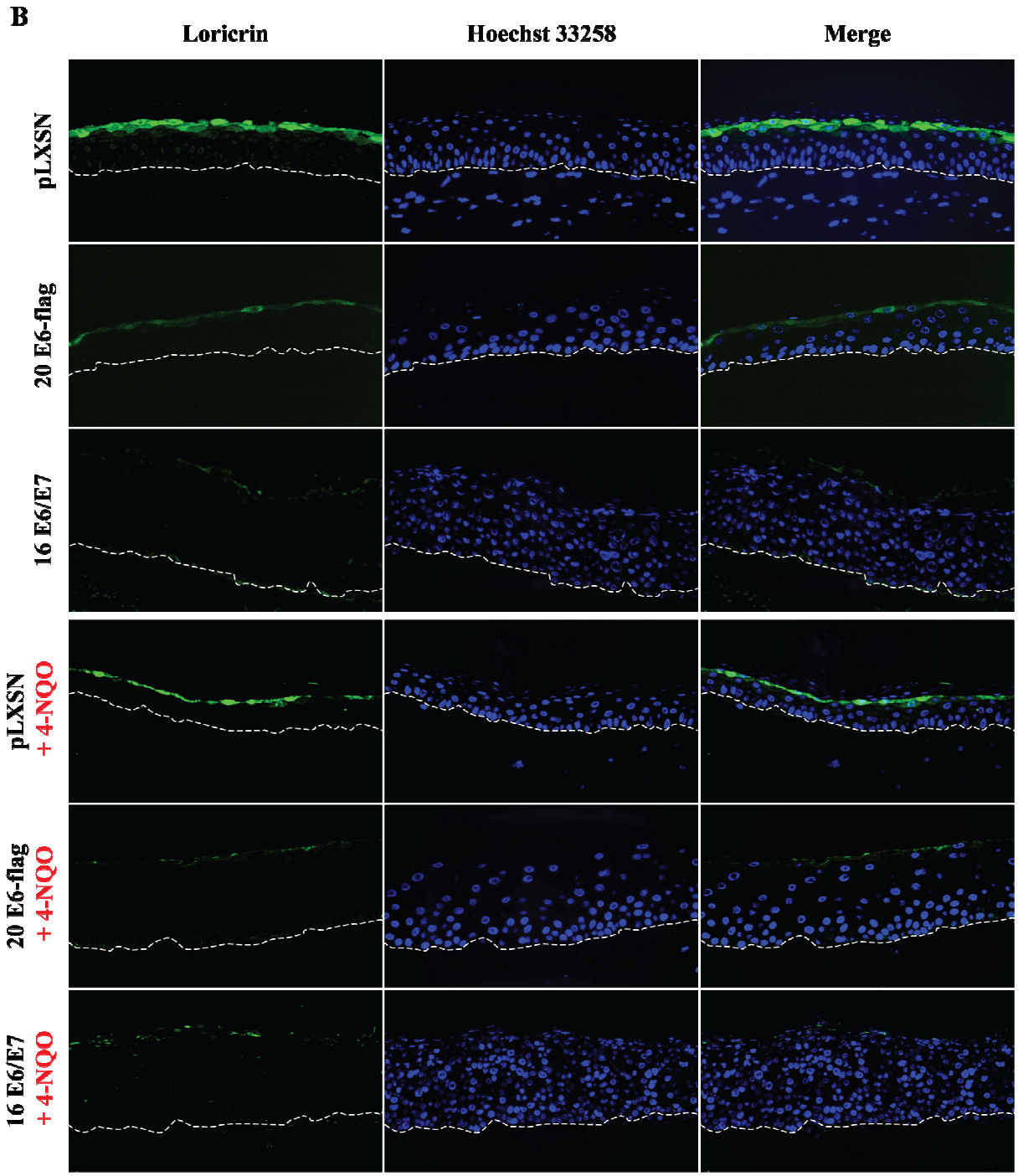

Figure 30. Immunofluorescence staining of late differentiation markers. **B.** Loricrin (green) expression pattern was similar in pLXSN control vector and HPV20 E6-flag raft, being restricted to last uppermost layers, very reduced in HPV20 E6-flag + 4-NQO and absent in HPV16E6/E7. However, HPV20 E6-flag contained a much lower amount of protein compared to pLXSN control. Dotted lines indicate separation from collagen raft. Nuclei were counterstained with Hoechst 33258 dye. Magnification 200x.

4.4.5 Proliferation measured by PCNA staining and BrdU incorporation

Proliferating cells were identified by PCNA staining and BrdU incorporation assay. PCNA is an auxiliary protein of DNA polymerase that is specifically expressed in cells during the S phase and it is used as a marker for cellular proliferation (Kelman, 1997). As keratinocytes proliferate from the stratum basale, PCNA-positive cells were observed only in this layer in pLXSN control and Flag-tagged HPV20 E6 organotypic cultures (**Fig. 31 C**). Western blot analysis showed a decrease in PCNA expression in the Flag-tagged HPV20 E6 samples (**Fig. 31 A and B**). $p21^{CIP1}$ and p53 down-regulate PCNA (Luo *et al.*, 1995; Mercer *et al.*, 1991). This PCNA down-regulation in Flag-tagged HPV20 E6 cultures is probably due to the simultaneous up-regulation of $p21^{CIP1}$ and p53 leading to a down-regulation of PCNA synthesis rather than a decreased proliferation rate *per se* (**Fig. 31 A and B**). In HPV16 E6/E7 epidermis PCNA staining was not only found in the stratum basale but also in the stratum spinosum, indicating hyperproliferation of abnormally differentiated keratinocytes (**Fig. 31 C**).

BrdU incorporation shared a similar labeling pattern with PCNA. No difference in BrdU incorporation was observed in Flag-tagged HPV20 E6-expressing cultures when comparing the pLXSN control, whereas unscheduled DNA synthesis in the differentiating compartment was demonstrated under the expression of HPV16 E6/E7 (**Fig. 31 D**). Both PCNA and BrdU incorporation studies demonstrated that proliferation rates are not modified when 4-NQO is added to the media.

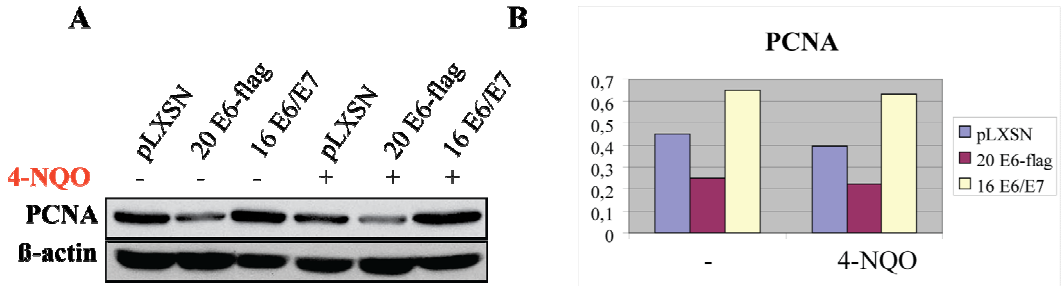

Figure 31. Proliferation levels showed to be similar in pLXSN control vector and HPV20 E6-flag, as demonstrated by BrdU incorporation and PCNA expression **A**. Western blot of raft total lysate. ß-actin was used as loading control. **B.** Quantification of protein bands normalized to ß-actin by densitometry.

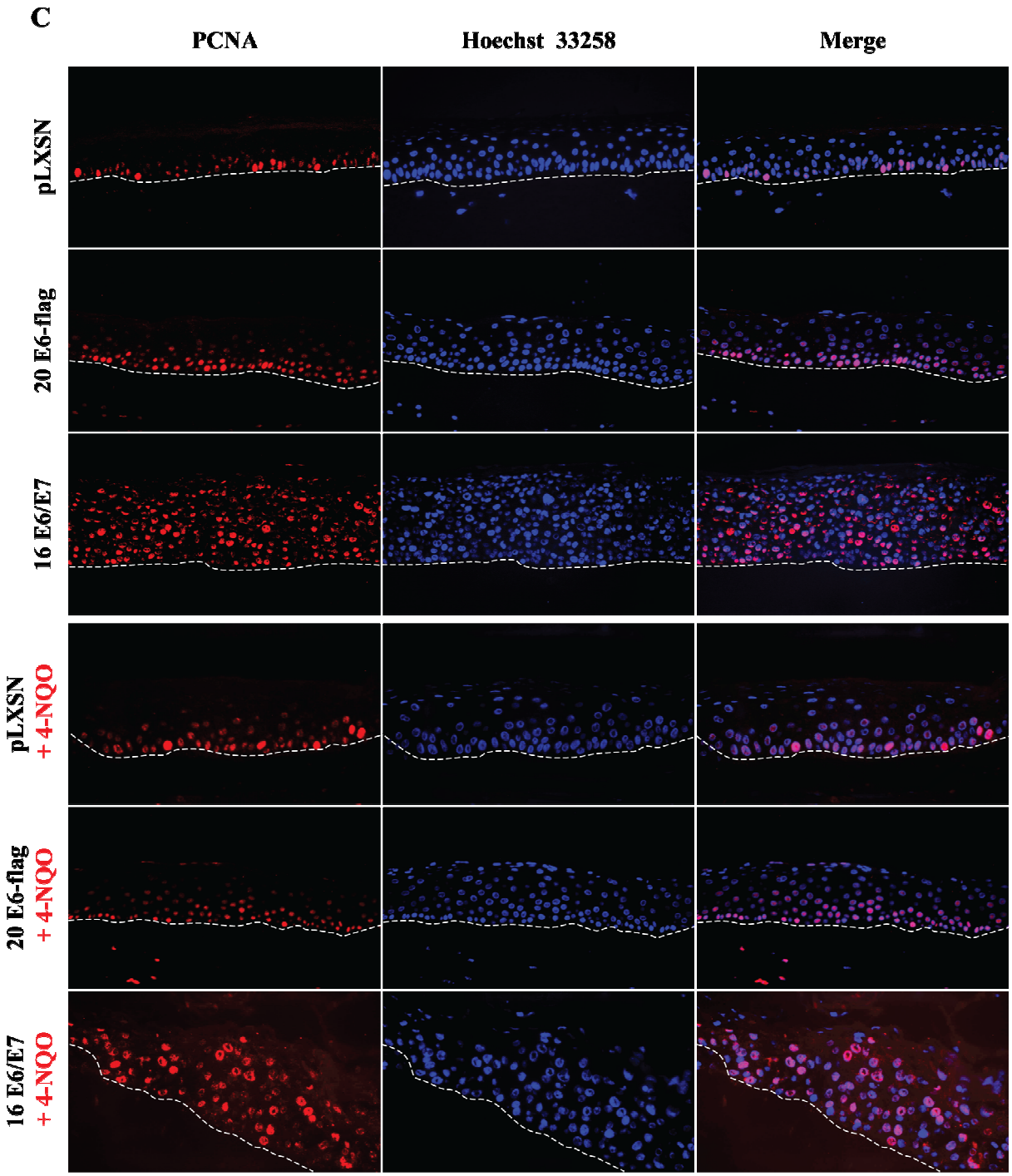

Figure 31. Proliferation levels showed to be similar in pLXSN control vector and HPV20 E6-flag, as demonstrated by BrdU incorporation and PCNA expression **C**. Immunofluorescence staining of PCNA. Dotted lines indicate separation from collagen raft. Nuclei were counterstained with Hoechst 33258 dye. Magnification 200x.

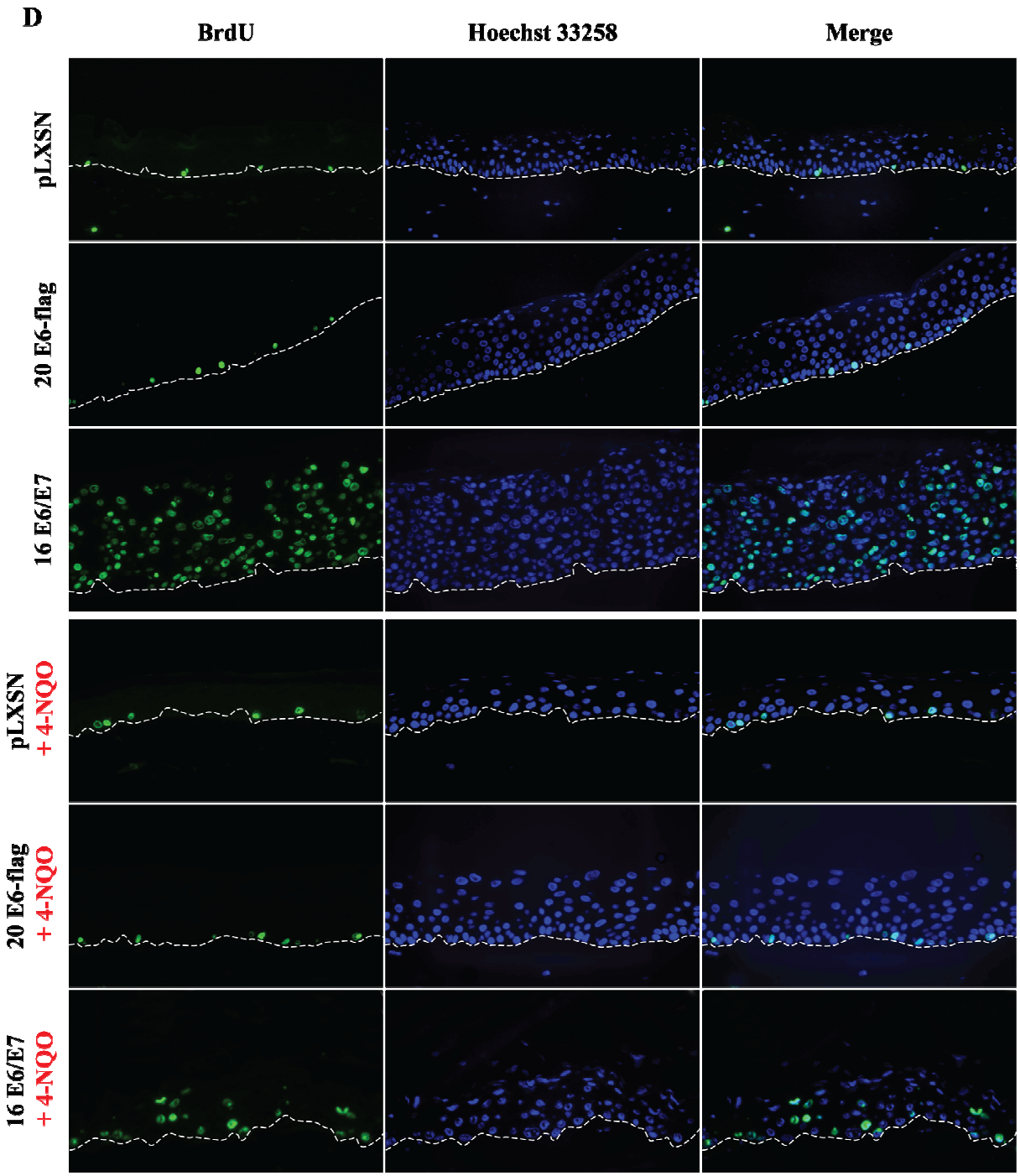

Figure 31. Proliferation level showed to be similar in pLXSN control vector and HPV20 E6-flag, as demonstrated by BrdU incorporation and PCNA expression. **D**. BrdU incorporation assay measured by immunofluorescence. Dotted lines indicate separation from collagen raft. Nuclei were counterstained with Hoechst 33258 dye. Magnification 200x.

4.4.6 Electron microscopy

In order to confirm the aberrant differentiation found in Flag-tagged HPV20 E6 expressing cultures (see 3.4.1 and 3.4.4), ultrastructural morphology was analyzed by transmission electron microscopy. In normal skin epidermis, the synthesis of keratin filaments starts in the stratum basale and continues into the stratum granulosum (Fuchs, 1993). In the stratum corneum cells become anucleated and compact. In accordance with these observations, ultrastructure analysis by transmission microscopy of the pLXSN control epidermis showed keratin accumulation in the stratum spinosum, small electro-dense granules in the stratum granulosum and compact stratum corneum where corneocytes can not be individually distinguished (**Fig. 32 A**). In Flag-tagged HPV20 E6 epidermis the stratum spinosum was not distinguishable. Stratum granulosum appeared thicker than in the pLXSN control, it was disorganized, with fewer keratin granules that highly differ in size from each other as well as accumulated of lipid droplets (**Fig. 32 A and C**). Moreover, Flag-tagged HPV20 E6 presented apoptotic figures in the upper granulosum and corneum strata (**Fig. 32 C**).

Intercellular spaces were not widened and the ultrastructure of desmosomes appeared normal in both pLXSN control and Flag-tagged HPV20 E6 samples (**Fig. 32 B**).

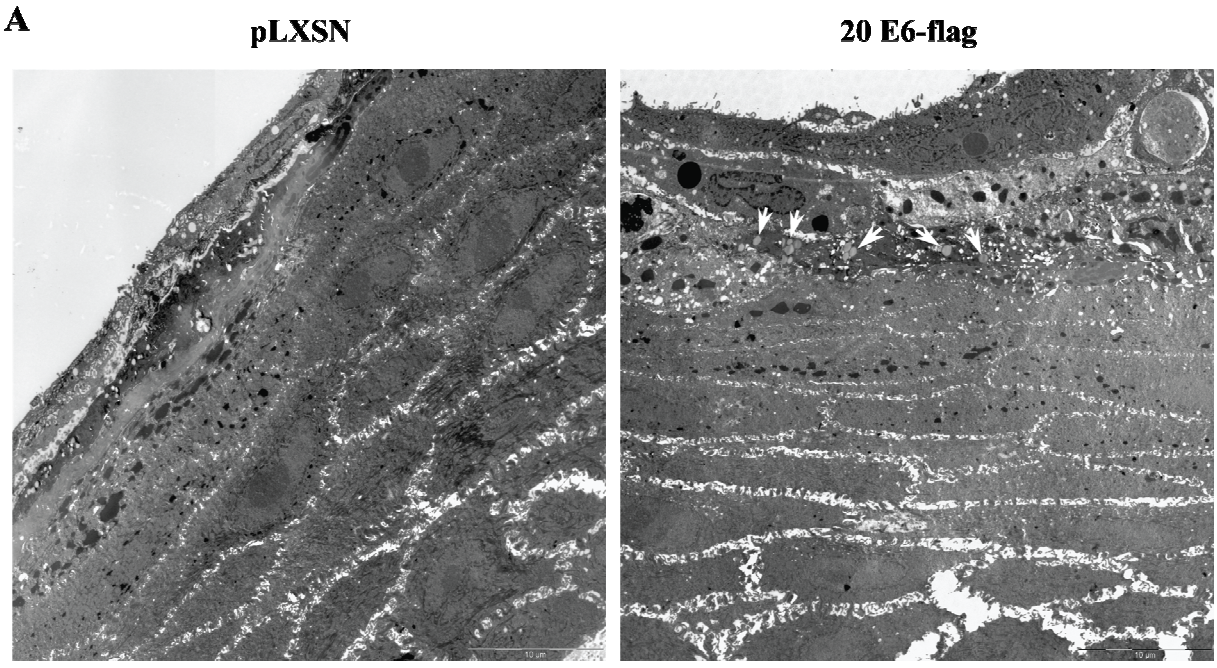

Figure 32. Ultrastructural analysis of raft cultures by electron microscopy. **A**. HPV20 E6-flag sample showed lipid accumulation and aberrant apoptotic bodies in the granular and cornified layer. Arrowheads indicate lipid droplets. Magnification 10 μm.

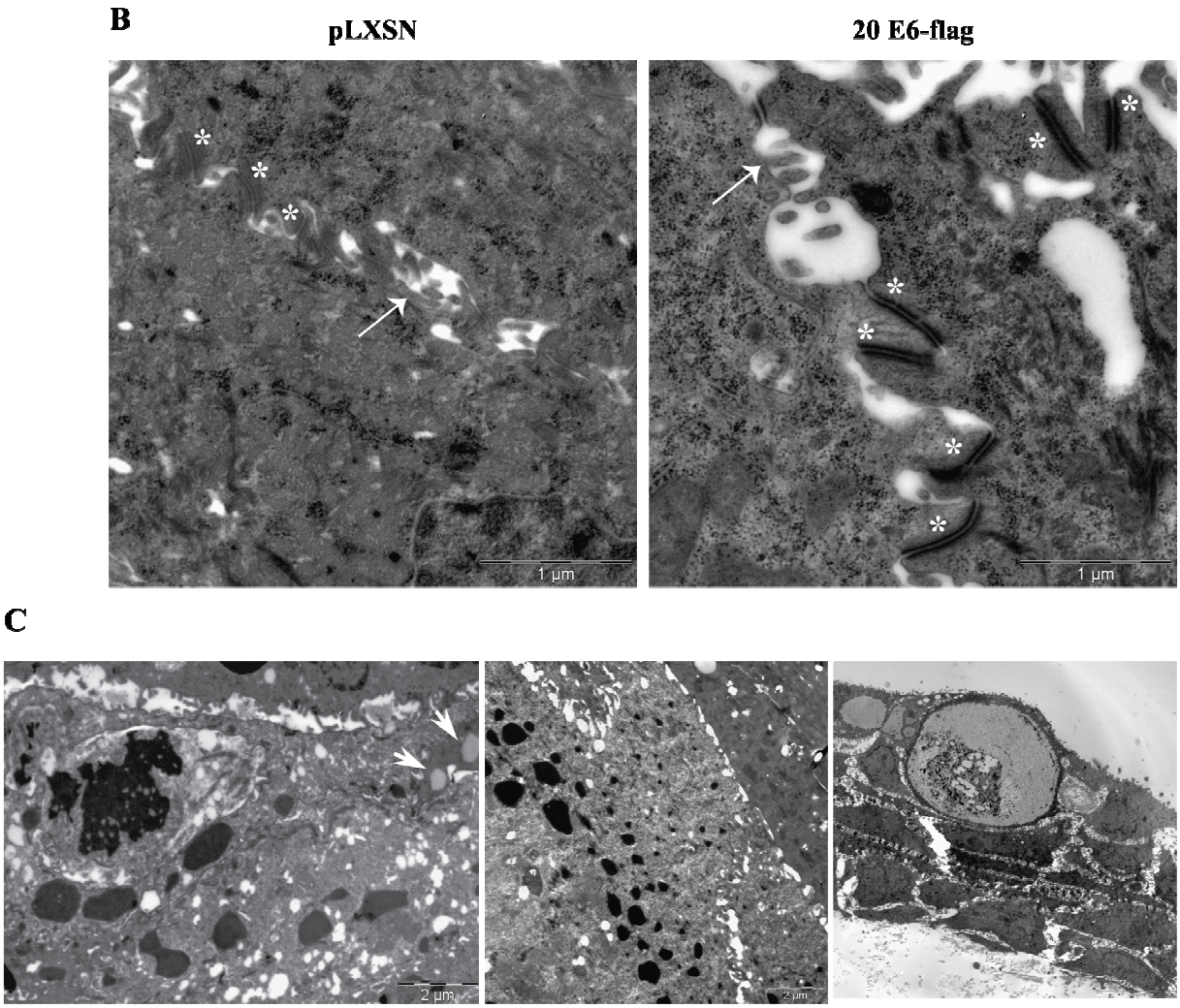

Figure 32. Ultrastructural analysis of raft cultures by electron microscopy. **B**. Desmosomes (*) were similar in pLXSN control and HPV20 E6-flag rafts and intercellular spaces (arrows) did not differ between both samples. Magnification 1 µm. **C.** Detail of Flag-tagged HPV20 E6 raft ultrastructure with lipid droplets (arrowheads), abnormal granules of different sizes in the stratum granulosum and apoptotic cell in the stratum corneum.

4.4.7 Loss of barrier function

4.4.7.1 Lipid quantification

Free fatty acids, ceramides and cholesterol are the main lipid constituents involved in maintenance of epidermal barrier function (Coderch *et al.*, 2003). We thus determined the levels of free fatty acids and cholesterol by Gas Chromatography-Mass Spectrometry (GC-MS). Differences in composition were observed between pLXSN control and Flag-tagged HPV20 E6 rafts (**Fig. 33**): pentadecanoic acid, linoleic acid, cis-10-Heptadecanoic acid, cis-10-Pentadecanoic acid, arachidonic acid, stearic acid, palmitoleic acid, oleic acid and total content of fatty acid were significantly increased in Flag-tagged HPV20 E6 organotypic cultures as determined by GC-MS whereas nervonic acid was significantly decreased.

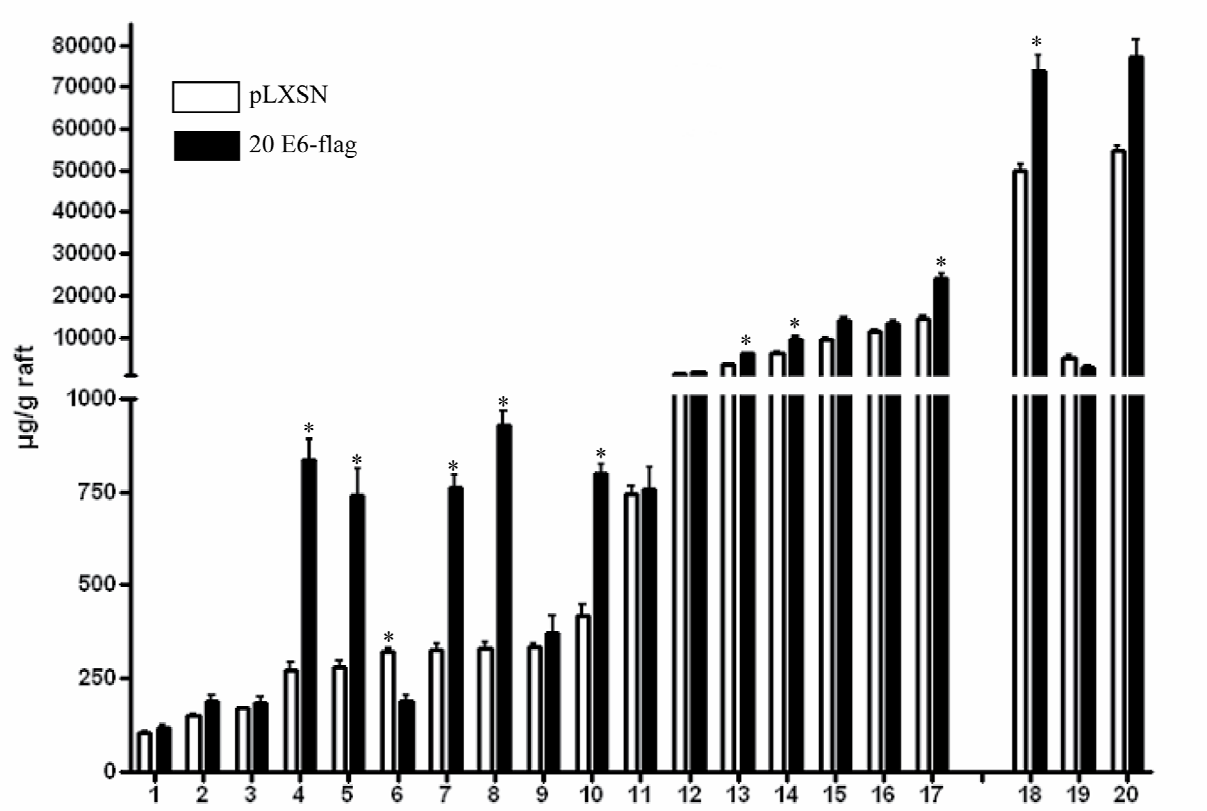

Figure 33. Lipid content analyzed by GC-MS. Content of individual fatty acids, cholesterol and total lipids was measured as µg/g raft tissue. 1. Erucic acid. 2. Behenic acid. 3. Arachidic acid. 4. Pentadecanoic acid. 5. Linoleic acid. 6. Nervonic acid. 7. cis-10-Heptadecanoic acid. 8. cis-10-Pentadecanoic acid. 9. Lignoceric acid. 10. Arachidonic acid. 11. cis-11-Eicosenoic acid. 12. Myristic acid. 13. Stearic acid. 14. Palmitoleic acid. 15. Palmitic acid. 16. Elaidic acid. 17. Oleic acid. 18. Total fatty acids. 19. Cholesterol. 20. Total lipids. * indicates significance calculated by stepdown Bonferroni method ($p<=0.05$).

4.4.7.2 Lipid droplets accumulate in organotypic cell cultures expressing Flag-tagged HPV20 E6

Flag-tagged HPV20 E6 expression induced changes in lipid composition (see 3.6.1) and lipid accumulation in the organotypic cultures as observed by electron microscopy (see 3.5). Therefore, lipid accumulation was suspected and staining with Oil Red O was performed. Both pLXSN control, as well as Flag-tagged HPV20 E6 showed intense lipid accumulation in the cornified layers. In addition, lipid droplets were seen in single cells of the basal compartment of Flag-tagged HPV20 E6 cultures at higher magnification (**Fig. 34**).

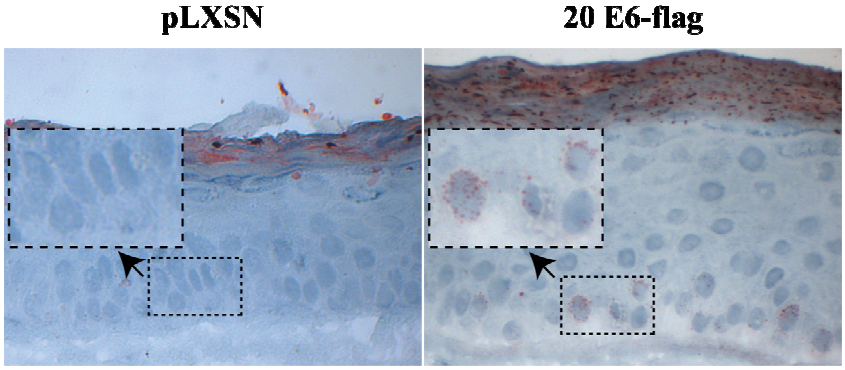

Figure 34. Lipid staining of cryosections. Lipids were detected by Oil Red O staining (red) and nuclei were counterstained with Meyers´ hemalaum. At magnification of 200x the cornified layer showed an intense lipid accumulation in both pLXSN control vector and HPV20 E6-flag rafts. HPV20 E6-flag presented accumulation of lipid droplets in the basal layer (see square detail).

4.4.8 Skin permeability assay

Stratum corneum is formed by ordered synthesis of different keratins and proteins in each stratum and it is crucial to develop the skin barrier function. The aberrant differentiation in Flag-tagged HPV20 E6 organotypic cultures (extended cytokeratin 14 expression, delay in cytokeratin 10 and involucrin expression; see 3.4.1 and 3.4.4), the altered lipid composition (see 3.6) and lipid accumulation (see 3.5 and 3.6) suggested a perturbed skin barrier. To examine this hypothesis, we performed skin permeability assay by Lucifer yellow penetration and Biotin uptake assays. Moreover, the presence of tight junctions was evaluated by cingulin staining.

4.4.8.1 The outside-in barrier is not functional in Flag-tagged HPV20 E6 rafts

The outside-in permeability of the stratum corneum was analyzed by its ability to take up a liquid dye. Lucifer yellow placed on top of the epithelia could not pass through the stratum corneum in control tissue. However, the dye penetrated through the epidermis in Flag-tagged HPV20 E6-expressing epidermis, demonstrating the defective skin barrier function (**Fig. 35**).

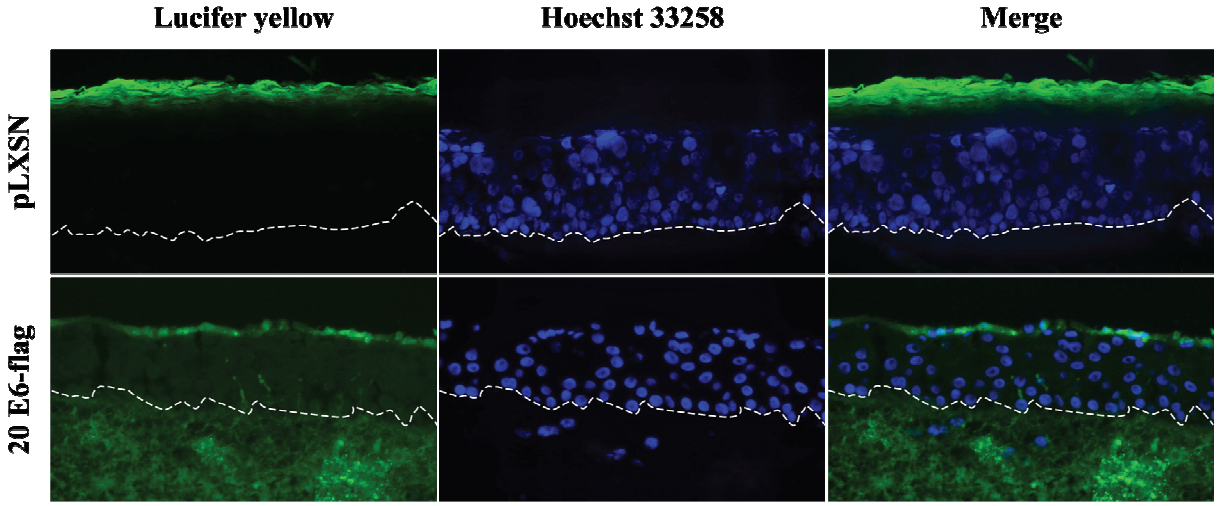

Figure 35. Lucifer yellow penetration assay showed that stratum corneum of pLXSN control raft was able to retain the dye whereas in Flag-tagged HPV20 E6 it diffused across the stratum corneum into the dermal equivalent. Dotted lines indicate basement membrane. Nuclei were counterstained with Hoechst 33258. Magnification 200x.

4.4.8.2 Increased permeability of tight junctions: altered inside-out barrier in Flag-tagged HPV20 E6 epithelia

In order to study how Flag-tagged HPV20 E6 expression affects the inside-out barrier function in stratifying epithelia, Biotin solution was added to the feeding medium of the raft cultures 30 min before harvesting. In pLXSN control tissue, Biotin moved up to the stratum granulosum (**Fig. 36 A**), where it was halted due to the presence of tight junctions, marked by cingulin staining (**Fig. 36 B**). However, Biotin penetrated the granular layer in Flag-tagged HPV20 E6-expressing epidermis and was able to reach the stratum corneum (**Fig. 36 A**). This observation was confirmed by the fact that Flag-tagged HPV20 E6 rafts were negative for cingulin staining (**Fig. 36 B**), indicating that the Biotin was not retained by the tight junctions and could reach the uppermost part of the tissue. Thus, tight junctions were disrupted in Flag-tagged HPV20 E6 samples and inside-out barrier was no longer functional.

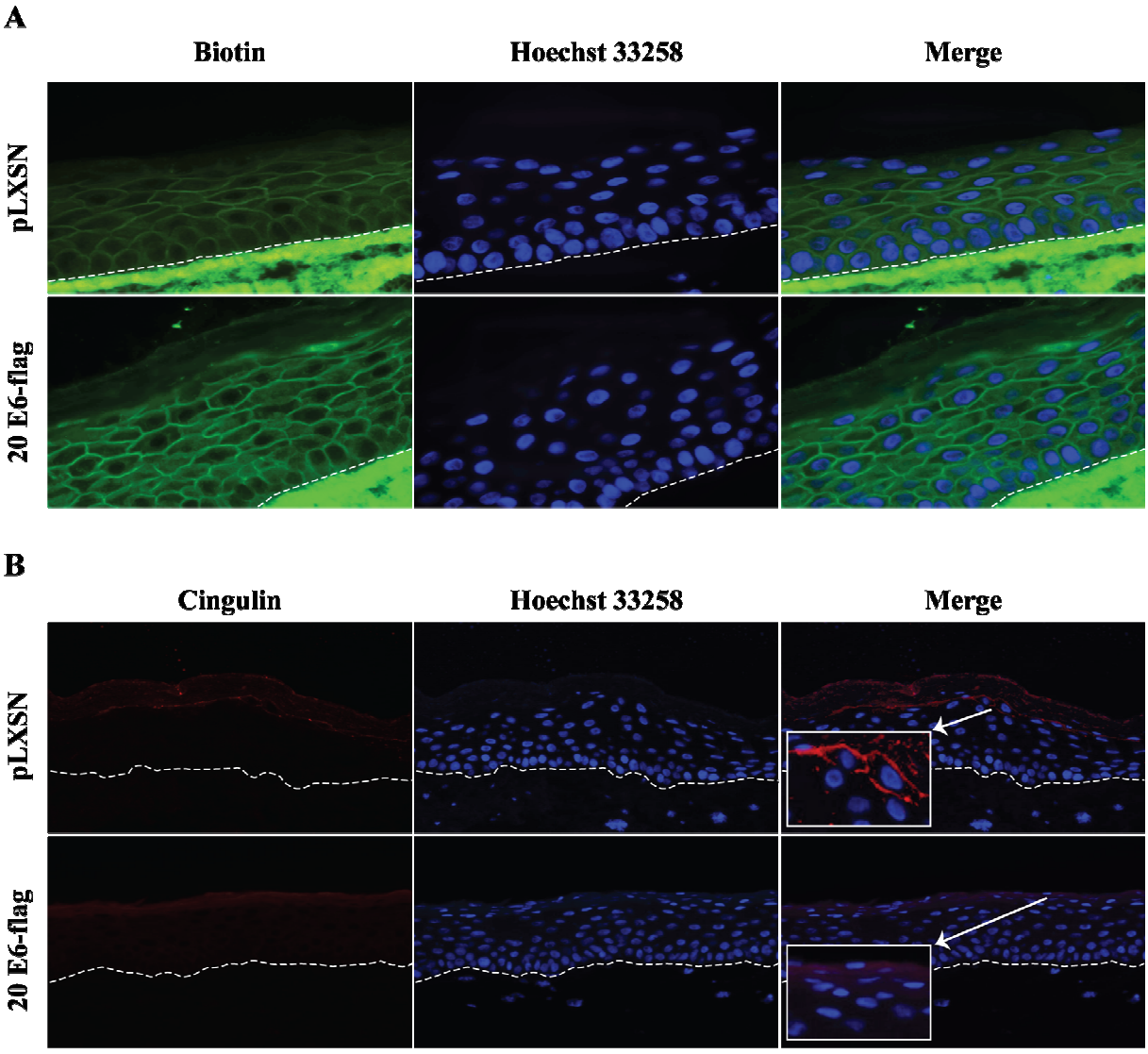

Figure 36. **A**. Biotin uptake assay. Inside-out barrier was functional in pLXSN control raft cultures whereas Biotin diffusion showed impaired barrier in HPV20 E6-flag raft culture. Dotted lines indicate basement membrane. Nuclei were counterstained with Hoechst 33258. Magnification 400x. **B**. Tight junction staining by localization of cingulin. In HPV20 E6-flag cultures the tight junctions were disrupted, in contrast to pLXSN control. Insert in merged picture shows detail of the upper stratum granulosum where tight junctions localise. Dotted lines indicate basement membrane. Magnification 200x.

4.4.9 Cell-cell communication: desmosomal distribution

Desmosomes are cell-to-cell adhesion structures that attach the cell surface adhesion proteins to intracellular keratin filaments (Langbein *et al.*, 2002). Differences in keratin expression profile and failure in barrier function suggested possible modifications in desmosome structure and/or localization. In order to examine the cellular distribution of desmosomes, desmoplakin staining was performed. This protein is an obligate component of

functional desmosomes which anchors intermediate filaments to desmosomal plaques in cell-to-cell adhesion complexes (Green *et al.*, 1990) and altered formation has been described in high-grade squamous intraepithelial lesions of the cervix (Alazawi *et al.*, 2003).

Immunofluorescence showed a similar distribution of desmosomes in Flag-tagged HPV20 E6 compared to control rafts as demonstrated by desmoplakin I/II staining (**Fig. 37**). Interestingly, desmoplakin staining made the presence of multilobular and pleomorfic nuclei more evident in Flag-tagged HPV20 E6 organotypic culture (**Fig. 37,** arrows).

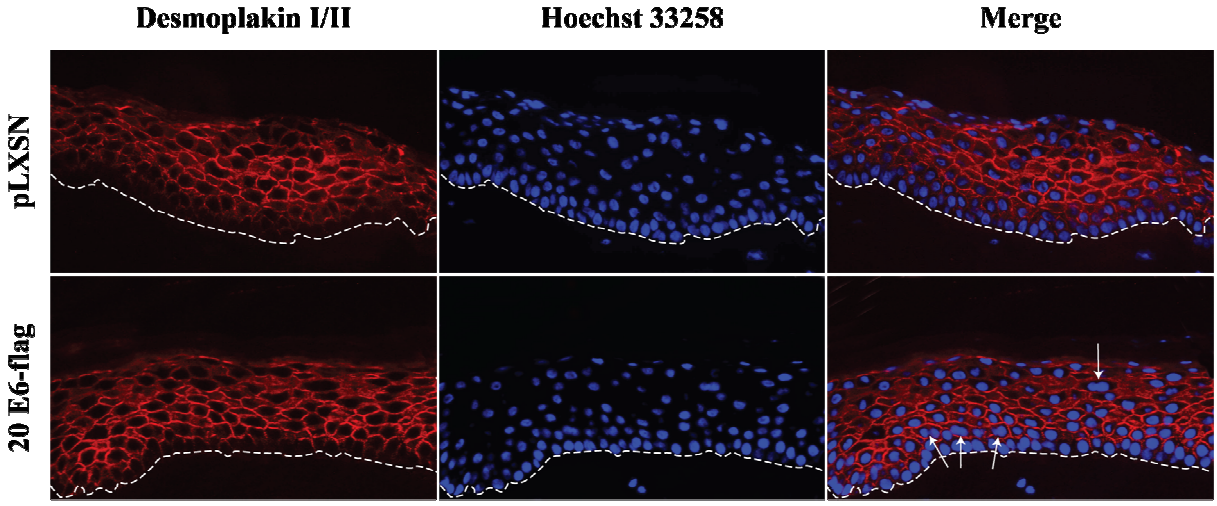

Figure 37. Study of desmosomal distribution by immunofluorescence staining showed correct desmosomal formation in HPV20 E6-flag and pLXSN control samples. Arrows indicate multilobular nuclei in HPV20 E6-flag raft cultures. Dotted lines indicate basement membrane. Nuclei counterstained with Hoechst 33258. Magnification 200x.

5 Discussion

Squamous cell cancer of the oral cavity is the third most common cancer in developing countries whereas esophageal cancer corresponds to the fifth most common cancer in males worldwide (Opitz *et al.*, 2002). Oropharyngeal and esophageal cancer are considered multifactorial, alcohol consumption and tobacco-use being the main risk factors (Castellsague *et al.*, 2004; Franceschi *et al.*, 1990; Ogden, 2005; Warnakulasuriya *et al.*, 2005). Smokers have a 4-7 times higher incidence for oropharyngeal and esophageal tumors than non-smokers. When tobacco is combined with alcohol consumption, the risk is further increased 19-fold (Zheng *et al.*, 1997). On the other hand, oropharyngeal and esophageal cancer patients infected with high risk HPV and with no alcohol or tobacco-use history have also been described (Loning *et al.*, 1985; Syrjanen *et al.*, 1983; Syrjanen *et al.*, 1982). Epidemiological differences between patients suggest the existence of two groups in the etiology of these malignancies corresponding to either viral infection or alcohol/tobacco consumption (Smith *et al.*, 2004).

HPV may cooperate with carcinogens in the development of oropharyngeal and esophageal tumors. It has been reported in nude mice that the early region of HPV16 is able to immortalize oral keratinocytes but only after 6 months of chronic exposure to the tobacco carcinogen Benzo[a]pyrene (BaP) (Li *et al.*, 1992). Oral keratinocytes isolated from these mice containing the HPV16 early region and exposed to BaP presented a malignant phenotype in organotypic raft culture (Park *et al.*, 1995). Moreover, it has been demonstrated that organotypic keratinocyte cultures exposed to BaP shown an increase in HPV16, 18 and 31 viral titers (Alam *et al.*, 2008). In addition, increased cervical cancer risk has been reported in smoking women (Nischan *et al.*, 1988; Stockwell and Lyman, 1987), as well as enhanced tumor progression (Phillips and Ni She, 1993) and invasive cervical cancer (Vaccarella *et al.*, 2008). BaP and other tobacco compounds such as 4-(methylnitrosamino)-1-(3-pyridyl)-1-butanone (NNK) have been found in the cervical mucus of smoker patients with cervical dysplasia (Holly *et al.*, 1993). This anatomical co-localization of both virus and carcinogen allows their interaction in the genital tract.

Cutaneous HPV have been found in skin SCC and HNSCC. Possible mechanisms through which genus Beta papillomaviruses types are involved in pathogenesis of disease are slowly evolving. Earlier epidemiological evidence high-lighted UV-irradiation as being an important co-factor in the development of pre- or malignant skin lesions (Brash *et al.*, 1991). *In vivo* and *in vitro* studies describing interactions of cutaneous HPV E6 and E7 genes with

cellular proteins confirm these data by indicating a necessity for additional UV-irradiation in the pathogenesis of skin disease in the presence of HPV (Dong *et al.*, 2008; Jackson *et al.*, 2000; Michel *et al.*, 2006; Struijk *et al.*, 2008; Underbrink *et al.*, 2008).

HPV20 belongs to the Genus Beta papillomavirus and it has been detected in NMSC (de Villiers, 1998; Feltkamp *et al.*, 2003). The involvement of HPV20 infection in the onset of skin papillomas and malignant transformation was demonstrated in HPV20 E6/E7 transgenic mice chronically exposed to UV-irradiation (Michel *et al.*, 2006). Interestingly, HPV20 has been also found in patients with head and neck and esophageal SCC (de Villiers *et al.*, 1999; Lavergne and de Villiers, 1999). However, the role of HPV20 in oropharyngeal and esophageal cancer onset and progression has not yet been elucidated.

DNA repair and apoptosis are induced in skin tissue as defense mechanisms after UV damage. However, it has been described that primary keratinocytes expressing HPV20 E6/E7 or E6 proteins prevent apoptosis after UV exposure (Struijk *et al.*, 2008), promoting the viral infection in UV-exposed sites. Similarly to the situation in the skin, where HPV20 acts in cooperation with UV-irradiation, we speculated that the virus might interact with carcinogens (e.g. tobacco and alcohol) in the oropharyngeal and esophageal epithelia to cause malignancy.

4-NQO is a synthetic carcinogen which induces oral SCC in rodents which undergo chronic 4-NQO uptake in the drinking water (Miyamoto *et al.*, 2008; Srinivasan *et al.*, 2008; Vered *et al.*, 2005). This chemical mimics the effect of UV irradiation by formation of guanine adducts, inducing DNA damage (Snyderwine and Bohr, 1992). 4-NQO behaves similarly to tobacco, creating DNA adducts, single-strand DNA breaks, pyrimidine dimmers and formation of oxidized bases (Kim *et al.*, 2006). 4-NQO has been largely used in *in vitro* models because, contrary to tobacco compounds, does not need metabolic activation.

Studying the cellular and viral factors involved in HPV20 promoter activation is important to understand the infection mechanism of this cutaneous virus. Promoter activation assays demonstrated a 4-fold activation of HPV20 URR by wtp53 whereas mutp53R248W expression did not modify the promoter activity (**Fig. 10**). When TAp63α or ΔNp63α were expressed, HPV20 URR was highly up-regulated, 25-fold and 35-fold respectively (**Fig. 11**), in accordance with previous reports (Fei *et al.*, 2006; Fei *et al.*, 2005). Interestingly, Flag-tagged HPV20 E6, Flag-tagged HPV20 E7 and Flag-tagged HPV20 E6/E7 expression led to an enhancement in HPV20 URR activity, indicating that the viral proteins themselves are able to induce promoter activation (**Fig. 12 and 19**). Flag-tagged HPV20 E6 expression did not influence the activation pattern of wtp53, TAp63α or ΔNp63α on HPV20 URR (**Fig. 13 and 14**). When cells were treated for 24 h with the carcinogen 4-NQO, HPV20 promoter was

activated and the chemical enhanced the Flag-tagged HPV20 E6, Flag-tagged HPV20 E7 as well as Flag-tagged HPV20 E6/E7 effect on HPV20 URR activation (**Fig. 19**). Thus, our results indicated the possible cooperation of cellular factors (wtp53, TAp63α and ΔNp63α), viral proteins (HPV20 E6 and E7) and chemical carcinogens (4-NQO) in the pathogenesis of HPV-associated cutaneous lesions. Experimental approaches with the presence of the complete HPV genome are necessary to elucidate the exact mechanistic action of HPV20.

Our results in HPV20 promoter activation studies prompted us to investigate the effect of Flag-tagged HPV20 E6 expression and/or 4-NQO treatment in organotypic cell culture where keratinocytes differentiate, mimicing the *in vivo* situation in epidermal tissue. In the organotypic culture model, epidermal stratification and expression of differentiation-specific proteins occurs, allowing the characterization of Flag-tagged HPV20 E6 constitutive expression and 4-NQO treatment in epidermal development and the determination of cellular factors that may be affected.

NIKS cells grown on a collagen matrix underwent terminal epidermal differentiation and stratified. Flag-tagged HPV20 E6 expression altered the epidermal morphology, showing clear features of disturbed stratification and dyskeratosis (**Fig. 24**). The epidermal basal cell layer remained intact but the stratum spinosum was poorly developed and normal orientation of the epidermal layers was lost. Flag-tagged HPV20 E6 rafts presented a stratum granulosum that differ from the typical layer with dense basophilic keratohyalin granules of a healthy epidermis (Gartner and Hiatt, 2007). Instead, ultrastructural examination revealed fewer keratin granules very heterogeneous in size and lipid droplets accumulation (**Fig. 32 C**). The parabasal layer showed basophilic nuclei as observed for *Epidermodysplasia verruciformis* HPV types (Alpsoy *et al.*, 2002) as well as anucleated eosinophilic inclusions resembling dyskeratotic cells.

Foamy-like keratinocytes were present in the upper layers of the Flag-tagged HPV20 E6 rafts. These aberrant keratinocytes have been found in lesions infected with *Epidermodysplasia verruciformis*-HPV types (Berger *et al.*, 1991), and also in pityriasis versicolor-like lesions infected with HPV20 (Weber *et al.*, 1994). These previous reports combined with our results open the question whether HPV20 E6 expression is responsible for the formation of foamy-like keratinocytes observed in patients and how other HPV20 viral proteins contribute to it. It still remains to be elucidated whether this ability of HPV20 E6 to form foamy-like keratinocytes is a unique feature of HPV20 or it is shared by other HPV types. Flag-tagged HPV20 E6 rafts also showed bubble-like cavernae formations in the

stratum corneum that probably corresponded to failures in cell-cell adherence, alterations in cellular composition and lipid extrusion (**Fig. 24**).

Aberrant morphology of Flag-tagged HPV20 E6 organotypic cultures suggested possible differences in the stage of keratinocyte differentiation, as measured by occurrence and distribution of specific keratins and proteins of the cornified envelope:

- Cytokeratin 14 is present in the epidermal undifferentiated compartment that contains the stem cells of the skin (reviewed in Moll *et al.*, 2008). This protein is highly up-regulated in oral carcinomas of snuff dippers patients (Ibrahim *et al.*, 1998) as well as in both keratinizing and non-keratinizing squamous cell cervical carcinomas, where cytokeratin 14 is not only confined to the basal cells but it also localizes in suprabasal layers (Smedts *et al.*, 1992). In our organotypic system, cytokeratin 14 was up-regulated and expressed throughout the entire suprabasal compartment in Flag-tagged HPV20 E6-expressing epidermis, with a prominent staining of the eosinophilic dyskeratotic cells of the upper layers (**Fig. 29 A and B**). In contrast, it was confined to the basal layer in the pLXSN control raft. The up-regulation of cytokeratin 14, typical of undifferentiated cells, indicates that Flag-tagged HPV20 E6 organotypic cultures retain features of a simpler epidermis, corresponding to a less differentiated phenotype.
- Cytokeratin 10 is normally expressed in all suprabasal layers of the skin. Down-regulation of this early differentiation marker has been reported in invasive cervical SCC (Carrilho *et al.*, 2004; Maddox *et al.*, 1999). In addition, organotypic cultures of primary keratinocytes expressing HPV20 E6/E7 showed a delay in cytokeratin 10 expression (Boxman *et al.*, 2001). Interestingly, we observed the same tendency without the involvement of HPV20 E7. Cytokeratin 10 protein localization was delayed to the second and third suprabasal layers of Flag-tagged HPV20 E6 rafts, being more obvious in HPV16 E6/E7 samples (**Fig. 29 A and C**).
- Late differentiation markers staining revealed delayed differentiation in Flag-tagged HPV20 E6 as well as 16 E6/E7 organotypic cultures. Involucrin is a keratin-associated protein indicative of epithelial differentiation (Rossi *et al.*, 1998). Rafts harboring Flag-tagged HPV20 E6 manifested a delay in the onset of involucrin expression in the lower spinosum layer (**Fig. 30 A**), contrary to pLXSN control raft culture where involucrin was detected throughout the entire suprabasal compartment. Similarly, the late differentiation marker loricrin was reduced in Flag-tagged HPV20 E6 organotypic cultures, as previously reported in HPV20 E6/E7 and HPV27 E6/E7 transgenic mice chronically exposed to UV (Michel *et al.*, 2006), while it disappeared in HPV16 E6/E7 (**Fig. 30 B**).

Epithelial cancers are characterized by immortalization and inhibition of terminal differentiation. When taken together, our results indicate that HPV20 E6 by itself induces aberrant and incomplete differentiation in raft cultures as evidenced by over-expression and altered expression profile of cytokeratin 14 and delayed expression of cytokeratin 10, involucrin and loricrin. Similar results has been previously shown for HPV16 E7, HPV16 E1^E4, HPV18 E6/E7, HPV6, HPV11, EV-HPV5, 12, 15, 17, 20 and HPV38 E6/E7 (Boxman *et al.*, 2001; Flores *et al.*, 2000; Garner-Hamrick *et al.*, 2004; Mullink *et al.*, 1991; Nakahara *et al.*, 2005; Woodworth *et al.*, 1992).

HPV protein expression alters several cellular factors of the host cell. E6 protein of high risk HPV types targets p53 tumor suppressor to proteosomal degradation through complex formation with ubiquitin ligase E6AP (Huibregtse *et al.*, 1991). In contrast, cutaneous HPV E6 proteins are unable to promote p53 degradation (Pim *et al.*, 2002). In our studies p53 levels were increased in Flag-tagged HPV20 E6 monolayer (**Fig. 20**) and rafts cultures, where expression was extended into the suprabasal compartment (**Fig. 28 A and B**). Over-expression of p53 may lead to G1 cell cycle arrest and apoptosis (reviewed in Vogelstein *et al.*, 2000). However, p53 accumulation in Flag-tagged HPV20 E6 rafts did not alter proliferation rates (**Fig. 31**). A similar p53 expression pattern was observed in HPV20 E6/E7-expressing transgenic mice chronically exposed to UV (Michel *et al.*, 2006), indicating the influence of HPV20 E6 in p53 over-expression or stabilization. Furthermore, it has been reported p53 accumulation in different tissues infected by several HPV types: E7 of high risk genital HPV types led to increased p53 levels but the protein activity was impaired (Munger *et al.*, 2001). Cutaneous HPV38 E6/E7 are able to immortalize keratinocytes and lead to accumulation of wtp53 (Accardi *et al.*, 2006); in those HPV38 E6/E7- expressing keratinocytes, stabilized p53 has changes in the phosphorylation pattern, localizes exclusively in the nucleus and cells proliferate normally, without increased apoptosis. In addition, this impairment in p53 functionality was found to be induced by up-regulation of ΔNp73, which inhibits the transcriptional regulatory properties of p53 in growth arrest and apoptosis. Further investigation of p53 mutations, phosphorylation pattern, localization and functionality under the context of HPV20 E6 expression is necessary for understanding the relevance of p53 accumulation.

The cyclin-dependent kinase inhibitor $p21^{CIP1}$ is a transcriptional target of p53 that induces G1 arrest after DNA damage (Waldman *et al.*, 1995). However, it is also involved in terminal differentiation and senescence independently of p53 (Macleod *et al.*, 1995; Parker *et al.*, 1995). $p21^{CIP1}$ was up-regulated in Flag-tagged HPV20 E6 and HPV16 E6/E7 organotypic

cultures (**Fig. 28 A and C**), probably induced by $p21^{CIP1}$ protein stabilization and not by transcription activation (Jones *et al.*, 1997). $p21^{CIP1}$ has p53-dependent and independent functions in cell cycle and differentiation. The role of $p21^{CIP1}$ accumulation in Flag-tagged HPV20 E6 and HPV16 E6/E7 organotypic cultures remains to be elucidated. However, a perturbed function of $p21^{CIP1}$ cannot be excluded considering that its up-regulation did not negatively influence cell proliferation in the organotypic cell cultures (**Fig. 31**).

ΔNp63α is mainly expressed in the basal cells of normal epithelium and plays a crucial role in epithelial morphogenesis and differentiation (reviewed in Candi *et al.*, 2007). An organotypic culture model where ΔNp63α was knocked-down by siRNA techniques showed that several proteins involved in skin development (cytokeratin 1 and 10, involucrin, loricrin and corneodesmin) have an altered expression profile in the absence of ΔNp63α (McKeon, 2004). This protein has the transactivation domain present in the TAp53 isoforms partially deleted. It can block the function of p53, TAp63 and TAp73 proteins -that may occur by DNA binding site competition in the promoter of target genes and by formation of hetero-oligomers through binding to the transactivation domain of p53 family TA isoforms (reviewed in Yang and McKeon, 2000). ΔNp63α is up-regulated when Flag-tagged HPV20 E6 is expressed in monolayer (**Fig. 20**) and organotypic cultures (**Fig. 28 A and D**). ΔNp63α accumulation has been observed in bladder, breast, cervix, head and neck, lung and prostrate cancer (reviewed in Westfall and Pietenpol, 2004), pointing to a possible role of this protein as oncogene (Hagiwara *et al.*, 1999). A previous report from our lab described wtp53-mediated degradation of HPV20 E6 whereas the UV-induced mutant p53R248W and ΔNp63α exerted a protective effect on HPV20 E6 (Fei and de Villiers, 2008). In our system, p53 was accumulated in Flag-tagged HPV20 E6 organotypic cultures. Whether accumulated p53 targeted HPV20 E6 to degradation remains uncertain. However, one can speculate that HPV20 E6 degradation may be protected by the observed ΔNp63α up-regulation, as well as by a possible p53 impaired function.

Uncontrolled cellular proliferation is characteristic of carcinogenesis (reviewed in Golias *et al.*, 2004). Therefore, possible changes in proliferation rates induced by Flag-tagged HPV20 E6 were studied. E7 plays a key role in promoting proliferation and deregulating cell cycle as demonstrated in HPV16 and 18 types (Boulet *et al.*, 2007; Munger *et al.*, 2001) as well as HPV10, 32, 48, 54 and 77 (Caldeira *et al.*, 2000) whereas E6 seems to help E7´s action in unscheduled proliferation. Flag-tagged HPV20 E6 expression did not alter proliferation in differentiated keratinocytes of the epidermal layer, showing similar BrdU incorporation rates when compared to pLXSN control rafts (**Fig. 31 C**). In agreement with our

observation, organotypic cultures of primary foreskin keratinocytes expressing HPV20 E6/E7 proteins did not present alterations in BrdU incorporation or PCNA staining (Boxman *et al.*, 2001). It has been demonstrated that HPV16 E6 constitutive expression in rafts does not lead to an increase proliferation rate (Halbert *et al.*, 1992). In contrast, BrdU incorporation and PCNA labeling in HPV16 E6/E7 raft cultures were extended to the suprabasal layers (**Fig. 31 B and C**), as previously reported in organotypic cultures of primary keratinocytes (Blanton *et al.*, 1992; Halbert *et al.*, 1992).

PCNA is an auxiliary factor for DNA polymerase δ and ε, important during DNA replication and repair. It is a cellular target of $p21^{CIP1}$, which binds it inducing cell cycle arrest (Li *et al.*, 1994). Western blot analysis of proteins extracted from raft cultures showed a down-regulation of PCNA levels in Flag-tagged HPV20 E6 samples (**Fig. 31 A**). PCNA constitutes a downstream target of p53 (Mercer *et al.*, 1991), indicating that p53 accumulation increases $p21^{CIP1}$ levels, that binds and blocks PCNA expression. Our results might indicate the decreased levels of PCNA as a consequence of p53 and $p21^{CIP1}$ accumulation. Proliferation rates were indeed not altered, as demonstrated by BrdU incorporation. However, analysis of other proliferation markers such as Ki67 or cyclin D1 may corroborate these results.

Flag-tagged HPV20 E6 organotypic cultures of keratinocytes showed differences in epidermal morphology and differentiation pattern, as well as overexpression of cellular factors p53, $p21^{CIP1}$ and ΔNp63α, in contrast to the pLXSN control rafts. Flag-tagged HPV20 E6 expressing rafts showed failures in the apoptosis program as observed by the formation of apoptotic figures in the uppermost parts of the epidermis (**Fig. 32 C**). In addition, stratum corneum was present in Flag-tagged HPV20 E6 and HPV16 E6/E7 organotypic cultures (**Fig. 24 and 25**) but its appearance was thinner and less compact than in control pLXSN epidermis, indicating a disturbed and delayed differentiation program. A functional epidermal barrier needs a correct balance between differentiation, proliferation and apoptosis rates (Presland and Dale, 2000). Because of the alterations observed in epidermal morphology, apoptosis and differentiation pattern, aberrations in barrier function were suspected. Disturbance was studied by Lucifer yellow dye penetration (**Fig. 35**) and Biotin uptake (**Fig. 36 A**) assays. Our results indicated that the cornified layer of Flag-tagged HPV20 E6 rafts presented a perturbed barrier function both outside-in and inside-out.

The defective barrier prompted us to analyze the desmosomal localization and presence of tight junctions in the stratum granulosum. Desmosomes play an important role in tissue integrity of epithelia by linking cytoskeletal components such as keratin filaments to

cellular membranes (Herve, 2008; Langbein *et al.*, 2002; Stokes, 2007). Altered desmosomes has been described in high-grade squamous intraepithelial lesions of the cervix (Alazawi *et al.*, 2003). In Flag-tagged HPV20 E6 expressing rafts, the desmosomal number and architecture was normal, comparable to the pLXSN control rafts (**Fig. 32 B and 37**). A recent report showed the degradation of the multi-PDZ protein PATJ, a critical component of tight junction, by HPV18 E6 and E6* proteins (Storrs and Silverstein, 2007). Adenovirus E4-ORF1 protein also binds to several PDZ proteins that complexes to tight junctions, inhibiting the formation of these structures (Latorre *et al.*, 2005). In our system, tight junctions were disrupted in the Flag-tagged HPV20 E6-expressing rafts as demonstrated by cingulin staining (**Fig. 36 B**), thus explaining the impaired inside-out barrier observed by Biotin uptake (**Fig. 36 A**). PDZ binding motifs is a specific feature of high risk mucosal HPV E6 proteins (Watson *et al.*, 2003) whereas cutaneous HPV E6 are not able to target proteosome-mediated PDZ proteins degradation (Elbel *et al.*, 1997; Fei and de Villiers, 2008; Pim *et al.*, 2002). Therefore, HPV20 E6 can not interfere with PDZ proteins and its molecular mechanism for targeting tight junction disruption requires further investigation.

Ceramides, fatty acids and cholesterol form the extracellular lamellar membrane, a densely packed structure in the stratum corneum (Bouwstra and Ponec, 2006; Elias and Menon, 1991). Alteration in these components leads to an accumulation of fatty acids and impairment of the barrier function (Feingold, 2007). These modifications may occur without alterations in proliferation and stratified organization in the keratinocytes as demonstrated in transgenic mice with inactivating mutations in 12R-lipoxigenase (12R-LOX) and epidermal LOX-3 (Epp *et al.*, 2007) and in patients with autosomal recessive congenital ichthyosis (ARCI) (Eckl *et al.*, 2005). Topical application of oleic acid and palmitoleic acid on hairless mouse skin induces increased transepidermal water loss (TEWL) as well as scaly skin, abnormal keratinization and hyperplasia (Katsuta *et al.*, 2005). In our system, the lipid composition of the organotypic raft cultures was analyzed, and several unsaturated fatty acids were found to be significantly up-regulated (**Fig. 33**). Interestingly, both oleic acid and palmitoleic acid were increased in Flag-tagged HPV20 E6 organotypic cultures, which may contribute to the observed loss of epidermal barrier function. It has recently been reported that the cornified envelope is not only formed by covalent bonds between glutamic acid residues of proteins and ceramides but also between free fatty acids and serine residues (Lopez *et al.*, 2007),. Alterations in fatty acid content lead to pertubance of the cornified envelope, as observed in Flag-tagged HPV20 E6 organotypic cultures. Aberrant lipid metabolism was also revealed by lipid accumulation into lipid droplets in the stratum granulosum and the basal

membrane, as demonstrated by electron microscopy (**Fig. 32 C**) and Oil Red O staining of organotypic culture cryosections (**Fig. 34**). Lipids present in the skin are particularly susceptible to oxidation. Unsaturated fatty acids oxidation occurs either spontaneously by reaction with oxygen on exposure to air or in the presence of light. Lipid peroxidation produces free radicals that are mutagenic and carcinogenic (reviewed in Briganti and Picardo, 2003). Flag-tagged HPV20 E6 induced abnormal lipid synthesis and accumulation, what may lead to increased formation of free radical species, especially after UV radiation, facilitating the onset of malignancies in viral infected epithelia. In summary, Flag-tagged HPV20 E6 expression leads to impaired barrier function, disruption of tight junctions and altered lipid composition. These alterations in the epidermis may be crucial during HPV infection and its molecular mechanisms and relevance in disease requires further investigation.

HPV20 requires UV-irradiation for inducing skin carcinogenesis. In a similar way, oropharyngeal and esophageal cancer may be promoted by the interaction and cooperation of different risk factors. In order to investigate the possible synergistic effect of tobacco/alcohol use and HPV20 infection, HPV monolayer and organotypic raft cultures models were treated with the UV-mimetic 4-NQO. This chemical was used as carcinogen model, comparable with the tobacco effect in the oral and laryngeal mucosa. In our studies, the influence of short term 4-NQO treatment in cell death, regulation of cell cycle, activation profile of HPV20 viral promoter and epidermal morphology and development was investigated combined with the expression of Flag-tagged HPV20 E6 protein. 4-NQO promotes apoptosis at high doses via p53-dependent mitochondrial signalling pathway (Han *et al.*, 2007). Low dose ($\leq$ 3 μM) 4-NQO treatment in immortalized keratinocytes induced minimal cell death (**Fig. 17**) and facilitated entry into S-phase and G2/M (**Fig. 18**), as previously described (Heron-Milhavet *et al.*, 2001). In accordance with Han *et al*. (2007), we observed G1 arrest and apoptosis when 4-NQO was used at high concentration (**Fig. 18 B**). It has been reported that E6 proteins of HPV8 and 38 of the Genus Beta papillomavirus are able to expand keratinocyte life span whereas E6 of HPV20 and HPV5 do not significantly change the population doublings (Bedard *et al.*, 2008). In our studies, we confirmed that Flag-tagged HPV20 E6 was not able to extend life span of the cells (**Fig. 22**). One single report described immortalization of normal human fibroblasts by chronic exposure to 4-NQO (Bai *et al.*, 1993). However, in our system 4-NQO short term treatment was not sufficient for immortalizing primary keratinocytes alone or expressing Flag-tagged HPV20 E6, suggesting that the chemical action varies upon different cell types and/or there is a need to perform the studies with longer 4-NQO exposure time in order to achieve immortalization. 4-NQO induces $p21^{CIP1}$ over-

expression allowing DNA repair and p53-dependent apoptosis through mitochondrial signaling pathway when damage can not be repaired (Han *et al.*, 2007). Interestingly, p53 was up-regulated in keratinocytes cells transiently transfected with Flag-tagged HPV20 E6 and treated with 4-NQO in comparison to control and Flag-tagged HPV20 E6-transfected cells not incubated with the chemical (**Fig. 20**). However, in organotypic cultures, 4-NQO did not alter the p53 and $p21^{CIP1}$ expression and localization pattern in the epidermis. Expression levels of Flag-tagged HPV20 E6 were slightly increased after 4-NQO treatment (**Fig. 20 and 27 B**), suggesting that chemical exposure stabilizes the viral protein, which might have a positive effect in the pathogenesis of the virus.

Li and coworkers demonstrated an increase in mRNA of PCNA after short exposure to 4-NQO in human hepatoblastoma cell line Hep G_2 and the human cervical epithelial cell line HeLa (Li *et al.*, 2005). In our monolayer and organotypic raft culture system, no difference in PCNA expression was found after 4-NQO treatment (**Fig. 20 and 31 A, B**). This difference could be attributed to a short 4-NQO treatment as well as differences in cellular type and protein levels of PCNA upstream targets like p53.

Taken together, the delay in cytokeratin 10 and involucrin expression (**Fig. 29 C and 30 A**) and absence of loricrin staining (**Fig. 30 B**) when 4-NQO was applied to the Flag-tagged HPV20 E6 organotypic culture medium points the possible synergistic effect of virus infection and chemical treatment in malignant conversion by formation of a less differentiated epidermis. Moreover, HPV20 URR up-regulation in monolayer keratinocytes (**Fig. 19**) together with increased Flag-tagged HPV20 E6 levels (**Fig. 20 and 27 B**) indicate that the chemical has a positive influence on the viral protein expression and therefore cooperates with HPV20 during infection and tumor progression. Longer chemical treatments are necessary to test the viral influence in cells chronically exposed to 4-NQO, mimicing the natural situation that occurs in oropharyngeal and esophageal cancer patients with alcohol/tobacco use and who are positive for HPV20 viral infection.

Organotypic raft culture studies show that keratinocytes expressing Flag-tagged HPV20 E6 are able to stratify but fail to form a normal epidermis and present aberrant differentiation. The normal keratin pattern is disturbed, resembling simpler epithelia and this phenotype is enhanced after 4-NQO treatment. Cellular protein p53 accumulates whereas $p21^{CIP1}$ and ΔNp63α modify their expression pattern in the epithelia. Organotypic raft cultures expressing Flag-tagged HPV20 E6 present foamy-like keratinocytes resembling the typical structures found in *Epidermodysplasia verruciformis* patients and pityriasis versicolor-like lesions infected with HPV20, indicating a probably involvement of HPV20 E6 in the

formation of such aberrant keratinocytes. In addition, Flag-tagged HPV20 E6 expression is capable of altering the functionality of the skin barrier function. That is probably done by abrogation of tight junction formation in the stratum granulosum and changes in the lipid metabolism of the skin leading to its accumulation and deregulated composition. Disruption of the skin barrier is related to a number of cutaneous diseases, all connected with underlying genetic and immune disorders. These include different forms of ichthyosis, atopic dermatitis and other eczemas (Elias *et al.*, 2008; Hanifin, 2008; Hoffjan and Stemmler, 2007). Correlation between these diseases and cutaneous HPV requires further investigation. Future studies with other cutaneous HPV and different E6 proteins will provide insight into HPV type specificity in the observed features and relevance in the pathogenesis of disease.

6 References

Aaltonen LM, Rihkanen H, Vaheri A (2002). Human papillomavirus in larynx. *Laryngoscope* **112:** 700-7.

Agarwal ML, Agarwal A, Taylor WR, Stark GR (1995). p53 controls both the G2/M and the G1 cell cycle checkpoints and mediates reversible growth arrest in human fibroblasts. *Proc Natl Acad Sci USA* **92:** 8493-7.

Akgul B, Cooke JC, Storey A (2006). HPV-associated skin disease. *J Pathol* **208:** 165-75.

Alam M, Ratner D (2001). Cutaneous squamous-cell carcinoma. *N Engl J Med* **344:** 975-83.

Alam S, Conway MJ, Chen HS, Meyers C (2008). The cigarette smoke carcinogen benzo[a]pyrene enhances human papillomavirus synthesis. *J Virol* **82:** 1053-8.

Alazawi WO, Morris LS, Stanley MA, Garrod DR, Coleman N (2003). Altered expression of desmosomal components in high-grade squamous intraepithelial lesions of the cervix. *Virchows Arch* **443:** 51-6.

Allen-Hoffmann BL, Schlosser SJ, Ivarie CA, Sattler CA, Meisner LF, O'Connor SL (2000). Normal growth and differentiation in a spontaneously immortalized near-diploid human keratinocyte cell line, NIKS. *J Invest Dermatol* **114:** 444-55.

Antonsson A, Forslund O, Ekberg H, Sterner G, Hansson BG (2000). The ubiquity and impressive genomic diversity of human skin papillomaviruses suggest a commensalic nature of these viruses. *J Virol* **74:** 11636-41.

Arima Y, Nishigori C, Takeuchi T, Oka S, Morimoto K, Utani A *et al* (2006). 4-Nitroquinoline 1-oxide forms 8-hydroxydeoxyguanosine in human fibroblasts through reactive oxygen species. *Toxicol Sci* **91:** 382-92.

Arroyo M, Bagchi S, Raychaudhuri P (1993). Association of the human papillomavirus type 16 E7 protein with the S-phase-specific E2F-cyclin A complex. *Mol Cell Biol* **13:** 6537-46.

Asgari MM, Kiviat NB, Critchlow CW, Stern JE, Argenyi ZB, Raugi GJ *et al* (2008). Detection of human papillomavirus DNA in cutaneous squamous cell carcinoma among immunocompetent individuals. *J Invest Dermatol* **128:** 1409-17.

Astori G, Lavergne D, Benton C, Hockmayr B, Egawa K, Garbe C *et al* (1998). Human papillomaviruses are commonly found in normal skin of immunocompetent hosts. *J Invest Dermatol* **110:** 752-5.

Aubry K, Paraf F, Monteil J, Bessede JP, Rigaud M (2008). Characterization of a new rat model of head and neck squamous cell carcinoma. *In Vivo* **22:** 403-8.

Babawale M, Seth R, Christian A, Al-Utayem W, Narula R, Jenkins D (2005). Histological analysis of cervical intraepithelial neoplasia. *Methods Mol Med* **119:** 41-8.

Bai L, Mihara K, Kondo Y, Honma M, Namba M (1993). Immortalization of normal human fibroblasts by treatment with 4-nitroquinoline 1-oxide. *Int J Cancer* **53:** 451-6.

Bailleul B, Daubersies P, Galiegue-Zouitina S, Loucheux-Lefebvre MH (1989). Molecular basis of 4-nitroquinoline 1-oxide carcinogenesis. *Jpn J Cancer Res* **80:** 691-7.

Baker TS, Newcomb WW, Olson NH, Cowsert LM, Olson C, Brown JC (1991). Structures of bovine and human papillomaviruses. Analysis by cryoelectron microscopy and three-dimensional image reconstruction. *Biophys J* **60:** 1445-56.

Banerjee NS, Genovese NJ, Noya F, Chien WM, Broker TR, Chow LT (2006). Conditionally activated E7 proteins of high-risk and low-risk human papillomaviruses induce S phase in postmitotic, differentiated human keratinocytes. *J Virol* **80:** 6517-24.

Bedard KM, Underbrink MP, Howie HL, Galloway DA (2008). The E6 oncoproteins from human betapapillomaviruses differentially activate telomerase through an E6AP-dependent mechanism and prolong the lifespan of primary keratinocytes. *J Virol* **82:** 3894-902.

Berezutskaya E, Yu B, Morozov A, Raychaudhuri P, Bagchi S (1997). Differential regulation of the pocket domains of the retinoblastoma family proteins by the HPV16 E7 oncoprotein. *Cell Growth Differ* **8:** 1277-86.

Berger TG, Sawchuk WS, Leonardi C, Langenberg A, Tappero J, Leboit PE (1991). Epidermodysplasia verruciformis-associated papillomavirus infection complicating human immunodeficiency virus disease. *Br J Dermatol* **124:** 79-83.

Berkhout RJ, Tieben LM, Smits HL, Bavinck JN, Vermeer BJ, ter Schegget J (1995). Nested PCR approach for detection and typing of epidermodysplasia verruciformis-associated human papillomavirus types in cutaneous cancers from renal transplant recipients. *J Clin Microbiol* **33:** 690-5.

Besson A, Dowdy SF, Roberts JM (2008). CDK inhibitors: cell cycle regulators and beyond. *Dev Cell* **14:** 159-69.

Biliris KA, Koumantakis E, Dokianakis DN, Sourvinos G, Spandidos DA (2000). Human papillomavirus infection of non-melanoma skin cancers in immunocompetent hosts. *Cancer Lett* **161:** 83-8.

Blanton RA, Coltrera MD, Gown AM, Halbert CL, McDougall JK (1992). Expression of the HPV16 E7 gene generates proliferation in stratified squamous cell cultures which is independent of endogenous p53 levels. *Cell Growth Differ* **3:** 791-802.

Blanton RA, Perez-Reyes N, Merrick DT, McDougall JK (1991). Epithelial cells immortalized by human papillomaviruses have premalignant characteristics in organotypic culture. *Am J Pathol* **138:** 673-85.

Borradori L, Sonnenberg A (1996). Hemidesmosomes: roles in adhesion, signaling and human diseases. *Curr Opin Cell Biol* **8:** 647-56.

Boukamp P, Breitkreutz D, Stark HJ, Fusenig NE (1990). Mesenchyme-mediated and endogenous regulation of growth and differentiation of human skin keratinocytes derived from different body sites. *Differentiation* **44:** 150-61.

Boulet G, Horvath C, Vanden Broeck D, Sahebali S, Bogers J (2007). Human papillomavirus: E6 and E7 oncogenes. *Int J Biochem Cell Biol* **39:** 2006-11.

Bourdon JC (2007). p53 Family isoforms. *Curr Pharm Biotechnol* **8:** 332-6.

Bourdon JC, Fernandes K, Murray-Zmijewski F, Liu G, Diot A, Xirodimas DP *et al* (2005). p53 isoforms can regulate p53 transcriptional activity. *Genes Dev* **19:** 2122-37.

Boxman IL, Mulder LH, Noya F, de Waard V, Gibbs S, Broker TR *et al* (2001). Transduction of the E6 and E7 genes of epidermodysplasia-verruciformis-associated human papillomaviruses alters human keratinocyte growth and differentiation in organotypic cultures. *J Invest Dermatol* **117:** 1397-404.

Bradford MM (1976). A rapid and sensitive method for the quantitation of microgram quantities of protein utilizing the principle of protein-dye binding. *Anal Biochem* **72:** 248-54.

Brash DE, Rudolph JA, Simon JA, Lin A, McKenna GJ, Baden HP *et al* (1991). A role for sunlight in skin cancer: UV-induced p53 mutations in squamous cell carcinoma. *Proc Natl Acad Sci USA* **88:** 10124-8.

Briganti S, Picardo M (2003). Antioxidant activity, lipid peroxidation and skin diseases. What's new. *J Eur Acad Dermatol Venereol* **17:** 663-9.

Buck CB, Cheng N, Thompson CD, Lowy DR, Steven AC, Schiller JT *et al* (2008). Arrangement of L2 within the papillomavirus capsid. *J Virol* **82:** 5190-7.

Butz K, Hoppe-Seyler F (1993). Transcriptional control of human papillomavirus (HPV) oncogene expression: composition of the HPV type 18 upstream regulatory region. *J Virol* **67:** 6476-86.

Caldeira S, de Villiers EM, Tommasino M (2000). Human papillomavirus E7 proteins stimulate proliferation independently of their ability to associate with retinoblastoma protein. *Oncogene* **19:** 821-6.

Caldeira S, Zehbe I, Accardi R, Malanchi I, Dong W, Giarre M *et al* (2003). The E6 and E7 proteins of the cutaneous human papillomavirus type 38 display transforming properties. *J Virol* **77:** 2195-206.

Candi E, Dinsdale D, Rufini A, Salomoni P, Knight RA, Mueller M *et al* (2007). TAp63 and DeltaNp63 in cancer and epidermal development. *Cell Cycle* **6:** 274-85.

Candi E, Melino G, Mei G, Tarcsa E, Chung SI, Marekov LN *et al* (1995). Biochemical, structural, and transglutaminase substrate properties of human loricrin, the major epidermal cornified cell envelope protein. *J Biol Chem* **270:** 26382-90.

Candi E, Schmidt R, Melino G (2005). The cornified envelope: a model of cell death in the skin. *Nat Rev Mol Cell Biol* **6:** 328-40.

Cason J, Mant CA (2005). High-risk mucosal human papillomavirus infections during infancy & childhood. *J Clin Virol* **32 Suppl 1:** S52-8.

Castellsague X, Quintana MJ, Martinez MC, Nieto A, Sanchez MJ, Juan A *et al* (2004). The role of type of tobacco and type of alcoholic beverage in oral carcinogenesis. *Int J Cancer* **108:** 741-9.

Chan PK, Cheung JL, Cheung TH, Lo KW, Yim SF, Siu SS *et al* (2007). Profile of viral load, integration, and E2 gene disruption of HPV58 in normal cervix and cervical neoplasia. *J Infect Dis* **196:** 868-75.

Chang YE, Laimins LA (2000). Microarray analysis identifies interferon-inducible genes and Stat-1 as major transcriptional targets of human papillomavirus type 31. *J Virol* **74:** 4174-82.

Cheng S, Schmidt-Grimminger DC, Murant T, Broker TR, Chow LT (1995). Differentiation-dependent up-regulation of the human papillomavirus E7 gene reactivates cellular DNA replication in suprabasal differentiated keratinocytes. *Genes Dev* **9:** 2335-49.

Chiang CM, Ustav M, Stenlund A, Ho TF, Broker TR, Chow LT (1992). Viral E1 and E2 proteins support replication of homologous and heterologous papillomaviral origins. *Proc Natl Acad Sci USA* **89:** 5799-803.

Chipuk JE, Kuwana T, Bouchier-Hayes L, Droin NM, Newmeyer DD, Schuler M *et al* (2004). Direct activation of Bax by p53 mediates mitochondrial membrane permeabilization and apoptosis. *Science* **303:** 1010-4.

Clifford GM, Smith JS, Aguado T, Franceschi S (2003). Comparison of HPV type distribution in high-grade cervical lesions and cervical cancer: a meta-analysis. *Br J Cancer* **89:** 101-5.

Coderch L, Lopez O, de la Maza A, Parra JL (2003). Ceramides and skin function. *Am J Clin Dermatol* **4:** 107-29.

Conrad M, Bubb VJ, Schlegel R (1993). The human papillomavirus type 6 and 16 E5 proteins are membrane-associated proteins which associate with the 16-kilodalton pore-forming protein. *J Virol* **67:** 6170-8.

Crusius K, Auvinen E, Steuer B, Gaissert H, Alonso A (1998). The human papillomavirus type 16 E5-protein modulates ligand-dependent activation of the EGF receptor family in the human epithelial cell line HaCaT. *Exp Cell Res* **241:** 76-83.

Dahlstrand HM, Dalianis T (2005). Presence and influence of human papillomaviruses (HPV) in Tonsillar cancer. *Adv Cancer Res* **93:** 59-89.

Darroudi F, Natarajan AT, Lohman PH (1989). Cytogenetical characterization of UV-sensitive repair-deficient CHO cell line 43-3B. II. Induction of cell killing, chromosomal aberrations and sister-chromatid exchanges by 4NQO, mono- and bi-functional alkylating agents. *Mutat Res* **212:** 103-12.

Davis HE, Morgan JR, Yarmush ML (2002). Polybrene increases retrovirus gene transfer efficiency by enhancing receptor-independent virus adsorption on target cell membranes. *Biophys Chem* **97:** 159-72.

Davy CD, J. (2005). Human papillomaviruses. Methods and protocols. *Humana Press Inc.*: Totowa, New Jersey.

de Jong-Tieben LM, Berkhout RJ, Smits HL, Bouwes Bavinck JN, Vermeer BJ, van der Woude FJ *et al* (1995). High frequency of detection of epidermodysplasia verruciformis-associated human papillomavirus DNA in biopsies from malignant and premalignant skin lesions from renal transplant recipients. *J Invest Dermatol* **105:** 367-71.

de Villiers EM (1995). Importance of human papillomavirus DNA typing in the diagnosis of anogenital warts in children. *Arch Dermatol* **131:** 366-7.

de Villiers EM (1998). Human papillomavirus infections in skin cancers. *Biomed Pharmacother* **52:** 26-33.

de Villiers EM, Fauquet C, Broker TR, Bernard HU, zur Hausen H (2004). Classification of papillomaviruses. *Virology* **324:** 17-27.

de Villiers EM, Lavergne D, McLaren K, Benton EC (1997). Prevailing papillomavirus types in non-melanoma carcinomas of the skin in renal allograft recipients. *Int J Cancer* **73:** 356-61.

de Villiers EM, Ruhland A, Sekaric P (1999). Human papillomaviruses in non-melanoma skin cancer. *Semin Cancer Biol* **9:** 413-22.

Dean PN, Jett JH (1974). Mathematical analysis of DNA distributions derived from flow microfluorometry. *J Cell Biol* **60:** 523-7.

del Mar Pena LM, Laimins LA (2001). Differentiation-dependent chromatin rearrangement coincides with activation of human papillomavirus type 31 late gene expression. *J Virol* **75:** 10005-13.

Deyrup AT (2008). Epstein-Barr virus-associated epithelial and mesenchymal neoplasms. *Hum Pathol* **39:** 473-83.

Dieffenbach CW, Lowe TM, Dveksler GS (1993). General concepts for PCR primer design. *PCR Methods Appl* **3:** S30-7.

DiMaio D, Mattoon D (2001). Mechanisms of cell transformation by papillomavirus E5 proteins. *Oncogene* **20:** 7866-73.

Doorbar J (2005). The papillomavirus life cycle. *J Clin Virol* **32 Suppl 1:** S7-15.

Doorbar J (2006). Molecular biology of human papillomavirus infection and cervical cancer. *Clin Sci (Lond)* **110:** 525-41.

Doorbar J, Coneron I, Gallimore PH (1989). Sequence divergence yet conserved physical characteristics among the E4 proteins of cutaneous human papillomaviruses. *Virology* **172:** 51-62.

Dowhanick JJ, McBride AA, Howley PM (1995). Suppression of cellular proliferation by the papillomavirus E2 protein. *J Virol* **69:** 7791-9.

Duensing S, Lee LY, Duensing A, Basile J, Piboonniyom S, Gonzalez S *et al* (2000). The human papillomavirus type 16 E6 and E7 oncoproteins cooperate to induce mitotic defects and genomic instability by uncoupling centrosome duplication from the cell division cycle. *Proc Natl Acad Sci USA* **97:** 10002-7.

Durst M, Gallahan D, Jay G, Rhim JS (1989). Glucocorticoid-enhanced neoplastic transformation of human keratinocytes by human papillomavirus type 16 and an activated ras oncogene. *Virology* **173:** 767-71.

Dyson N, Howley PM, Munger K, Harlow E (1989). The human papilloma virus-16 E7 oncoprotein is able to bind to the retinoblastoma gene product. *Science* **243:** 934-7.

Eckert RL, Crish JF, Robinson NA (1997). The epidermal keratinocyte as a model for the study of gene regulation and cell differentiation. *Physiol Rev* **77:** 397-424.

el-Deiry WS, Tokino T, Velculescu VE, Levy DB, Parsons R, Trent JM *et al* (1993). WAF1, a potential mediator of p53 tumor suppression. *Cell* **75:** 817-25.

Elbel M, Carl S, Spaderna S, Iftner T (1997). A comparative analysis of the interactions of the E6 proteins from cutaneous and genital papillomaviruses with p53 and E6AP in correlation to their transforming potential. *Virology* **239:** 132-49.

Elder, DE, Elenitsas R, Johnson BL Jr, Murphy GF (2005). Lever's Histopathology of the Skin, 9th ed. *Lippincott Williams and Wilkins*: Philadelphia, PA.

Elias PM, Williams ML, Holleran WM, Jiang YJ, Schmuth M (2008). Pathogenesis of permeability barrier abnormalities in the ichthyoses: inherited disorders of lipid metabolism. *J Lipid Res* **49:** 697-714.

Epp N, Furstenberger G, Muller K, de Juanes S, Leitges M, Hausser I *et al* (2007). 12R-lipoxygenase deficiency disrupts epidermal barrier function. *J Cell Biol* **177:** 173-82.

Fakhry C, Gillison ML (2006). Clinical implications of human papillomavirus in head and neck cancers. *J Clin Oncol* **24:** 2606-11.

Fei JW, Angel P, Wei QX, de Villiers EM (2006). TAp63α indirectly regulates a cutaneous HPV promoter through complex formation with Jun family members. *Oncogene* **25:** 3914-23.

Fei JW, de Villiers EM (2008). Degradation of HPV20E6 by p53: ΔNp63 alpha and mutant p53R248W protect the wild type p53 mediated caspase-degradation. *Int J Cancer* **123:** 108-16.

Fei JW, Wei QX, Angel P, de Villiers EM (2005). Differential enhancement of a cutaneous HPV promoter by ΔNP63alpha, Jun and mutant p53. *Cell Cycle* **4:** 689-96.

Feingold KR (2007). The importance of lipids in cutaneous function. *J Lipid Res* **48:** 2529-30.

Feltkamp MC, Broer R, di Summa FM, Struijk L, van der Meijden E, Verlaan BP *et al* (2003). Seroreactivity to epidermodysplasia verruciformis-related human papillomavirus types is associated with nonmelanoma skin cancer. *Cancer Res* **63:** 2695-700.

Fillies T, Werkmeister R, Packeisen J, Brandt B, Morin P, Weingart D *et al* (2006). Cytokeratin 8/18 expression indicates a poor prognosis in squamous cell carcinomas of the oral cavity. *BMC Cancer* **6:** 10.

Forslund O, Iftner T, Andersson K, Lindelof B, Hradil E, Nordin P *et al* (2007). Cutaneous human papillomaviruses found in sun-exposed skin: Beta-papillomavirus species 2 predominates in squamous cell carcinoma. *J Infect Dis* **196:** 876-83.

Franceschi S, Talamini R, Barra S, Baron AE, Negri E, Bidoli E *et al* (1990). Smoking and drinking in relation to cancers of the oral cavity, pharynx, larynx, and esophagus in northern Italy. *Cancer Res* **50:** 6502-7.

Frattini MG, Laimins LA (1994). Binding of the human papillomavirus E1 origin-recognition protein is regulated through complex formation with the E2 enhancer-binding protein. *Proc Natl Acad Sci USA* **91:** 12398-402.

Frattini MG, Lim HB, Doorbar J, Laimins LA (1997). Induction of human papillomavirus type 18 late gene expression and genomic amplification in organotypic cultures from transfected DNA templates. *J Virol* **71:** 7068-72.

Frazer IH (2004). Prevention of cervical cancer through papillomavirus vaccination. *Nat Rev Immunol* **4:** 46-54.

Fuchs E (1993). Epidermal differentiation and keratin gene expression. *J Cell Sci Suppl* **17:** 197-208.

Furuse M, Hata M, Furuse K, Yoshida Y, Haratake A, Sugitani Y *et al* (2002). Claudin-based tight junctions are crucial for the mammalian epidermal barrier: a lesson from claudin-1-deficient mice. *J Cell Biol* **156:** 1099-111.

Gabet AS, Accardi R, Bellopede A, Popp S, Boukamp P, Sylla BS *et al* (2008). Impairment of the telomere/telomerase system and genomic instability are associated with keratinocyte immortalization induced by the skin human papillomavirus type 38. *FASEB J* **22:** 622-32.

Galiegue-Zouitina S, Bailleul B, Loucheux-Lefebvre MH (1985). Adducts from in vivo action of the carcinogen 4-hydroxyaminoquinoline 1-oxide in rats and from in vitro reaction of 4-acetoxyaminoquinoline 1-oxide with DNA and polynucleotides. *Cancer Res* **45:** 520-5.

Gartner LP, Hiatt JL (2007). Color Textbook of Histology. *Sanders E*, 3rd edition.

Genther Williams SM, Disbrow GL, Schlegel R, Lee D, Threadgill DW, Lambert PF (2005). Requirement of epidermal growth factor receptor for hyperplasia induced by E5, a high-risk human papillomavirus oncogene. *Cancer Res* **65:** 6534-42.

Gillison ML, Koch WM, Capone RB, Spafford M, Westra WH, Wu L *et al* (2000). Evidence for a causal association between human papillomavirus and a subset of head and neck cancers. *J Natl Cancer Inst* **92:** 709-20.

Giroglou T, Florin L, Schafer F, Streeck RE, Sapp M (2001). Human papillomavirus infection requires cell surface heparan sulfate. *J Virol* **75:** 1565-70.

Gloss B, Bernard HU, Seedorf K, Klock G (1987). The upstream regulatory region of the human papilloma virus-16 contains an E2 protein-independent enhancer which is specific for cervical carcinoma cells and regulated by glucocorticoid hormones. *EMBO J* **6:** 3735-43.

Golias CH, Charalabopoulos A, Charalabopoulos K (2004). Cell proliferation and cell cycle control: a mini review. *Int J Clin Pract* **58:** 1134-41.

Grassmann K, Rapp B, Maschek H, Petry KU, Iftner T (1996). Identification of a differentiation-inducible promoter in the E7 open reading frame of human papillomavirus type 16 (HPV-16) in raft cultures of a new cell line containing high copy numbers of episomal HPV-16 DNA. *J Virol* **70:** 2339-49.

Green KJ, Parry DA, Steinert PM, Virata ML, Wagner RM, Angst BD *et al* (1990). Structure of the human desmoplakins. Implications for function in the desmosomal plaque. *J Biol Chem* **265:** 2603-12.

Habig M, Smola H, Dole VS, Derynck R, Pfister H, Smola-Hess S (2006). E7 proteins from high- and low-risk human papillomaviruses bind to TGF-beta-regulated Smad proteins and inhibit their transcriptional activity. *Arch Virol* **151:** 1961-72.

Hagiwara K, McMenamin MG, Miura K, Harris CC (1999). Mutational analysis of the p63/p73L/p51/p40/CUSP/KET gene in human cancer cell lines using intronic primers. *Cancer Res* **59:** 4165-9.

Halbert CL, Demers GW, Galloway DA (1991). The E7 gene of human papillomavirus type 16 is sufficient for immortalization of human epithelial cells. *J Virol* **65:** 473-8.

Halbert CL, Demers GW, Galloway DA (1992). The E6 and E7 genes of human papillomavirus type 6 have weak immortalizing activity in human epithelial cells. *J Virol* **66:** 2125-34.

Hall PA, Campbell SJ, O'Neill M, Royston DJ, Nylander K, Carey FA *et al* (2000). Expression of the p53 homologue p63α and ΔNp63α in normal and neoplastic cells. *Carcinogenesis* **21:** 153-60.

Han H, Pan Q, Zhang B, Li J, Deng X, Lian Z *et al* (2007). 4-NQO induces apoptosis via p53-dependent mitochondrial signaling pathway. *Toxicology* **230:** 151-63.

Handley J, Hanks E, Armstrong K, Bingham A, Dinsmore W, Swann A *et al* (1997). Common association of HPV 2 with anogenital warts in prepubertal children. *Pediatr Dermatol* **14:** 339-43.

Harwood CA, Surentheran T, Sasieni P, Proby CM, Bordea C, Leigh IM *et al* (2004). Increased risk of skin cancer associated with the presence of epidermodysplasia verruciformis human papillomavirus types in normal skin. *Br J Dermatol* **150:** 949-57.

Hebner C, Beglin M, Laimins LA (2007). Human papillomavirus E6 proteins mediate resistance to interferon-induced growth arrest through inhibition of p53 acetylation. *J Virol* **81:** 12740-7.

Heron-Milhavet L, Karas M, Goldsmith CM, Baum BJ, LeRoith D (2001). Insulin-like growth factor-I (IGF-I) receptor activation rescues UV-damaged cells through a p38 signaling pathway. Potential role of the IGF-I receptor in DNA repair. *J Biol Chem* **276:** 18185-92.

Hibi K, Trink B, Patturajan M, Westra WH, Caballero OL, Hill DE *et al* (2000). AIS is an oncogene amplified in squamous cell carcinoma. *Proc Natl Acad Sci USA* **97:** 5462-7.

Hohl D, Mehrel T, Lichti U, Turner ML, Roop DR, Steinert PM (1991). Characterization of human loricrin. Structure and function of a new class of epidermal cell envelope proteins. *J Biol Chem* **266:** 6626-36.

Hohl D, Ruf Olano B, de Viragh PA, Huber M, Detrisac CJ, Schnyder UW *et al* (1993). Expression patterns of loricrin in various species and tissues. *Differentiation* **54:** 25-34.

Hollstein M, Sidransky D, Vogelstein B, Harris CC (1991). p53 mutations in human cancers. *Science* **253:** 49-53.

Holly EA, Cress RD, Ahn DK, Aston DA, Kristiansen JJ, Wu R *et al* (1993). Detection of mutagens in cervical mucus in smokers and nonsmokers. *Cancer Epidemiol Biomarkers Prev* **2:** 223-8.

Houben E, De Paepe K, Rogiers V (2007). A keratinocyte's course of life. *Skin Pharmacol Physiol* **20:** 122-32.

Hozumi M (1969). Production of hydrogen peroxide by 4 hydroxyaminoquinoline 1-oxide. *Gann* **60:** 83-90.

Hsu TC SN, Trizna Z, Feun L, Furlong C, Schantz S (1993). Cytogenetic studies on the in vitro genotoxicity of 4-nitroquinoline-1-oxide on human lymphocytes. *Int J Oncol* **3:** 823-6.

Huber M, Rettler I, Bernasconi K, Frenk E, Lavrijsen SP, Ponec M *et al* (1995). Mutations of keratinocyte transglutaminase in lamellar ichthyosis. *Science* **267:** 525-8.

Hughes FJ, Romanos MA (1993). E1 protein of human papillomavirus is a DNA helicase/ATPase. *Nucleic Acids Res* **21:** 5817-23.

Huibregtse JM, Scheffner M, Howley PM (1991). A cellular protein mediates association of p53 with the E6 oncoprotein of human papillomavirus types 16 or 18. *EMBO J* **10:** 4129-35.

Hurford RK, Jr., Cobrinik D, Lee MH, Dyson N (1997). pRB and p107/p130 are required for the regulated expression of different sets of E2F responsive genes. *Genes Dev* **11:** 1447-63.

IARC (2005). Monographs on Evaluation of Carcinogenic Risks of Humans. Human Papillomaviruses, vol. Volume 90. *International Agency for Research on Cancer*.

Irwin MS, Kaelin WG (2001). p53 family update: p73 and p63 develop their own identities. *Cell Growth Differ* **12:** 337-49.

Ishida-Yamamoto A, Tanaka H, Nakane H, Takahashi H, Hashimoto Y, Iizuka H (1999). Programmed cell death in normal epidermis and loricrin keratoderma. Multiple functions of profilaggrin in keratinization. *J Investig Dermatol Symp Proc* **4:** 145-9.

Ishiji T, Lace MJ, Parkkinen S, Anderson RD, Haugen TH, Cripe TP *et al* (1992). Transcriptional enhancer factor (TEF)-1 and its cell-specific co-activator activate human papillomavirus-16 E6 and E7 oncogene transcription in keratinocytes and cervical carcinoma cells. *EMBO J* **11:** 2271-81.

Jablonska S, Majewski S (1994). Epidermodysplasia verruciformis: immunological and clinical aspects. *Curr Top Microbiol Immunol* **186:** 157-75.

Jackson ME, Pennie WD, McCaffery RE, Smith KT, Grindlay GJ, Campo MS (1991). The B subgroup bovine papillomaviruses lack an identifiable E6 open reading frame. *Mol Carcinog* **4:** 382-7.

Jackson S, Harwood C, Thomas M, Banks L, Storey A (2000). Role of Bak in UV-induced apoptosis in skin cancer and abrogation by HPV E6 proteins. *Genes Dev* **14:** 3065-73.

Ji L, Fang B, Yen N, Fong K, Minna JD, Roth JA (1999). Induction of apoptosis and inhibition of tumorigenicity and tumor growth by adenovirus vector-mediated fragile histidine triad (FHIT) gene overexpression. *Cancer Res* **59:** 3333-9.

Jones DL, Alani RM, Munger K (1997). The human papillomavirus E7 oncoprotein can uncouple cellular differentiation and proliferation in human keratinocytes by abrogating p21Cip1-mediated inhibition of cdk2. *Genes Dev* **11:** 2101-11.

Joyce JG, Tung JS, Przysiecki CT, Cook JC, Lehman ED, Sands JA *et al* (1999). The L1 major capsid protein of human papillomavirus type 11 recombinant virus-like particles interacts with heparin and cell-surface glycosaminoglycans on human keratinocytes. *J Biol Chem* **274:** 5810-22.

Kalinin AE, Kajava AV, Steinert PM (2002). Epithelial barrier function: assembly and structural features of the cornified cell envelope. *Bioessays* **24:** 789-800.

Kamper N, Day PM, Nowak T, Selinka HC, Florin L, Bolscher J *et al* (2006). A membrane-destabilizing peptide in capsid protein L2 is required for egress of papillomavirus genomes from endosomes. *J Virol* **80:** 759-68.

Kanojia D, Vaidya MM (2006). 4-nitroquinoline-1-oxide induced experimental oral carcinogenesis. *Oral Oncol* **42:** 655-67.

Kaur P, McDougall JK (1989). HPV-18 immortalization of human keratinocytes. *Virology* **173:** 302-10.

Kelman Z (1997). PCNA: structure, functions and interactions. *Oncogene* **14:** 629-40.

Kiviat NB (1999). Papillomaviruses in non-melanoma skin cancer: epidemiological aspects. *Semin Cancer Biol* **9:** 397-403.

Kiyono T, Foster SA, Koop JI, McDougall JK, Galloway DA, Klingelhutz AJ (1998). Both Rb/p16INK4a inactivation and telomerase activity are required to immortalize human epithelial cells. *Nature* **396:** 84-8.

Klingelhutz AJ, Foster SA, McDougall JK (1996). Telomerase activation by the E6 gene product of human papillomavirus type 16. *Nature* **380:** 79-82.

Koch PJ, de Viragh PA, Scharer E, Bundman D, Longley MA, Bickenbach J *et al* (2000). Lessons from loricrin-deficient mice: compensatory mechanisms maintaining skin barrier function in the absence of a major cornified envelope protein. *J Cell Biol* **151:** 389-400.

Koong SL, Yen AM, Chen TH (2006). Efficacy and cost-effectiveness of nationwide cervical cancer screening in Taiwan. *J Med Screen* **13 Suppl 1:** S44-7.

Koopman R, Schaart G, Hesselink MK (2001). Optimisation of oil red O staining permits combination with immunofluorescence and automated quantification of lipids. *Histochem Cell Biol* **116:** 63-8.

Koster MI, Kim S, Mills AA, DeMayo FJ, Roop DR (2004). p63 is the molecular switch for initiation of an epithelial stratification program. *Genes Dev* **18:** 126-31.

Krawczyk E, Suprynowicz FA, Liu X, Dai Y, Hartmann DP, Hanover J *et al* (2008). Koilocytosis: a cooperative interaction between the human papillomavirus E5 and E6 oncoproteins. *Am J Pathol* **173:** 682-8.

Kreimer AR, Clifford GM, Boyle P, Franceschi S (2005). Human papillomavirus types in head and neck squamous cell carcinomas worldwide: a systematic review. *Cancer Epidemiol Biomarkers Prev* **14:** 467-75.

Kyng KJ, May A, Stevnsner T, Becker KG, Kolvra S, Bohr VA (2005). Gene expression responses to DNA damage are altered in human aging and in Werner Syndrome. *Oncogene* **24:** 5026-42.

Kyo S, Klumpp DJ, Inoue M, Kanaya T, Laimins LA (1997). Expression of AP1 during cellular differentiation determines human papillomavirus E6/E7 expression in stratified epithelial cells. *J Gen Virol* **78 (Pt 2):** 401-11.

Lancaster WD, Olson C (1982). Animal papillomaviruses. *Microbiol Rev* **46:** 191-207.

Langbein L, Grund C, Kuhn C, Praetzel S, Kartenbeck J, Brandner JM *et al* (2002). Tight junctions and compositionally related junctional structures in mammalian stratified epithelia and cell cultures derived therefrom. *Eur J Cell Biol* **81:** 419-35.

Langbein L, Rogers MA, Praetzel S, Cribier B, Peltre B, Gassler N *et al* (2005). Characterization of a novel human type II epithelial keratin K1b, specifically expressed in eccrine sweat glands. *J Invest Dermatol* **125:** 428-44.

Lavergne D, de Villiers EM (1999). Papillomavirus in esophageal papillomas and carcinomas. *Int J Cancer* **80:** 681-4.

Lechner MS, Laimins LA (1994). Inhibition of p53 DNA binding by human papillomavirus E6 proteins. *J Virol* **68:** 4262-73.

Lee C, Cho Y (2002). Interactions of SV40 large T antigen and other viral proteins with retinoblastoma tumour suppressor. *Rev Med Virol* **12:** 81-92.

Lee C, Laimins LA (2004). Role of the PDZ domain-binding motif of the oncoprotein E6 in the pathogenesis of human papillomavirus type 31. *J Virol* **78:** 12366-77.

Li B, Dou QP (2000). Bax degradation by the ubiquitin/proteasome-dependent pathway: involvement in tumor survival and progression. *Proc Natl Acad Sci USA* **97:** 3850-5.

Li R, Waga S, Hannon GJ, Beach D, Stillman B (1994). Differential effects by the p21 CDK inhibitor on PCNA-dependent DNA replication and repair. *Nature* **371:** 534-7.

Li SL, Kim MS, Cherrick HM, Doniger J, Park NH (1992). Sequential combined tumorigenic effect of HPV-16 and chemical carcinogens. *Carcinogenesis* **13:** 1981-7.

Li Y, Wang L, Li S, Guo T, Guo X, Yan P *et al* (2005). p53 protein activates the transcription of human proliferating cell nuclear antigen in response to 4-nitroquinoline N-oxide treatment. *Int J Biochem Cell Biol* **37:** 416-26.

Liu X, Clements A, Zhao K, Marmorstein R (2006). Structure of the human Papillomavirus E7 oncoprotein and its mechanism for inactivation of the retinoblastoma tumor suppressor. *J Biol Chem* **281:** 578-86.

Liu Y, Chen JJ, Gao Q, Dalal S, Hong Y, Mansur CP *et al* (1999). Multiple functions of human papillomavirus type 16 E6 contribute to the immortalization of mammary epithelial cells. *J Virol* **73:** 7297-307.

Longworth MS, Laimins LA (2004). Pathogenesis of human papillomaviruses in differentiating epithelia. *Microbiol Mol Biol Rev* **68:** 362-72.

Loning T, Ikenberg H, Becker J, Gissmann L, Hoepfer I, zur Hausen H (1985). Analysis of oral papillomas, leukoplakias, and invasive carcinomas for human papillomavirus type related DNA. *J Invest Dermatol* **84:** 417-20.

Lopez O, Cocera M, Wertz PW, Lopez-Iglesias C, de la Maza A (2007). New arrangement of proteins and lipids in the stratum corneum cornified envelope. *Biochim Biophys Acta* **1768:** 521-9.

Luo Y, Hurwitz J, Massague J (1995). Cell-cycle inhibition by independent CDK and PCNA binding domains in p21Cip1. *Nature* **375:** 159-61.

Malzahn K, Mitze M, Thoenes M, Moll R (1998). Biological and prognostic significance of stratified epithelial cytokeratins in infiltrating ductal breast carcinomas. *Virchows Arch* **433:** 119-29.

Mansbridge J, Knapp M (1987). Effects of filaggrin breakdown products on the growth and maturation of keratinocytes. *Arch Dermatol Res* **279:** 465-9.

Marekov LN, Steinert PM (1998). Ceramides are bound to structural proteins of the human foreskin epidermal cornified cell envelope. *J Biol Chem* **273:** 17763-70.

McDonald LA, Walker DM, Gibbins JR (1998). Cervical lymph node involvement in head and neck cancer detectable as expression of a spliced transcript of type II keratin K5. *Oral Oncol* **34:** 276-83.

McGowan K, Coulombe PA (1998). The wound repair-associated keratins 6, 16, and 17. Insights into the role of intermediate filaments in specifying keratinocyte cytoarchitecture. *Subcell Biochem* **31:** 173-204.

McKeon F (2004). p63 and the epithelial stem cell: more than status quo? *Genes Dev* **18:** 465-9.

Mercer WE, Shields MT, Lin D, Appella E, Ullrich SJ (1991). Growth suppression induced by wild-type p53 protein is accompanied by selective down-regulation of proliferating-cell nuclear antigen expression. *Proc Natl Acad Sci USA* **88:** 1958-62.

Michel A, Kopp-Schneider A, Zentgraf H, Gruber AD, de Villiers EM (2006). E6/E7 expression of human papillomavirus type 20 (HPV-20) and HPV-27 influences proliferation and differentiation of the skin in UV-irradiated SKH-hr1 transgenic mice. *J Virol* **80:** 11153-64.

Middleton K, Peh W, Southern S, Griffin H, Sotlar K, Nakahara T *et al* (2003). Organization of human papillomavirus productive cycle during neoplastic progression provides a basis for selection of diagnostic markers. *J Virol* **77:** 10186-201.

Miller CS, Johnstone BM (2001). Human papillomavirus as a risk factor for oral squamous cell carcinoma: a meta-analysis, 1982-1997. *Oral Surg Oral Med Oral Pathol Oral Radiol Endod* **91:** 622-35.

Mills AA (2006). p63: oncogene or tumor suppressor? *Curr Opin Genet Dev* **16:** 38-44.

Mischke D, Wille G, Wild AG (1990). Allele frequencies and segregation of human polymorphic keratins K4 and K5. *Am J Hum Genet* **46:** 548-52.

Mistry N, Wibom C, Evander M (2008). Cutaneous and mucosal human papillomaviruses differ in net surface charge, potential impact on tropism. *Virol J* **5:** 118.

Miyamoto S, Yasui Y, Kim M, Sugie S, Murakami A, Ishigamori-Suzuki R *et al* (2008). A novel rasH2 mouse carcinogenesis model that is highly susceptible to 4-NQO-induced tongue and esophageal carcinogenesis is useful for preclinical chemoprevention studies. *Carcinogenesis* **29:** 418-26.

Modis Y, Trus BL, Harrison SC (2002). Atomic model of the papillomavirus capsid. *EMBO J* **21:** 4754-62.

Moll I, Heid H, Franke WW, Moll R (1987). Distribution of a special subset of keratinocytes characterized by the expression of cytokeratin 9 in adult and fetal human epidermis of various body sites. *Differentiation* **33:** 254-65.

Moll R (1998). Cytokeratins as markers of differentiation in the diagnosis of epithelial tumors. *Subcell Biochem* **31:** 205-62.

Moll R, Divo M, Langbein L (2008). The human keratins: biology and pathology. *Histochem Cell Biol* **129:** 705-33.

Moll R, Franke WW, Schiller DL, Geiger B, Krepler R (1982). The catalog of human cytokeratins: patterns of expression in normal epithelia, tumors and cultured cells. *Cell* **31:** 11-24.

Morse DE, Psoter WJ, Cleveland D, Cohen D, Mohit-Tabatabai M, Kosis DL *et al* (2007). Smoking and drinking in relation to oral cancer and oral epithelial dysplasia. *Cancer Causes Control* **18:** 919-29.

Munger K, Basile JR, Duensing S, Eichten A, Gonzalez SL, Grace M *et al* (2001). Biological activities and molecular targets of the human papillomavirus E7 oncoprotein. *Oncogene* **20:** 7888-98.

Munger K, Howley PM (2002). Human papillomavirus immortalization and transformation functions. *Virus Res* **89:** 213-28.

Munger K, Scheffner M, Huibregtse JM, Howley PM (1992). Interactions of HPV E6 and E7 oncoproteins with tumour suppressor gene products. *Cancer Surv* **12:** 197-217.

Murphy GF, Flynn TC, Rice RH, Pinkus GS (1984). Involucrin expression in normal and neoplastic human skin: a marker for keratinocyte differentiation. *J Invest Dermatol* **82:** 453-7.

Nakahara T, Peh WL, Doorbar J, Lee D, Lambert PF (2005). Human papillomavirus type 16 E1^E4 contributes to multiple facets of the papillomavirus life cycle. *J Virol* **79:** 13150-65.

Nakahara W, Fukuoka F, Sugimura T (1957). Carcinogenic action of 4-nitroquinoline-N-oxide. *Gan* **48:** 129-37.

Nakano K, Vousden KH (2001). PUMA, a novel proapoptotic gene, is induced by p53. *Mol Cell* **7:** 683-94.

Narisawa-Saito M, Kiyono T (2007). Basic mechanisms of high-risk human papillomavirus-induced carcinogenesis: roles of E6 and E7 proteins. *Cancer Sci* **98:** 1505-11.

Ninomiya Y, Suzuki K, Ishii C, Inoue H (2004). Highly efficient gene replacements in Neurospora strains deficient for nonhomologous end-joining. *Proc Natl Acad Sci U S A* **101:** 12248-53.

Nishimura A (1999). Changes in Bcl-2 and Bax expression in rat tongue during 4-nitroquinoline 1-oxide-induced carcinogenesis. *J Dent Res* **78:** 1264-9.

Nunoshiba T, Demple B (1993). Potent intracellular oxidative stress exerted by the carcinogen 4-nitroquinoline-N-oxide. *Cancer Res* **53:** 3250-2.

O'Connor M, Bernard HU (1995). Oct-1 activates the epithelial-specific enhancer of human papillomavirus type 16 via a synergistic interaction with NFI at a conserved composite regulatory element. *Virology* **207:** 77-88.

O'Guin WM, Galvin S, Schermer A, Sun TT (1987). Patterns of keratin expression define distinct pathways of epithelial development and differentiation. *Curr Top Dev Biol* **22:** 97-125.

Opitz OG, Suliman Y, Hahn WC, Harada H, Blum HE, Rustgi AK (2001). Cyclin D1 overexpression and p53 inactivation immortalize primary oral keratinocytes by a telomerase-independent mechanism. *J Clin Invest* **108:** 725-32.

Parkin DM, Bray F (2006). Chapter 2: The burden of HPV-related cancers. *Vaccine* **24 Suppl 3:** S11-25.

Parkin DM, Bray F, Ferlay J, Pisani P (2005). Global cancer statistics, 2002. *CA Cancer J Clin* **55:** 74-108.

Patel KR, Smith KT, Campo MS (1987). The nucleotide sequence and genome organization of bovine papillomavirus type 4. *J Gen Virol* **68 (Pt 8):** 2117-28.

Pear WS, M.; Nolan, G.P. (1997). Methods in Molecular Medicine: Gene Therapy Protocols. *Humana Press Inc.*: Totowa, New Jersey.

Peto J, Gilham C, Fletcher O, Matthews FE (2004). The cervical cancer epidemic that screening has prevented in the UK. *Lancet* **364:** 249-56.

Pett M, Coleman N (2007). Integration of high-risk human papillomavirus: a key event in cervical carcinogenesis? *J Pathol* **212:** 356-67.

Phillips DH, Ni She M (1993). Smoking-related DNA adducts in human cervical biopsies. *IARC Sci Publ***:** 327-30.

Pim D, Massimi P, Banks L (1997). Alternatively spliced HPV-18 E6* protein inhibits E6 mediated degradation of p53 and suppresses transformed cell growth. *Oncogene* **15:** 257-64.

Pim D, Storey A, Thomas M, Massimi P, Banks L (1994). Mutational analysis of HPV-18 E6 identifies domains required for p53 degradation in vitro, abolition of p53 transactivation in vivo and immortalisation of primary BMK cells. *Oncogene* **9:** 1869-76.

Pim D, Thomas M, Banks L (2002). Chimaeric HPV E6 proteins allow dissection of the proteolytic pathways regulating different E6 cellular target proteins. *Oncogene* **21:** 8140-8.

Ponting CP (1997). Evidence for PDZ domains in bacteria, yeast, and plants. *Protein Sci* **6:** 464-8.

Presland RB, Dale BA (2000). Epithelial structural proteins of the skin and oral cavity: function in health and disease. *Crit Rev Oral Biol Med* **11:** 383-408.

Preston DS, Stern RS (1992). Nonmelanoma cancers of the skin. *N Engl J Med* **327:** 1649-62.

Quade BJ, Yang A, Wang Y, Sun D, Park J, Sheets EE *et al* (2001). Expression of the p53 homologue p63 in early cervical neoplasia. *Gynecol Oncol* **80:** 24-9.

Radtke F, Raj K (2003). The role of Notch in tumorigenesis: oncogene or tumour suppressor? *Nat Rev Cancer* **3:** 756-67.

Ramoz N, Rueda LA, Bouadjar B, Montoya LS, Orth G, Favre M (2002). Mutations in two adjacent novel genes are associated with epidermodysplasia verruciformis. *Nat Genet* **32:** 579-81.

Riley RR, Duensing S, Brake T, Munger K, Lambert PF, Arbeit JM (2003). Dissection of human papillomavirus E6 and E7 function in transgenic mouse models of cervical carcinogenesis. *Cancer Res* **63:** 4862-71.

Roberts S, Ashmole I, Johnson GD, Kreider JW, Gallimore PH (1993). Cutaneous and mucosal human papillomavirus E4 proteins form intermediate filament-like structures in epithelial cells. *Virology* **197:** 176-87.

Robles AI, Bemmels NA, Foraker AB, Harris CC (2001). APAF-1 is a transcriptional target of p53 in DNA damage-induced apoptosis. *Cancer Res* **61:** 6660-4.

Roden RB, Day PM, Bronzo BK, Yutzy WHt, Yang Y, Lowy DR *et al* (2001). Positively charged termini of the L2 minor capsid protein are necessary for papillomavirus infection. *J Virol* **75:** 10493-7.

Romanczuk H, Villa LL, Schlegel R, Howley PM (1991). The viral transcriptional regulatory region upstream of the E6 and E7 genes is a major determinant of the differential immortalization activities of human papillomavirus types 16 and 18. *J Virol* **65:** 2739-44.

Roninson IB (2002). Oncogenic functions of tumour suppressor p21 (Waf1/Cip1/Sdi1): association with cell senescence and tumour-promoting activities of stromal fibroblasts. *Cancer Lett* **179:** 1-14.

Rossi A, Jang SI, Ceci R, Steinert PM, Markova NG (1998). Effect of AP1 transcription factors on the regulation of transcription in normal human epidermal keratinocytes. *J Invest Dermatol* **110:** 34-40.

Sambrook JF, E.F. und Maniatis, T. (1989). Molecular Cloning: A Laboratory Manual. *NY Cold Spring Harbor Laboratory Press*: Cold Spring Harbor.

Sanclemente G, Gill DK (2002). Human papillomavirus molecular biology and pathogenesis. *J Eur Acad Dermatol Venereol* **16:** 231-40.

Sang BC, Barbosa MS (1992). Single amino acid substitutions in "low-risk" human papillomavirus (HPV) type 6 E7 protein enhance features characteristic of the "high-risk" HPV E7 oncoproteins. *Proc Natl Acad Sci USA* **89:** 8063-7.

Schaper ID, Marcuzzi GP, Weissenborn SJ, Kasper HU, Dries V, Smyth N *et al* (2005). Development of skin tumors in mice transgenic for early genes of human papillomavirus type 8. *Cancer Res* **65:** 1394-400.

Scheffner M, Werness BA, Huibregtse JM, Levine AJ, Howley PM (1990). The E6 oncoprotein encoded by human papillomavirus types 16 and 18 promotes the degradation of p53. *Cell* **63:** 1129-36.

Schiffman M, Herrero R, Desalle R, Hildesheim A, Wacholder S, Rodriguez AC *et al* (2005). The carcinogenicity of human papillomavirus types reflects viral evolution. *Virology* **337:** 76-84.

Schmitt A, Harry JB, Rapp B, Wettstein FO, Iftner T (1994). Comparison of the properties of the E6 and E7 genes of low- and high-risk cutaneous papillomaviruses reveals strongly transforming and high Rb-binding activity for the E7 protein of the low-risk human papillomavirus type 1. *J Virol* **68:** 7051-9.

Schwarz E, Freese UK, Gissmann L, Mayer W, Roggenbuck B, Stremlau A *et al* (1985). Structure and transcription of human papillomavirus sequences in cervical carcinoma cells. *Nature* **314:** 111-4.

Segre JA (2006). Epidermal barrier formation and recovery in skin disorders. *J Clin Invest* **116:** 1150-8.

Selinka HC, Florin L, Patel HD, Freitag K, Schmidtke M, Makarov VA *et al* (2007). Inhibition of transfer to secondary receptors by heparan sulfate-binding drug or antibody induces noninfectious uptake of human papillomavirus. *J Virol* **81:** 10970-80.

Seo YR, Lee SH, Han SS, Ryu JC (1999). Effect of p53 tumor suppressor on nucleotide excision repair in human colon carcinoma cells treated with 4-nitroquinoline 1-oxide. *Res Commun Mol Pathol Pharmacol* **104:** 157-64.

Sevilla LM, Nachat R, Groot KR, Klement JF, Uitto J, Djian P *et al* (2007). Mice deficient in involucrin, envoplakin, and periplakin have a defective epidermal barrier. *J Cell Biol* **179:** 1599-612.

Shah NG, Trivedi TI, Tankshali RA, Goswami JA, Shah JS, Jetly DH *et al* (2007). Molecular alterations in oral carcinogenesis: significant risk predictors in malignant transformation and tumor progression. *Int J Biol Markers* **22:** 132-43.

Shamanin V, Glover M, Rausch C, Proby C, Leigh IM, zur Hausen H *et al* (1994). Specific types of human papillomavirus found in benign proliferations and carcinomas of the skin in immunosuppressed patients. *Cancer Res* **54:** 4610-3.

Shamanin V, zur Hausen H, Lavergne D, Proby CM, Leigh IM, Neumann C *et al* (1996). Human papillomavirus infections in nonmelanoma skin cancers from renal transplant recipients and nonimmunosuppressed patients. *J Natl Cancer Inst* **88:** 802-11.

Sherr CJ, Roberts JM (1999). CDK inhibitors: positive and negative regulators of G1-phase progression. *Genes Dev* **13:** 1501-12.

Shibue T, Takeda K, Oda E, Tanaka H, Murasawa H, Takaoka A *et al* (2003). Integral role of Noxa in p53-mediated apoptotic response. *Genes Dev* **17:** 2233-8.

Smedts F, Ramaekers F, Troyanovsky S, Pruszczynski M, Link M, Lane B *et al* (1992). Keratin expression in cervical cancer. *Am J Pathol* **141:** 497-511.

Smith EM, Ritchie JM, Summersgill KF, Hoffman HT, Wang DH, Haugen TH *et al* (2004). Human papillomavirus in oral exfoliated cells and risk of head and neck cancer. *J Natl Cancer Inst* **96:** 449-55.

Smotkin D, Wettstein FO (1986). Transcription of human papillomavirus type 16 early genes in a cervical cancer and a cancer-derived cell line and identification of the E7 protein. *Proc Natl Acad Sci U S A* **83:** 4680-4.

Snyderwine EG, Bohr VA (1992). Gene- and strand-specific damage and repair in Chinese hamster ovary cells treated with 4-nitroquinoline 1-oxide. *Cancer Res* **52:** 4183-9.

Soussi T, Beroud C (2001). Assessing TP53 status in human tumours to evaluate clinical outcome. *Nat Rev Cancer* **1:** 233-40.

Srinivasan P, Suchalatha S, Babu PV, Devi RS, Narayan S, Sabitha KE *et al* (2008). Chemopreventive and therapeutic modulation of green tea polyphenols on drug metabolizing enzymes in 4-Nitroquinoline 1-oxide induced oral cancer. *Chem Biol Interact* **172:** 224-34.

Stark HJ, Breitkreutz D, Limat A, Bowden P, Fusenig NE (1987). Keratins of the human hair follicle: "hyperproliferative" keratins consistently expressed in outer root sheath cells in vivo and in vitro. *Differentiation* **35:** 236-48.

Stark HJ, Szabowski A, Fusenig NE, Maas-Szabowski N (2004). Organotypic cocultures as skin equivalents: A complex and sophisticated in vitro system. *Biol Proced Online* **6:** 55-60.

Stauffer Y, Raj K, Masternak K, Beard P (1998). Infectious human papillomavirus type 18 pseudovirions. *J Mol Biol* **283:** 529-36.

Steger G, Corbach S (1997). Dose-dependent regulation of the early promoter of human papillomavirus type 18 by the viral E2 protein. *J Virol* **71:** 50-8.

Steinert PM (1993). Structure, function, and dynamics of keratin intermediate filaments. *J Invest Dermatol* **100:** 729-34.

Steinert PM (2000). The complexity and redundancy of epithelial barrier function. *J Cell Biol* **151:** F5-8.

Sterling J, Tyring S (2001). Human papillomaviruses. Clinical and Scientific Advances. *Arnold Publisher*: London.

Stohr M, Vogt-Schaden M, Knobloch M, Vogel R, Futterman G (1978). Evaluation of eight fluorochrome combinations for simultaneous DNA-protein flow analyses. *Stain Technol* **53:** 205-15.

Stoler A, Kopan R, Duvic M, Fuchs E (1988). Use of monospecific antisera and cRNA probes to localize the major changes in keratin expression during normal and abnormal epidermal differentiation. *J Cell Biol* **107:** 427-46.

Storrs CH, Silverstein SJ (2007). PATJ, a tight junction-associated PDZ protein, is a novel degradation target of high-risk human papillomavirus E6 and the alternatively spliced isoform 18 E6. *J Virol* **81:** 4080-90.

Struijk L, van der Meijden E, Kazem S, ter Schegget J, de Gruijl FR, Steenbergen RD *et al* (2008). Specific betapapillomaviruses associated with squamous cell carcinoma of the skin inhibit UVB-induced apoptosis of primary human keratinocytes. *J Gen Virol* **89:** 2303-14.

Sugimura T, Otake H, Matsushima T (1968). Single strand scissions of DNA caused by a carcinogen, 4-hydroxylaminoquinoline 1-oxide. *Nature* **218:** 392.

Sun T-T, Eichner, R, Schermer, A, Copper, D, Nelson, WG, Weiss, RA (1984). Classification, expression, and possible mechanisms of evolution of mammalian epithelial keratins, a unifying model. Vol. 1. Cold Spring Harbor Laboratory, *Cold Spring Harbor*: New York.

Sun TT, Eichner R, Nelson WG, Tseng SC, Weiss RA, Jarvinen M *et al* (1983). Keratin classes: molecular markers for different types of epithelial differentiation. *J Invest Dermatol* **81:** 109s-15s.

Syrjanen K, Syrjanen S, Lamberg M, Pyrhonen S, Nuutinen J (1983). Morphological and immunohistochemical evidence suggesting human papillomavirus (HPV) involvement in oral squamous cell carcinogenesis. *Int J Oral Surg* **12:** 418-24.

Syrjanen K, Syrjanen S, Pyrhonen S (1982). Human papilloma virus (HPV) antigens in lesions of laryngeal squamous cell carcinomas. *ORL J Otorhinolaryngol Relat Spec* **44:** 323-34.

Tachezy R, Klozar J, Salakova M, Smith E, Turek L, Betka J *et al* (2005). HPV and other risk factors of oral cavity/oropharyngeal cancer in the Czech Republic. *Oral Dis* **11:** 181-5.

Tang XH, Knudsen B, Bemis D, Tickoo S, Gudas LJ (2004). Oral cavity and esophageal carcinogenesis modeled in carcinogen-treated mice. *Clin Cancer Res* **10:** 301-13.

Thomas JT, Laimins LA (1998). Human papillomavirus oncoproteins E6 and E7 independently abrogate the mitotic spindle checkpoint. *J Virol* **72:** 1131-7.

Thomas M, Banks L (1999). Human papillomavirus (HPV) E6 interactions with Bak are conserved amongst E6 proteins from high and low risk HPV types. *J Gen Virol* **80 (Pt 6):** 1513-7.

Thomas MC, Chiang CM (2005). E6 oncoprotein represses p53-dependent gene activation via inhibition of protein acetylation independently of inducing p53 degradation. *Mol Cell* **17:** 251-64.

Tieben LM, Berkhout RJ, Smits HL, Bouwes Bavinck JN, Vermeer BJ, Bruijn JA *et al* (1994). Detection of epidermodysplasia verruciformis-like human papillomavirus types in malignant and premalignant skin lesions of renal transplant recipients. *Br J Dermatol* **131:** 226-30.

Truong AB, Kretz M, Ridky TW, Kimmel R, Khavari PA (2006). p63 regulates proliferation and differentiation of developmentally mature keratinocytes. *Genes Dev* **20:** 3185-97.

Trus BL, Roden RB, Greenstone HL, Vrhel M, Schiller JT, Booy FP (1997). Novel structural features of bovine papillomavirus capsid revealed by a three-dimensional reconstruction to 9 A resolution. *Nat Struct Biol* **4:** 413-20.

Tsai TC, Chen SL (2003). The biochemical and biological functions of human papillomavirus type 16 E5 protein. *Arch Virol* **148:** 1445-53.

Tseng SC, Jarvinen MJ, Nelson WG, Huang JW, Woodcock-Mitchell J, Sun TT (1982). Correlation of specific keratins with different types of epithelial differentiation: monoclonal antibody studies. *Cell* **30:** 361-72.

Underbrink MP, Howie HL, Bedard KM, Koop JI, Galloway DA (2008). The E6 proteins from multiple beta HPV types degrade Bak and protect keratinocytes from apoptosis after UVB irradiation. *J Virol*. **82**:10408-17.

Ustav E, Ustav M, Szymanski P, Stenlund A (1993). The bovine papillomavirus origin of replication requires a binding site for the E2 transcriptional activator. *Proc Natl Acad Sci USA* **90:** 898-902.

Vasiljevic N, Nielsen L, Doherty G, Dillner J, Forslund O, Norrild B (2008). Differences in transcriptional activity of cutaneous human papillomaviruses. *Virus Res* **137:** 213-9.

Vered M, Yarom N, Dayan D (2005). 4NQO oral carcinogenesis: animal models, molecular markers and future expectations. *Oral Oncol* **41:** 337-9.

Vogelstein B, Lane D, Levine AJ (2000). Surfing the p53 network. *Nature* **408:** 307-10.

Walboomers JM, Jacobs MV, Manos MM, Bosch FX, Kummer JA, Shah KV *et al* (1999). Human papillomavirus is a necessary cause of invasive cervical cancer worldwide. *J Pathol* **189:** 12-9.

Waldman T, Kinzler KW, Vogelstein B (1995). p21 is necessary for the p53-mediated G1 arrest in human cancer cells. *Cancer Res* **55:** 5187-90.

Wang LE, Hsu TC, Xiong P, Strom SS, Duvic M, Clayman GL *et al* (2007). 4-Nitroquinoline-1-oxide-induced mutagen sensitivity and risk of nonmelanoma skin cancer: a case-control analysis. *J Invest Dermatol* **127:** 196-205.

Wang TY, Chen BF, Yang YC, Chen H, Wang Y, Cviko A *et al* (2001). Histologic and immunophenotypic classification of cervical carcinomas by expression of the p53 homologue p63: a study of 250 cases. *Hum Pathol* **32:** 479-86.

Watson RA, Thomas M, Banks L, Roberts S (2003). Activity of the human papillomavirus E6 PDZ-binding motif correlates with an enhanced morphological transformation of immortalized human keratinocytes. *J Cell Sci* **116:** 4925-34.

Watt FM, Boukamp P, Hornung J, Fusenig NE (1987). Effect of growth environment on spatial expression of involucrin by human epidermal keratinocytes. *Arch Dermatol Res* **279:** 335-40.

Watzig V, Jablonska S (1987). HPV-20-induced epidermodysplasia verruciformis. *Hautarzt* **38:** 521-4.

Wayne S, Robinson RA (2006). Upper aerodigestive tract squamous dysplasia: correlation with p16, p53, pRb, and Ki-67 expression. *Arch Pathol Lab Med* **130:** 1309-14.

Weber BP, Fierlbeck G, Kempf HG (1994). Multiple metachronous skin squamous cell carcinomas and epidermodysplasia verruciformis in the head region: a human papilloma virus-associated disease. *Eur Arch Otorhinolaryngol* **251:** 342-6.

Werness BA, Levine AJ, Howley PM (1990). Association of human papillomavirus types 16 and 18 E6 proteins with p53. *Science* **248:** 76-9.

Wertz PW, van den Bergh B (1998). The physical, chemical and functional properties of lipids in the skin and other biological barriers. *Chem Phys Lipids* **91:** 85-96.

Westfall MD, Pietenpol JA (2004). p63: Molecular complexity in development and cancer. *Carcinogenesis* **25:** 857-64.

Wrone DA, Yoo S, Chipps LK, Moy RL (2004). The expression of p63 in actinic keratoses, seborrheic keratosis, and cutaneous squamous cell carcinomas. *Dermatol Surg* **30:** 1299-302.

Wu YJ, Parker LM, Binder NE, Beckett MA, Sinard JH, Griffiths CT *et al* (1982). The mesothelial keratins: a new family of cytoskeletal proteins identified in cultured mesothelial cells and nonkeratinizing epithelia. *Cell* **31:** 693-703.

Yamashita T, Segawa K, Fujinaga Y, Nishikawa T, Fujinaga K (1993). Biological and biochemical activity of E7 genes of the cutaneous human papillomavirus type 5 and 8. *Oncogene* **8:** 2433-41.

Yang A, McKeon F (2000). P63 and P73: P53 mimics, menaces and more. *Nat Rev Mol Cell Biol* **1:** 199-207.

Yang YY, Koh LW, Tsai JH, Tsai CH, Wong EF, Lin SJ *et al* (2004). Involvement of viral and chemical factors with oral cancer in Taiwan. *Jpn J Clin Oncol* **34:** 176-83.

Zerfass-Thome K, Zwerschke W, Mannhardt B, Tindle R, Botz JW, Jansen-Durr P (1996). Inactivation of the cdk inhibitor p27KIP1 by the human papillomavirus type 16 E7 oncoprotein. *Oncogene* **13:** 2323-30.

Zheng T, Holford T, Chen Y, Jiang P, Zhang B, Boyle P (1997). Risk of tongue cancer associated with tobacco smoking and alcohol consumption: a case-control study. *Oral Oncol* **33:** 82-5.

Ziegler A, Leffell DJ, Kunala S, Sharma HW, Gailani M, Simon JA *et al* (1993). Mutation hotspots due to sunlight in the p53 gene of nonmelanoma skin cancers. *Proc Natl Acad Sci USA* **90:** 4216-20.

zur Hausen H (1996). Papillomavirus infections-a major cause of human cancers. *Biochim Biophys Acta* **1288:** F55-78.

zur Hausen H (2002). Papillomaviruses and cancer: from basic studies to clinical application. *Nat Rev Cancer* **2:** 342-50.

zur Hausen H, Meinhof W, Scheiber W, Bornkamm GW (1974). Attempts to detect virus-secific DNA in human tumors. I. Nucleic acid hybridizations with complementary RNA of human wart virus. *Int J Cancer* **13:** 650-6.

7 Publications and poster presentations

Publications:

Herráez-Hernández E, Nobre RG, Langbein L, Kaden S, Gröne HJ and de Villiers EM. HPV20 E6 Oncoprotein Modifies Epithelial Differentiation and Induces Lipid Accumulation. Submitted.

Nobre RG, **Herráez-Hernández E**, Fei JW, Langbein L, Kaden S, Gröne HJ and de Villiers EM. E7 oncoprotein of novel HPV108 lacking the E6 gene induces dysplasia in organotypic keratinocyte cultures. J Virol. Epub 2009 Jan 19.

Poster presentations:

Herráez-Hernández E and de Villiers EM. Interaction of HPV20 with chemical carcinogens in the pathogenesis of malignant tumors.24th International Papillomavirus Conference and Clinical Workshop. Beijing, China. November, 2007.

Herráez-Hernández E and de Villiers EM. Interaction of HPV20 with chemical carcinogens in the pathogenesis of malignant tumors. DKFZ PhD students meeting. Weil der Stadt, Germany. July, 2007.

8 Acknowledgements

First of all, I would like to express my gratitude to my supervisor Prof. de Villiers for giving me the opportunity of undertaking this project and for her invaluable expertise, understanding, and continous support. I also would like to thank the members of my committee, Prof. Dr. G. Hämmerling and Prof. Dr. P. Angel.

I am also grateful to all the members of the lab that contribute to a nice work atmosphere during these years. Thanks to Araceli Velázquez, for all her support in my professional and personal life. Very special thanks to my lab colleagues Sabine Serick for her endless support day by day, Andrés Báez for his friendship and good moments when everything started in the lab some years ago; meu amigo Rui (*quisiera ser un pexe*), for our great team inside and outside of the lab and Benancio-Bladimiro whose candies and kindness helped me during the last months.

I would like to thank my long distance friends Joan and Alberto (and the little Elisa), for all the conversations in the best and worst moments. To my transoceanic soul mate Adan, the closest support one could dream from so far away! I am very grateful to my family heidelberguensis Ton, Rosalinda, Marcelo, Dieter, Rubén (*y nuestras charlas por carreteras secundarias*), Jorham (*mi eterno bichito*) and the great *equipote* Marina, JuanPa and Jose Luis for all the good moments that we had together and will stay with me forever. My warmest thanks go to my closest friends, Estrella, Jose, Anita and Ana Laura: they have been part of my heart since many years ago and always had encouranging words and hugs waiting for me.

I want to express my deepest gratitude to family, especially to my parents, my dear brother Iván (Ñai) and Herena (*fueguito* number one!). *Esta fue una tesis compartida entre los cuatro!* Their inconditional support day by day, their care, complete understanding and love always travel with me. I dedicate this thesis to my grandmother Lilín who believed and encouraged me since the first day of my life and whose continous positivity and happiness will accompany me forever (*dedico esta tesis a mi abuela Lilín, que creyó en mi y me animó a seguir adelante desde mi primer día de vida y cuya continua alegría me acompañará siempre*).